AN ENGINEERING APPROACH TO IMPROVE CLINICAL USABILITY OF QUANTITATIVE ELECTROMYOGRAPHY

by

Alexander Arthur Brownell

A dissertation submitted to the faculty of
The University of Utah
in partial fulfillment of the requirements for the degree of

Doctor of Philosophy

Department of Bioengineering

The University of Utah

May 2011

The University of Utah Graduate School

STATEMENT OF DISSERTATION APPROVAL

The dissertation of Alexander Arthur Brownell

has been approved by the following supervisory committee members:

Mark B. Bromberg	, Chair	**17 Dec 10** Date Approved
Richard A. Normann	, Member	**17 Dec 10** Date Approved
Douglas A. Christensen	, Member	**17 Dec 10** Date Approved
Rob S. MacLeod	, Member	**21 Dec 10** Date Approved
J. Robinson Singleton	, Member	**4 Jan 11** Date Approved

and by **Richard D. Rabbitt**, Chair of the Department of **Bioengineering**

and by Charles A. Wight, Dean of The Graduate School.

ABSTRACT

Electromyography (EMG) is the record of the electrical activity from muscle fiber membranes. This invaluable clinical tool in neurology aids in the diagnosis and monitoring of disease affecting muscle and nerve. Routine clinical EMG studies rely on the experience of the physician to analyze the data in a qualitative manner. Quantitative EMG (QEMG) refers to a number of techniques that measure various aspects of the EMG signal and result in statistical data. These techniques are becoming broader in scope, more automated and increasingly available on EMG machines. However, QEMG studies have challenges in a number of operational parameters from the engineering perspective but may not accurately fit from the physiologic and pathologic perspectives, and a number of these issues have not been investigated in a systematic way.

Here we present a number of studies aimed at validating and improving clinical usability of QEMG. First, we compare three QEMG algorithms available on EMG machines for use in the clinic, a study not performed previously. We determined that two algorithms yield similar results with minimal user intervention, while the third requires considerable expert review of the results and which are less robust than with the first two. Second, we show that among available sizes of intramuscular needle electrodes the smaller diameter electrode yields data comparable to the larger diameter electrode for clinical QEMG. Third, we show that any needle electrode position along the longitudinal

axis of the muscle with respect to the distribution of neuromuscular junctions within the muscle is acceptable for clinical QEMG studies. Fourth, we investigate and find that high-pass filtering is not an effective means of extracting more sensitive information from the EMG signals. Finally, we determine that at each position of the electrode within the muscle, 10 s worth of data collection balances the need to collect sufficient data with the possibility of degrading the signal due to subtle physiologic movements. The results of these efforts are a better understanding of the practical limits of the QEMG algorithms and how operational parameters can be optimized for more accurate statistics, more rapid data acquisition, and greater patient tolerability.

To my loving wife Michelle, whose long-suffering made this possible. Also, to Mark, a wonderful friend and unparalleled mentor.

TABLE OF CONTENTS

1 INTRODUCTION

Electromyography (EMG) is the record of electrical activity generated by muscle fiber membranes measured by electrodes placed either within or external to muscle. The membrane depolarization that is measured is the signal that initiates muscle fiber contraction (excitation-contraction coupling). EMG techniques provide information directly about the function and pathology of muscles, and indirectly about the function and pathology of both the nerves that innervate them and neuromuscular junction transmission. Thus, EMG is a useful tool to determine if a muscle is normal or abnormal; and if abnormal, whether the primary disease process is of nerves innervating the muscle or of the muscle itself, and also the integrity and function of the neuromuscular junction. Simply stated, EMG can estimate the architectural arrangement of muscle fibers within the muscle and their activation.

This body of work bridges the two disciplines concerned with the improvement of EMG techniques. Engineers have the ability to create systems and algorithms which allow for the measurement of EMG signals and can create new techniques to improve accuracy and efficiency. Clinicians have an understanding of the anatomy, physiology and disease processes underlying the signals which are generated by the EMG study. We explore clinically relevant questions to refine and optimize data acquisition and

interpretation from an engineering perspective with consideration of practical clinical limitations.

Anatomy and Physiology of the Motor Unit

The motor unit is the basic unit of neuromuscular function, the quantal unit of movement. It is defined as a single α-motor neuron, originating from the anterior horn of the spinal cord, along with its axon, and all of the muscle fibers which it innervates (Figure 1.1). This concept of the motor unit as the final common pathway of movement was introduced in 1925 by Lidell and Sherrington (1). Interposed between the nerve ending and the muscle fiber is the neuromuscular junction.

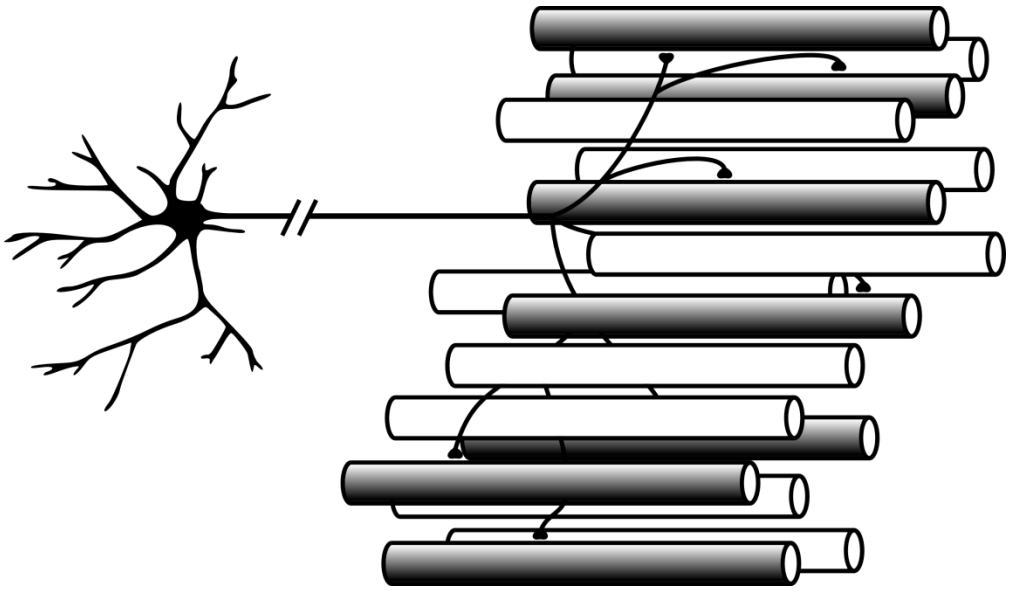

Figure 1.1: Representation of a motor unit. The α-motor neuron at the left is in the anterior horn of the spinal cord. Its axon exits the spinal cord through the anterior root and courses alongside other axons to a muscle. Within the muscle the axon branches up to several hundred times, and each branch innervates a single muscle fiber.

The architecture of muscle fibers of a motor unit within muscle has been determined by glycogen depletion studies. Edstrom and Kugelberg, in 1968, found that in rat preparations a single α-motor neuron (ventral rootlet) can be isolated and repeatedly stimulated thus depleting the glycogen stores in all muscle fibers innervated by that motor unit. When the muscle was removed and prepared for histology a cross section of the muscle, when stained for glycogen, revealed depleted fibers representing muscle fibers innervated by the stimulated neuron (2). An example of such a study is shown in Figure 1.2. These studies revealed many previously unconfirmed properties of motor units. Many motor units overlap—sharing much of the same territory in the muscle. Motor units cover relatively large areas of the overall axial territory of the muscle but vary greatly in area, but no motor unit in large skeletal muscle covers the entire cross-sectional area of the muscle. Importantly, relatively few neighboring muscle fibers belong to the same motor unit. Additionally, motor units are essentially uniform in

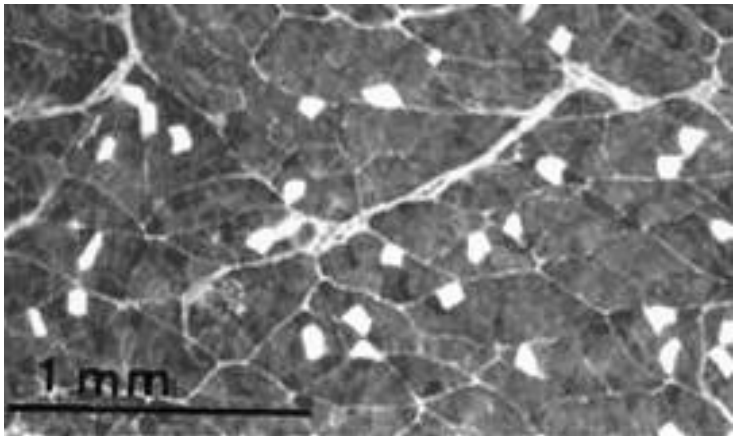

Figure 1.2: Glycogen depletion study in the rat showing muscle in cross section. Single motor neuron activated repeatedly until all glycogen stores are depleted. Excision of muscle and staining for glycogen reveals white muscle fibers belonging to stimulated unit. Modified from Edström and Kugelberg (1968).

regard to histochemical fiber type—the innervating α-motor neuron is the main factor determining muscle fiber type and its attendant properties. Studies on felines have suggested that a single muscle contains hundreds of motor units, each unit containing an average of 400-800 muscle fibers, and the overlap of such units is such that any area of the muscle may contain 20-50 overlapping units (3,4).

Glycogen depletion studies are still the only method of directly observing the arrangement of muscle fibers of a motor unit. However, this is a destructive procedure and cannot be used clinically. EMG studies remain the most widely used tool for determining the characteristics of motor units in the clinical setting.

An estimate of the motor unit territory within human muscle and the arrangement of muscle fibers therein were determined by two groups using different EMG techniques. Buchthal et al. showed that the motor unit could be discovered anywhere longitudinally within a muscle using two multielectrodes inserted into the muscle at right angles as at least a portion of the muscle fibers of the motor unit ran completely from one tendon to the other (5). They showed that most motor unit territories are basically circular. Stålberg and Antoni used a single fiber electrode as a trigger source and a concentric needle electrode as a sampling electrode moved through the muscle at defined steps and thus determined the cross-sectional area and fiber distribution within the motor unit (Figure 1.3). It was determined that most motor unit territories fall between 5 to 10 mm in diameter. Both of these studies showed that fibers within the motor unit are not evenly distributed throughout.

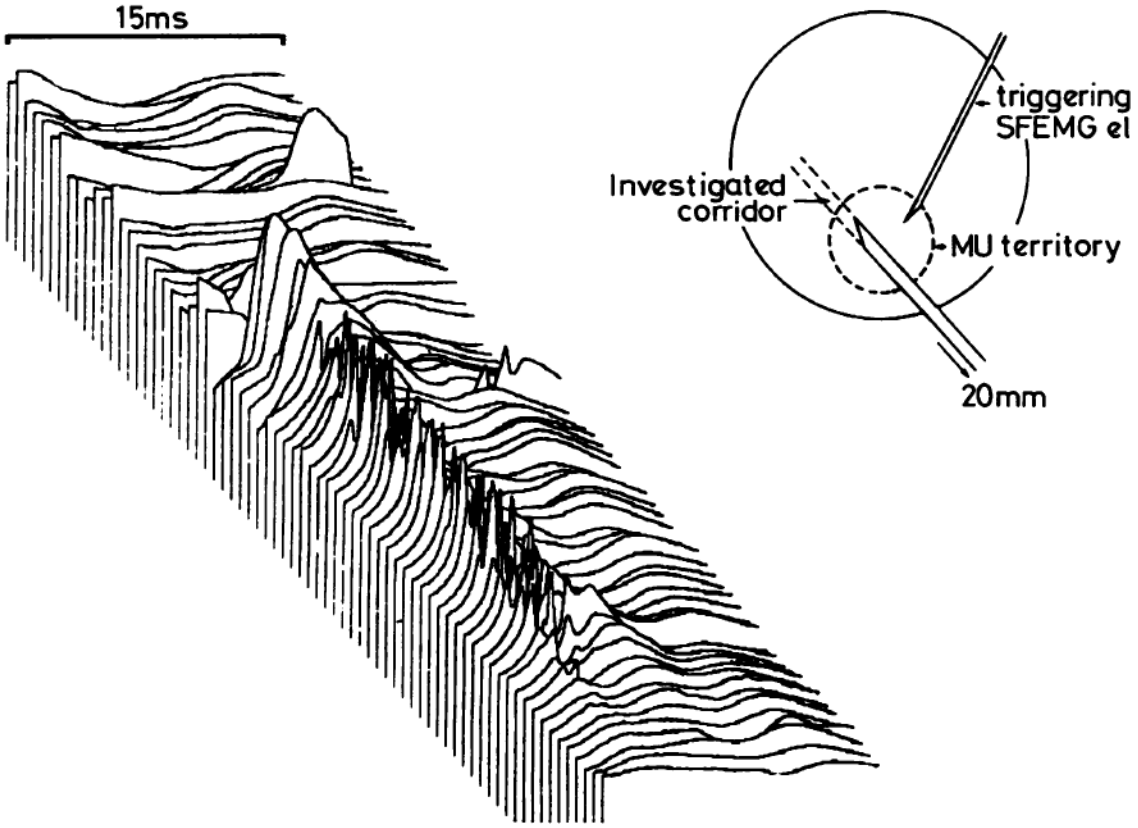

Figure 1.3: Scanning EMG study of a normal tibialis anterior muscle from Stålberg and Antoni (6). Of note, the resulting electrical potential varies greatly depending on the position of the electrode within the motor unit. The different action potential morphologies result from the spatial relationship of the needle to the nearest muscle fibers with a nonuniform distribution of muscle fibers within the motor unit.

Motor Unit Action Potential

The MUAP is the electrical view of the motor unit and consists of the combined potentials from all of the single muscle fiber action potentials within the uptake area of the electrode. Surface electrodes have a large uptake area. Intramuscular electrodes vary in size and hence uptake areas and yield a variety of restricted views of the electrical motor unit. In this regard, the electrode may be thought of as a probe and the muscle a

black box. This black box is unusually complex with respect to the number of motor units, the size of the motor units, the recruitment order with voluntary activation, and the arrangement of neuromuscular junctions. Further, the black box may be normal or abnormal due either to a neurogenic or myopathic process. In the clinical investigation the black box can be probed with a variety of electrode types whose position in the muscle and relation to fibers of the motor units is unknown to the investigator. We will deal with these issues in greater depth later in this section.

There are common metrics used to describe an MUAP waveform which include: peak-to-peak amplitude, duration, area, area-to-amplitude ratio, number of turns, and number of phases (shown in Figure 1.4). The metrics allow for quantitative statistics, and from clinical empiric experience, can help in distinguishing normal from pathologic muscle. Abnormal MUAPs exhibit characteristic features that, in combination with other clinical data, can confirm the diagnosis of a number of pathologic conditions. Initially, in the 1950's, motor units from normal subjects and those with known pathology were studied from photographs of the oscilloscope screen to quantify the range of metric values. It is from these laboriously collected data that qualitative interpretation of normal from abnormal motor units is determined during routine EMG studies. Normal values for these metrics differ among muscles and with age, and a sample recorded with a concentric needle electrode are shown in Table 1.1.

The concentric needle, monopolar needle, and single fiber needle are common intramuscular electrodes in clinical use (Figure 1.5). The concentric needle electrode consists of a stainless steel cannula, which acts as the reference electrode, and a central silver wire insulated from the cannula, which is the active electrode. The end of the

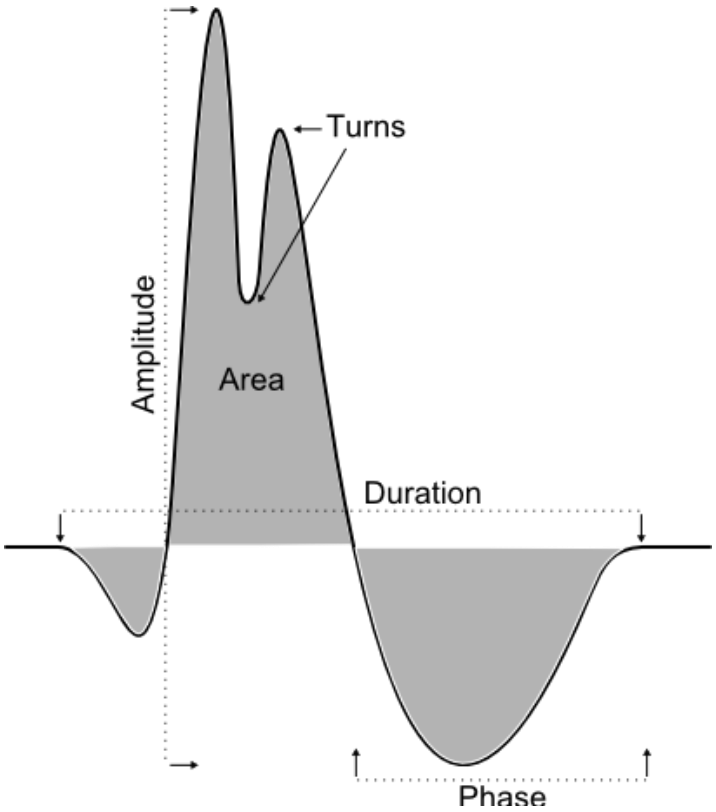

Figure 1.4: Common metrics obtained from motor unit action potential.

Table 1.1: Normal values for quantitative EMG studies recorded with a concentric needle electrode (7).

Mean values and standard deviations

	Amplitude (μV)		Duration (ms)		Area/Amplitude		Phases		Turns	
Muscle	Mean	SD	Mean	SD	Mean	SD	Mean	SD	Mean	SD
Deltoid	550	± 110	10	± 1.3	1.6	± 0.2	3	± 0.3	4.2	± 0.8
Biceps brachii	436	± 115	9.9	± 1.4	1.5	± 0.2	2.6	± 0.3	4.2	± 0.6
Dorsal interosseous (FDIH)	752	± 247	9.4	± 1.3	1.4	± 0.2	3.1	± 0.4	3.9	± 0.6
Vastus Lateralus	687	± 239	12	± 1.9	1.7	± 0.2	3	± 0.3	4.5	± 0.8
Anterior tibialis	666	± 254	11	± 1.2	1.7	± 0.2	3.2	± 0.3	4.7	± 0.9

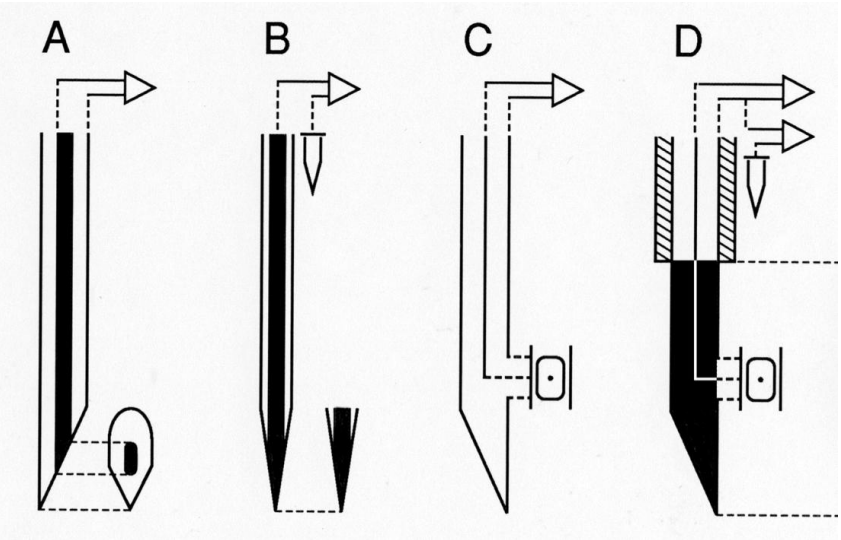

Figure 1.5: Representation of three different types of needle electrodes. A: concentric needle electrode—a solid conductive core is the active electrode which is insulated from the needle cannula that is used as the reference electrode. There are two sizes of concentric electrodes. B: monopolar needle electrode—a wire is insulated and the end tapered to a cone which is the active electrode and a separate electrode, often on the skin, is the reference electrode. C: single fiber needle electrode—a 25 μm insulated wire is brought out from the side of the cannula and is the active electrode and the cannula is the reference electrode. D: macroEMG needle electrode—longer single fiber EMG electrode with the distal 15 mm of the cannula uninsulated and used as recording surface. Figure modified from Bromberg 1993 (8).

standard sized needle is cut off at 15° to create an elliptical recording surface. There are practical limitations to concentric electrodes based on their stiffness and ability to pass through muscle and limitations to their recording uptake radius, resulting in two diameters for practical electrodes: the routine concentric electrode is a 26 gauge (0.46 mm diameter) needle with a recording ellipse of 580 x 150 μm (0.07 mm^2); and the pediatric concentric electrode is a 30 gauge (0.3 mm diameter) needle with a recording ellipse of 390 x 100 μm (0.03mm^2).

The monopolar needle electrode is an insulated straight wire electrolytically etched to an uninsulated conical tip that serves as the active surface. The reference electrode is a surface plate or disk electrode placed on the skin, preferably close to the intramuscular electrode to reduce extraneous intervening bioelectric noise. There are a several diameters of monopolar electrodes with the same limitations on electrode stiffness. They have different recording surface areas but there is less information available and basic studies have not been performed with monopolar electrodes.

The single fiber EMG needle electrode is based on the same cannula size as the routine concentric electrode but the active electrode comes out the side of the cannula 2.5 mm from the tip and is 25 μm in diameter. The cannula is used as the reference electrode. The macroEMG electrode is a longer single fiber EMG electrode with the distal 15 mm of the cannula uninsulated. The uninsulated 15 mm recording surface is large and can include all or most of a motor unit. Surface electrodes can record the entire motor unit and consists of two electrodes, the active generally placed over the belly of the muscle and the reference near either the insertion or origin of the same muscle.

The number of muscle fiber action potentials in the intramuscular MUAP recorded by the commonly used active electrodes depends upon the size of the active recording surface and the proximity to the muscle fibers. Except for the macroEMG electrode, the MUAPs recorded by concentric, monopolar and single fiber electrodes consists of relatively few individual muscle fibers of the motor unit. Concentric needle and single fiber electrodes were used in my studies exclusively. The uptake area from the standard sized concentric needle relative to the size of muscle fibers (average 50-60 microns) and their extracellular action potential voltages has been determined as the

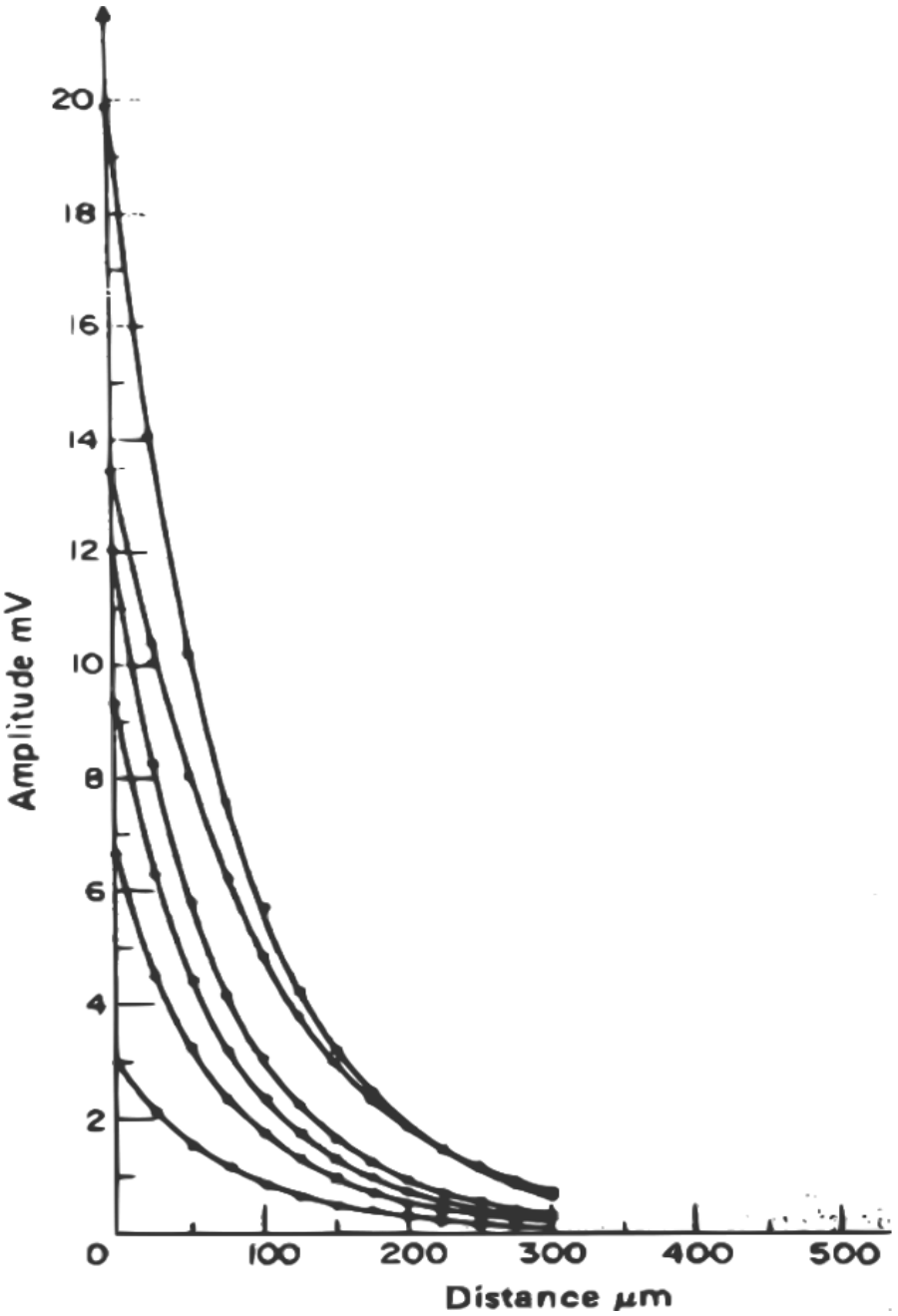

Figure 1.6: Decline of peak-peak amplitude as a function of distance of electrode from muscle fiber (11). A multi-electrode needle with an index active electrode used to measure the 0 µm by maximizing the action potential. Subsequent distance measurements were made using active electrodes along the axis of the needle with known distances between. Each line represents a different muscle fiber diameter. The difference in amplitudes at 0 µm from the muscle fiber is presumably due to differences in the muscle fiber diameter, but could be due in part to optimization of spatial orientation of the electrode to the muscle fiber.

distance where 90% attenuation in signal occurs, and is 350 μm from the electrode face, with negligible contribution from fibers beyond 500 μm (Figure 1.6) (9,10). In the setting of the density of muscle fibers within a motor unit this implies that perhaps only 2-4 fibers' action potentials will make up the largest part of the MUAP and overall only a mere 7-15 fibers will contribute to the waveform (Figure 1.7). As shown earlier, this is a very small portion of the fibers of a motor unit. Further, with random insertions of the electrode different portions of the motor unit will be sampled resulting in different waveforms due to the nonuniform distribution of muscle fibers within the motor unit. In addition, small movements of the electrode will change the contours of the MUAP.

Intramuscular electrodes are a blind probe of the motor unit. As mentioned above, the nearest several fibers make up the largest contribution to the shape of the

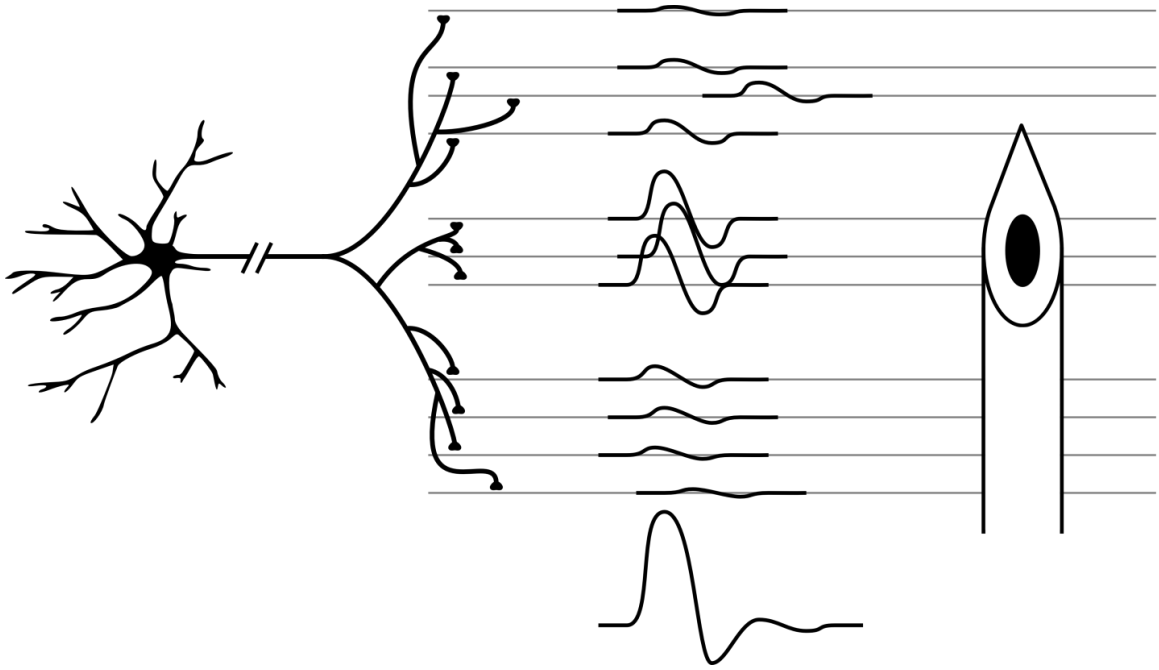

Figure 1.7: Schematic representation of the individual muscle fiber action potentials in relation to proximity to the recording electrode and the MUAP that results.

MUAP. These two facts mean that there may be considerable variability of the MUAP from the same motor unit depending upon the chance placement of the electrode (Figure 1.8). This blind approach dictates that many MUAPs must be recorded and statistically analyzed to achieve a representative estimate of muscle fiber architecture. A typical QEMG study requires the measurement of 20 separate MUAPs with no further change in metrics with the collection of additional MUAPs (12,13).

Currently there is no technique that allows for the reliable and clinically practical measurement of all muscle fibers of a sufficient number of motor units at one time. Because of attenuation MUAPs recorded from surface electrodes are very small and their size varies with their depth. Further, there is little or no selectivity with overlapping motor units. Intramuscular electrodes minimize the overlap of unit potentials due to

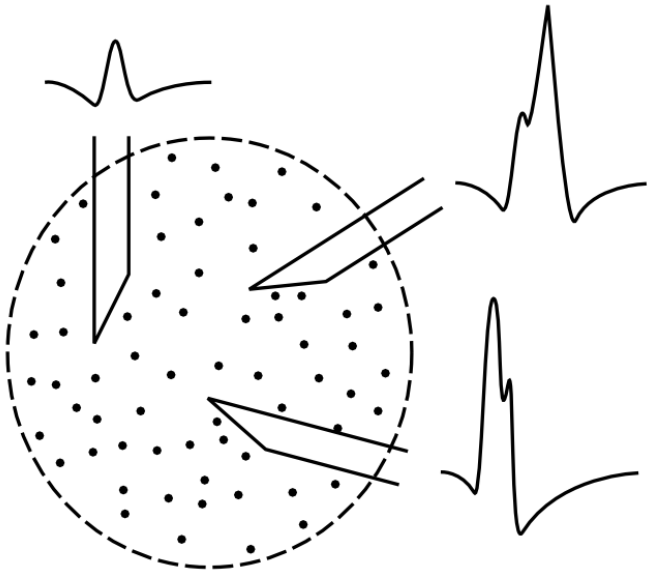

Figure 1.8: Schematic representation of various MUAPs of a single motor unit. The proximity of the active electrode surface to the nearest muscle fibers dictates the shape of the resulting MUAP. Therefore, many different MUAP morphologies can be represented from the same motor unit.

limited uptake areas and thus pick up potentials from fewer motor units. By positioning the concentric electrode nearer the muscle fibers the potentials are also larger, although the number of fibers contributing to the potentials is a very small percentage of the full motor unit. The single fiber electrode reduces the number of fibers contributing to the potentials measured, but also reduces the clinical usefulness of the information collected. Reducing the electrode size even farther would allow for truly single fiber measurement or even intracellular measurement—although this would be of little use in clinical decision making. We will discuss later, in the section about pathologic changes in the MUAP, why the concentric and monopolar needle provide the most appropriate mix of information for clinical studies, balancing selectivity and comprehensiveness.

Changes in the MUAP due to nerve injury: neuropathic motor units

Nerve injury leaves muscles with varying degrees of denervation. In cases of incomplete injury of the nerve supplying a muscle the orphaned muscle fibers regain neural control through collateral sprouting of remaining nerve terminal branches (14). This is the process whereby remaining α-motor neurons create new intramuscular sprouts either from a node of Ranvier or near the neuromuscular junction.

The degree of retained motor control and strength depends upon the extent of loss of nerve fibers and the time course of loss, monophasic or progressive (slowly or rapidly). The effect of collateral reinnervation is increased likelihood that muscle fibers from the same (reinnervating) motor unit will be adjacent or closer together than occurs normally (15-18). As a consequence, when there are even one or two more muscle fibers

within 500 μm of the recording face of the electrode both amplitude and area of the MUAP can increase measurably (Figure 1.9). In extreme cases where very few motor neurons remain, a single α-motor neuron might innervate every muscle fiber within the uptake area of the needle electrode. The pathologic marker of collateral reinnervation is fiber type grouping. The degree of collateral reinnervation of a motor unit is limited; the fiber density increases the radial territory (area) is limited to the original boundaries imposed by muscle fascicles resulting with extreme loss in areas of muscle with many permanently denervated muscle fibers.

New axonal sprouts may be smaller in diameter and have less myelination causing slower transmission of the depolarizing signal along terminal branches. This can mean that some muscle fibers of a motor unit will depolarize somewhat later than other fibers

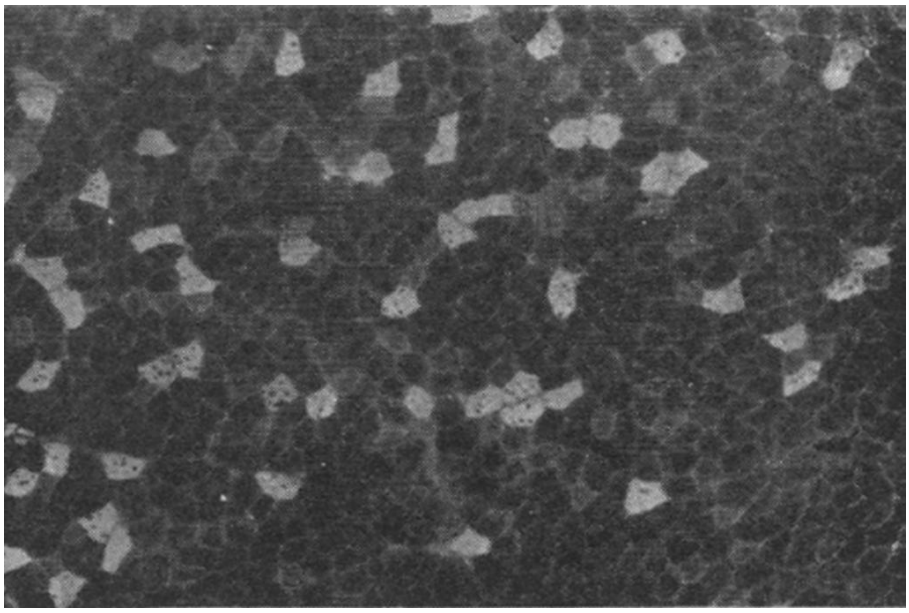

Figure 1.9: Glycogen depletion study in the rat after partial crush of the sciatic nerve showing the effects of collateral reinnervation. Note that there are many more immediately adjacent fibers than in the normal muscle (compare to Figure 1.2). Adapted from Kugleberg (16).

of the motor unit. In addition, muscle fibers will atrophy after denervation and will conduct muscle fiber action potentials more slowly from the neuromuscular junction to the recording electrode and arrive later than their normal counter parts. When one fiber within the uptake area of the electrode depolarizes at a different time than others it can be seen as an additional peak in the MUAP. The delay seen is inconsistent due to normal variability of alpha motor neuron discharge patterns and the changes in muscle fiber conduction velocities associated with the discharge variability, a phenomenon called velocity recovery function (19). These factors affect the MUAP waveform and result in increases in the number of turns and sometimes increases in the number of phases and a degree of waveform variability from discharge to discharge (see Figure 1.10). Higher than normal number of turns (polyturn; >5 turns) and phases (polyphasic; >four phases)

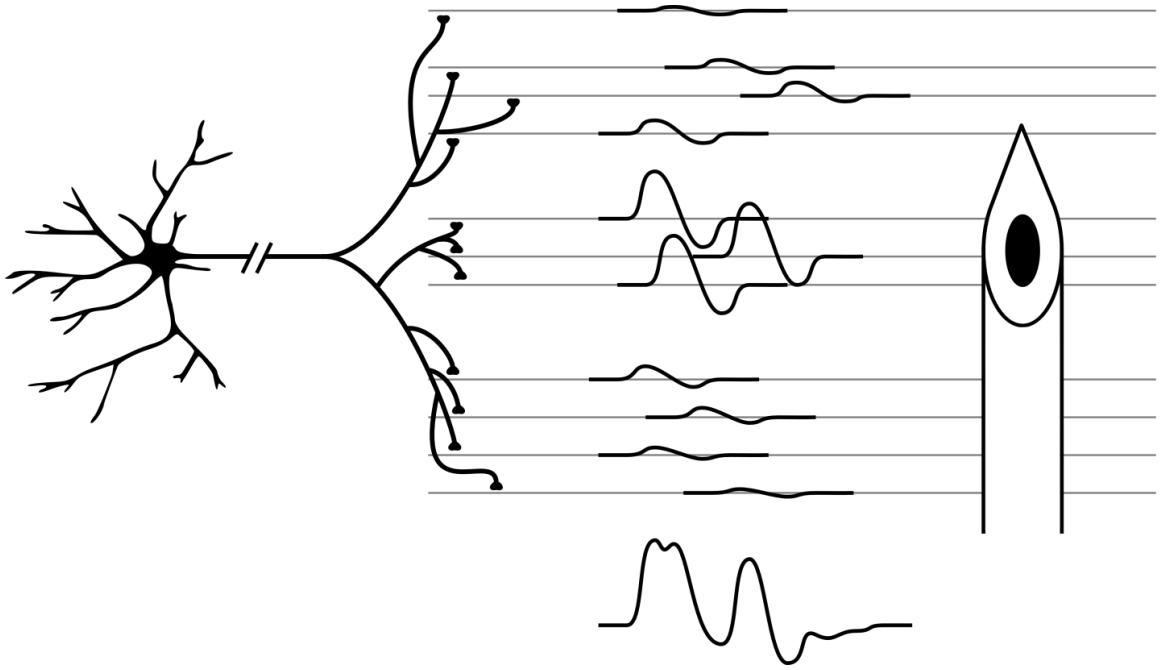

Figure 1.10: Schematic representation of individual muscle fiber action potentials from atrophic/reinnervated unit in relation to proximity to the recording electrode and the polyturn/polyphasic MUAP which results (compare with Figure 1.7).

is often called increased MUAP complexity, and suggests that there is some degree of nerve injury in the recent past with active reinnervation. However, polyturn/polyphasic phenomenon can also be seen in myopathic processes, which will be dealt with in the next section.

Additionally, newly sprouted nerve terminals and neuromuscular junctions may not have the same robust synaptic connections with the muscle fiber as more established neuromuscular junctions. The acetylcholine receptor is composed of five subunits and with reinnervation the normal gamma subunit is initially replaced by an epsilon subunit that imparts slower and less reliable receptor channel openings (20). When postsynaptic receptors are developing on reinnervated fibers, signals across the neuromuscular junction may be insufficient to cause propagating depolarization of the muscle fiber membrane, which is called transmission blocking. Signals may not block but transmission can be slowed (measured in microseconds and called "jitter" at the neuromuscular junction level). Both of these can lead to discharge to discharge variations in muscle fiber action potentials that contribute to the MUAP. The summed variations in transmission in the MUAP waveform is called "jiggle" and is an important EMG finding that support the diagnosis of ongoing denervation and reinnervation (21). Over time, postsynaptic receptors revert to more secure forms (gamma subunit in place of epsilon subunit) and transmission becomes more stable and jiggle is reduced.

When consideration is given to MUAP metrics of amplitude, area, and complexity a reliable estimate can be made of whether there is a high likelihood that an abnormality is due to nerve injury. For example, very high amplitude MUAPs with normal complexity indicates remote nerve injury with sufficient time for stable reinnervation.

Normal or very slightly increased amplitude with increased area and complexity and jiggle indicates relatively recent injury with new and active reinnervation. Low amplitude can mean that the electrode is not near enough to fibers from the motor unit, or that there has been denervation without reinnervation and subsequent reduced numbers of muscle fibers. In routine EMG studies these factors are weighed in a subjective manner. However, knowledge of the changes in the various metrics and their implications are based on quantification of metrics and correlations with clinical states.

Changes in the MUAP due to muscle fiber injury: myopathic motor units

Muscle fiber injury changes the MUAP without necessarily changing the relative cross-sectional position of muscle fibers in the motor unit. Many different diseases of muscle cause changes in the MUAP, including: inflammatory myopathies, metabolic myopathies, inherited dystrophies, and membrane disorders (channelopathies). These conditions result in changes to muscle fibers but the number of nerves reaching the muscle remain normal. The MUAP is affected in the following ways.

In cases of inflammatory myopathy the initial insult is often immune mediated, activating the body's immune system to degrade and destroy the muscle fiber at segmental sites along fibers. This leads to smaller diameter and less uniform muscle fibers (22). As propagation of the depolarizing signal is dependent on the radial diameter of the muscle fiber, if different fibers of the same unit have a range of diameters they will propagate signals at different rates. This can, in the extreme, lead to an MUAP where the action potential of each contributing muscle fiber is clearly differentiated from the others.

In other words, there is decreased overlap of individual muscle fiber action potentials. This phenomenon causes decreased MUAP amplitude, due to a lack of constructive interference, and increased waveform complexity (23).

In some myopathies damage to a muscle fiber is severe enough at a single point along its length that the fiber is no longer electrically contiguous. Loss of propagation of this muscle fiber action potential reduces the amplitude of the MUAP when recorded beyond the point of the damage. This leaves the distal segment of muscle fiber electrically denervated. Fiber atrophy occurs in this segment and it often is destroyed. However, with control of the inflammatory disease process repair is made and the distal segment is reanastamosed with the intact portion of the fiber. This will allow for propagation along the full length of the fiber, though it will be slower through the atrophied portion. This causes decreased amplitude and increased complexity as described earlier.

In general, MUAPs from myopathic units can be differentiated from normal units in their relatively low amplitude and markedly increased complexity. While increased complexity occurs in cases of neuropathic damage, the amount of complexity is generally far less than is the case from a myopathy. Also, myopathic units are generally smaller in amplitude and area than normal while neuropathic are almost always larger in both metrics. Though this is generally true, there is a lot of overlap of the distributions of MUAP metrics for normal and diseased states—thus the need for quantitative EMG studies which can more sensitively tease out the differences. Examples of changes due to the different pathologies are shown in Figure 1.11.

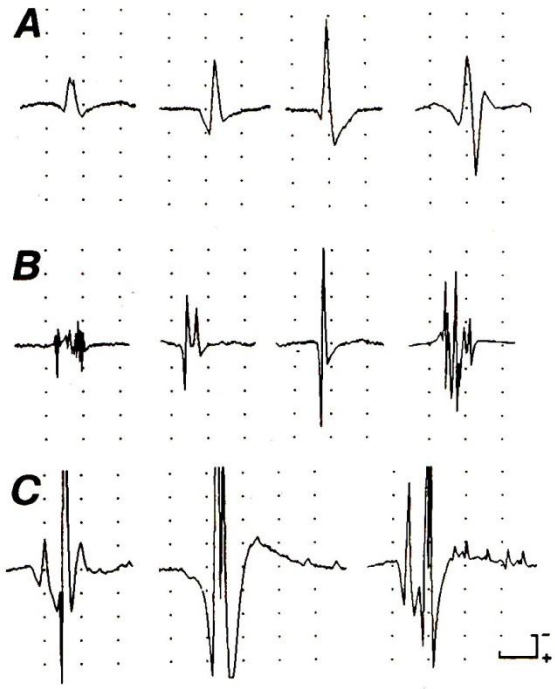

Figure 1.11: Examples of different characteristic MUAPs. Note that these are photographically isolated MUAP waveforms whereas during routine EMG studies there is a train of MUAPs discharging at different rates with overlap of waveforms leading to the possibility of "apparent" complexity. Row A: stereotypical MUAPs from normal muscles. Row B: MUAPs from myopathic muscles. Note that these are markedly more complex than the normal MUAPs, but that their amplitudes and areas are not comparably increased. Row C: MUAPs from neuropathic muscles. Note that these also show markedly increased complexity as well as much increased amplitudes (clipped in figure) and areas.

Single fiber EMG

Single fiber EMG is a set of techniques which use a special single fiber electrode to obtain unique information about the muscle and pathology that cannot be obtained otherwise. Due to the 25 μm diameter active recording surface and effective up take radius of less than 300 μm this electrode records from only one to three muscle fibers of a motor unit at a time (24).

One of the important studies performed with a single fiber electrode is determination of fiber density. This is done by positioning the active electrode as close as possible to an active muscle fiber—determined by a single muscle fiber action potential of greater and 200 μV amplitude and leading edge rise time of less than 300 ms. When these criteria are met the waveform is examined for evidence of additional muscle fiber action potentials—most commonly a second peak (example shown in Figure 1.12). The number of muscle fibers within the uptake radius of the electrode is recorded for that site, and the process is repeated until a total of 20 sites are sampled. The fiber density is an empiric number and provides information as to the packing density of muscle fibers in motor units. While an increased fiber density is suggestive of neural degeneration with

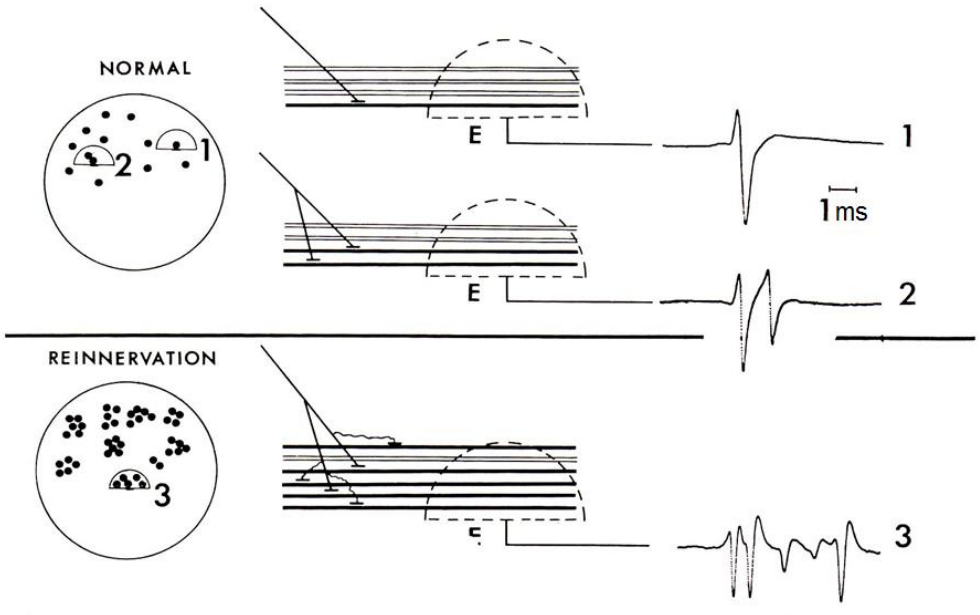

Figure 1.12: Schematic representation of fiber density study using a single fiber EMG electrode. The semicircle represents the 300 μm uptake area. In normal muscle one or two fibers at a single sight may be recorded. In reinnervated muscle many more may be recorded at one site.

reinnervation it can also be observed in myopathic disorders due to loss of muscle fibers and greater closeness of remaining fibers.

We have shown the characteristic changes which are common to the various categories of pathology measured with intramuscular electrodes. Changes in motor unit amplitude cannot be distinguished with surface or single fiber electrode. Using a surface electrode does not allow for the distinction between either small or large amplitude units because the size of the unit measured from the surface is due to the proximity of the motor unit to the electrode rather than the remodeling of the motor unit architecture as measured intramuscularly. Single fiber electrodes also fail to register changes in motor unit amplitude as they record from, at most, a few fibers and so sensitively that there is rarely constructive overlap of the fiber potentials. Increased MUAP complexity is also difficult to ascertain with surface or single fiber needle electrodes. The complexity in surface potentials is completely obscured by the overlap of many small and low frequency potentials contributing. Single fiber is somewhat more sensitive to complexity, but is limited by the number of fibers in the uptake area. Single fiber EMG can see increased complexity, which is the purpose of a fiber density study, but cannot distinguish complexity differences between myopathic and neuropathic processes as the larger concentric or monopolar needles can.

Frequency space of EMG signals

Frequency spectra of interference patterns and EMG signals are dependent on a number of factors. For individual action potentials the frequency spectrum is dependent

on the proximity of the active face of the electrode to the nearest muscle fibers. When the electrode is close to a muscle fiber the high frequency components will be more pronounced (25,26). Muscle tissue acts as a low-pass filter, filtering out higher frequency components more effectively as distance from the source increases (26,11,27). This is due to the impedance of charged molecule movement through the tissue. In a volume conductor there is no voltage without current, and current is impeded in muscle by various forces. There is natural impedance of ionic fluid, which is far more complex in the biologic environment from increased viscosity due to proteins, cellular and extracellular structural architecture. Cell membranes and connective tissue also impede the movement of ions. The nearness of the electrode to an action potential source (muscle fiber or fibers) can be judged by a rapid rise time of MUAP indicating high frequency components in the waveform.

Individual motor unit action potential frequency spectra will depend largely on the overall duration of the potential. Low frequency components will dominate if there is any significant portion of relatively flat baseline included in the analysis (see Figure 1.13). This is also true of interference pattern (sum of many motor unit action potential trains) frequency spectra (see Figure 1.14). When fewer motor units are recruited greater portions of the signal are at the low end of the spectrum. A fully activated muscle will exhibit a shift toward higher frequencies due to the lack of free baseline, though there is still a relatively smooth continuum of frequencies represented. Near the high end of the frequency spectrum the largest influence is the proximity of the electrode to the nearest active muscle fiber.

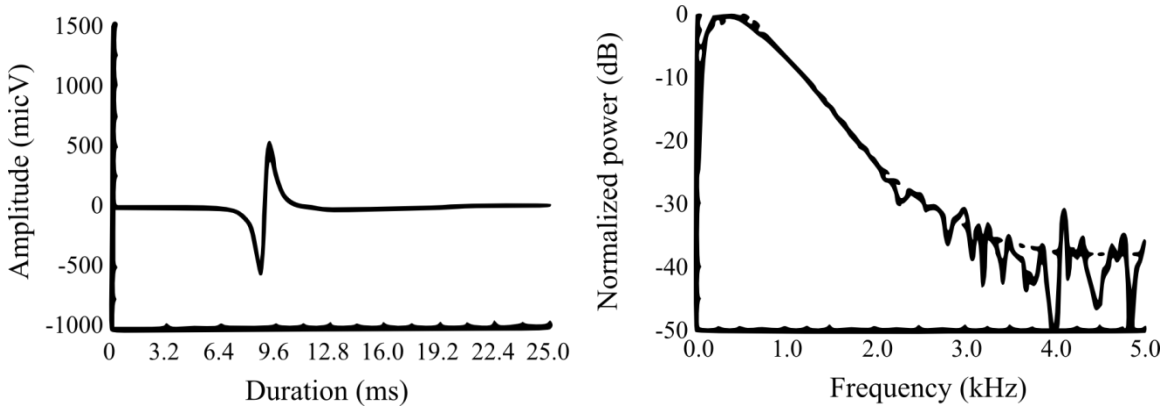

Figure 1.13: Sample MUAP with the corresponding fast Fourier transform spectral analysis. Modified from Pattichis (28).

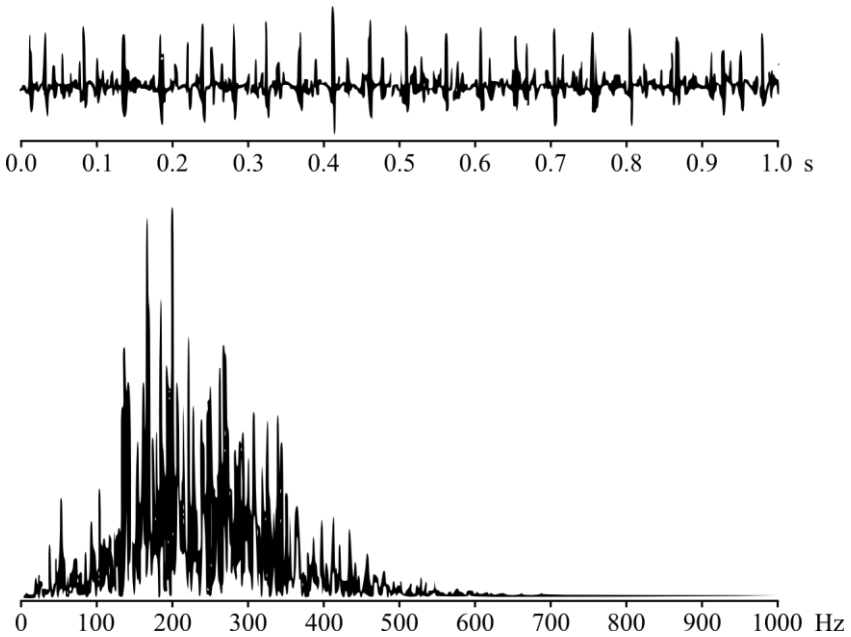

Figure 1.14: Time (upper) and frequency domain (lower) traces of 20% isometric contraction from biceps brachii muscle. Modified from Duchêne (29).

EMG Studies

EMG is used in a variety of settings, from clinical neurology and physical medicine and rehabilitation to academic research laboratories to visualize and quantify the activity of motor units. The studies included in this work focus on determining factors that influence the physiologic recording and algorithmic processing of the signals to make QEMG more applicable and more easily used in the clinical setting.

Clinical EMG

Clinical EMG studies are generally performed as part of a suite of electrodiagnostic studies to help arrive at a diagnosis of a disorder affecting the peripheral nervous system. Electrodiagnostic studies are unique clinical tests in that the clinician is actively involved in designing what tests will be performed and performs the tests him/herself, in contrast to, for example, imaging studies or electroencephalographic (EEG) studies, that are performed by technologists and interpreted at a later time by physicians. For electrodiagnostic studies, the clinician interviews the patient to clarify the clinical question and then performs a focused neurologic examination. From this information the appropriate tests are selected. Nerve conduction tests that can assess the function of sensory and motor nerves are usually performed first. The clinical EMG study focuses on the motor system. It is performed by a physician using a needle electrode which is inserted into the patient's muscle, or muscles, of interest. The clinician will listen to the amplified sound that the waveforms produce as well as watch the waveforms on the computer monitor (equivalent to a cathode ray oscilloscope). Of

note, listening to the waveforms is a sensitive means of distinguishing differences in amplitude (loudness) and complexity (splitting of sound components). However, this is qualitative with the high chance of over-recognition of rare events (loud and complex MUAPs). Once the clinician has obtained the desired information at a single site, the needle is repositioned a number of times within the muscle to examine a different group of muscle fibers and motor units. As with listening to motor units, there are statistical issues as not all areas of muscle are similarly affected by pathologic processes and a suitable sample must be obtained. Most important for the advantages of QEMG, abnormal MUAPs will be admixed with normal MUAPs, and a suitable sample size is necessary to avoid false positive and negative interpretations. Many EMG studies require examining several muscles, repeating the process described.

Clinical EMG studies are performed by clinicians who have been trained to recognize normal signals and differentiate them from abnormal. The patterns of abnormality discussed above are often very obvious to the clinician, who can then use this data to arrive at some clinical conclusion. Of note, the well trained ear can distinguish very subtle differences in MUAP waveform components, including component frequencies, changes in complexity (number of phases and turns), differences in timing of components (jiggle), and overall discharge rates. If, however, the EMG exhibits only mild abnormality there can be ambiguity for even an experienced clinician. Thus there is a need to increase the sensitivity of the studies performed in the clinic.

Quantitative EMG

Basic mechanics of QEMG analysis

QEMG is a term that broadly describes any of a number of techniques that attempt to quantify some aspect of the EMG signal. This body of work deals with quantitative multi-MUAP analysis. In the early days of EMG studies many attempts were made to quantitatively measure the waveforms, but were extremely tedious and time consuming. The earliest quantitative studies were performed by photographing waveforms from an oscilloscope and were measured by hand using calipers. This provided the MUAP data upon which qualitative EMG studies are based, but are not practical for anything but research purposes. Modern computing has made the QEMG study possible in a time domain that makes the analysis practical and also allows for determination of derived metrics such as waveform area and area-amplitude ratio, assessment of jiggle and fiber density.

QEMG focuses on the identification of individual MUAPs from a weak interference signal that includes the activation of several motor units. These techniques are called multi-MUP (for multiple motor unit potential analysis) or decomposition EMG techniques, based in part on different algorithmic approaches. The signal containing many MUAPs is most often analyzed using template matching (30-34). The different MUAPs are characterized and compared to determine if each recurring discharge is likely to belong to a single motor unit or several.

Template matching is performed by assigning an identifier to each extracted waveform isolated from baseline. After these waveforms are identified they are compared to each other to attempt to match them based on similar metrics and matching

morphologies. If a waveform is sufficiently similar, it is assumed to originate from the same motor unit (see Figure 1.15).

This determination is strengthened by analyzing the discharge pattern of the motor unit. Normal physiologic activation of motor units falls within a range of frequencies from approximately 8-20 Hz during a moderate contraction (35,36). During maximal contraction, which produces an interference pattern that is too complex for QEMG studies at this point, the motor neuron can fire with bursts of 60-140 Hz (37). This relatively regular motor unit firing pattern, during moderate contractions, allows for predicting a time window during which the same motor unit would be expected to discharge. Some algorithms exclude all waveforms that occur sooner than expected from

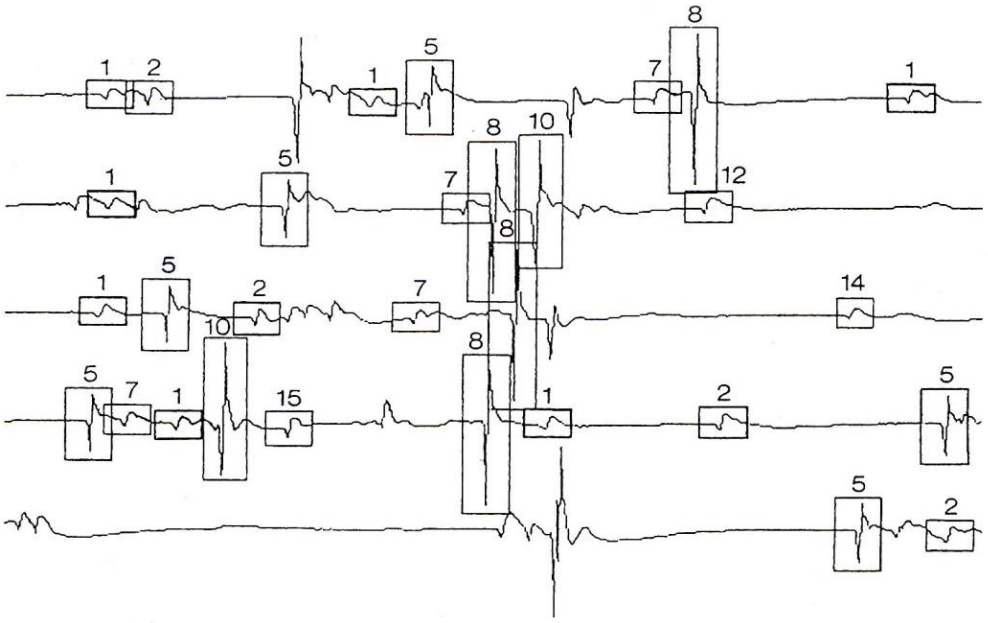

Figure 1.15: Stylized example of decomposition using template matching (32). In this drawing, recurring MUAPs are assigned an identifier while non-recurring waveforms are not—they are assumed to be several MUAPs overlapping.

the previous discharge due to the fact that it is extremely unlikely to be physiologically stimulated at such a close interval.

Once grouped into sets of similar waveform shapes, the many discharges of the various MUAPs are respectively averaged to remove random electric and physiologic noise. Averaged MUAPs are then automatically measured for each of the metrics of interest. Waveform marking is performed by algorithms that first indentify the onset and termination times of the MUAP. Once these two points are set, amplitude, area (and derived metrics such as area/amplitude ratio), and number of turns and phases is fairly straightforward. There are different approaches to identifying the onset and termination (Figure 1.16), and small variations in threshold settings can markedly affect the results (12). Generally accepted practice is to collect a number of trains of EMG signal in order to obtain a minimum of 20 averaged MUAPs for statistical rigor (38).

Advantages of QEMG

Quantitative EMG can become a more consistent and sensitive tool than the qualitative clinical EMG study. In most pathologic conditions the distinguishing motor units are in the minority (Figure 1.17). Subtle differences can be discovered in the QEMG study that may be overlooked in a qualitative study. Conversely, given the bias of the clinical exam, a qualitative study may overstate or understate any perceived abnormalities inappropriately where a QEMG study will not be biased.

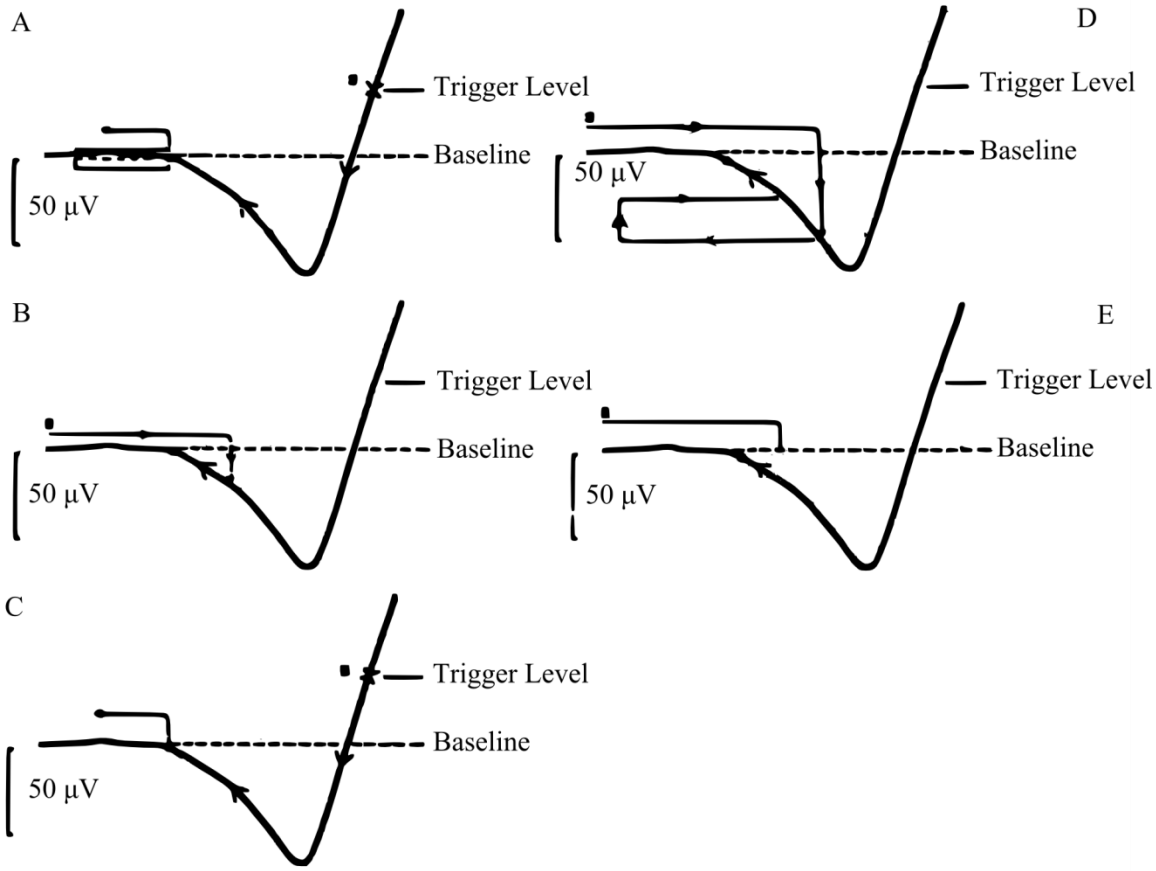

Figure 1.16: Various algorithmic methods for marking onset of MUAPs (12). Each example shows a trigger level which initiates the search for the initial excursion from baseline where the initial duration marker will be set. Methods A, B and C each work backward from the site of waveform onset to ensure that no earlier waveform component exists. Methods D and E work forward from some point a set distance far in front of the trigger to catch the earliest waveform component. Small changes in the values used in any of these algorithms result in large differences in the resulting placement of duration markers.

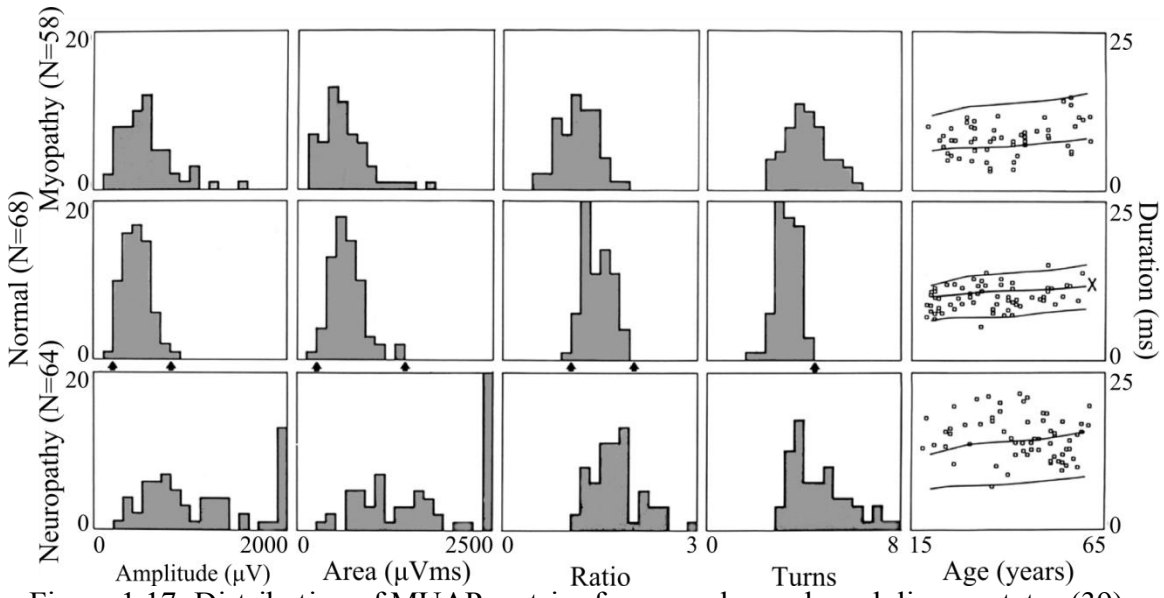

Figure 1.17: Distribution of MUAP metrics for normal muscle and disease states (39). The figure shows clearly that there is significant overlap of metrics measured and it is the outlying values that help to distinguish the pathologic from normal muscles.

Practical issues

Currently, very few clinicians use QEMG as part of their daily practice. The reasons range from ignorance of the techniques or lack of software to perform the analysis to dissatisfaction with the extra time the quantitative studies require. Though QEMG does legitimately take longer than a routine clinical examination, with refinements in the algorithms the time required is decreasing and will soon be only minimally longer.

Patient discomfort (and hence tolerance to the study), though not the primary consideration in any medical procedure, is important. Clinical observation shows that there is a full spectrum of pain and anxiety associated with EMG studies. An advantage of QEMG is that an informative study can be performed by investigating a few key muscles.

EMG machines, like all medical devices, require approval through the FDA. This means that each new component of the system, either hardware or software, requires an approval process which is lengthy and expensive. Therefore, if a component of the system could be improved there would have to be some financial incentive for the manufacturer to go through the process of development, testing, and approval before it would be available to the clinician. This argues for the improvement of QEMG techniques using tools readily available within the existing EMG systems so that such improvements can readily be employed broadly.

2 RATIONALE FOR THE WORK AND TECHNIQUES EMPLOYED

Bringing QEMG to the clinical laboratory is the ultimate goal for most investigators involved in the development of algorithms and new techniques. However, those who develop the algorithms are generally computer scientists, programmers, and basic scientists. Thus, there are many issues in the clinical realm not appreciated or identified and left unresolved. Without direct clinical experience the practical importance of certain aspects of QEMG may be inappropriately inflated or minimized. We can bridge this gap because of our experience in the clinic and background in physiology, engineering and biomedical research. We have explored some clinically practical problems from an engineering perspective.

The following studies address practical and theoretical questions that arose from clinical use of QEMG techniques and different algorithms. 1) MUAP detection algorithms are empirically based and some algorithms seemed more efficient than others: however, we found no such comparison in the literature, and thus we performed a comparison study to determine the performance of each. 2) Measurement of fiber density requires a special single fiber electrode and we investigated whether the same information could be obtained using simpler and more accessible QEMG techniques. 3) Basic physiology of signal propagation led us to investigate possible diagnostically significant differences in MUAP morphology when recorded near and far from the site of

the signal initiation (neuromuscular junctions). 4) There are two sizes of concentric needle electrodes available and the smaller size has been used for studies of neuromuscular jitter, and thus we studied whether there were significant differences with respect to MUAP metrics between the standard and smaller sizes to determine if the spectrum of QEMG could be expanded with the use of one electrode. 5) Recording conditions change over data acquisition time due to physiologic and adventitious movements of the patient and operator and we sought to determine the effects on signal stability on the time trying to keep the needle electrode in one position within the muscle.

In the following sections we also lay out the basic techniques used for each study. A more detailed description of the methods is found in the individual publications, though we also include additional information not found in the articles due to space restrictions.

Algorithm Comparison

A number of different computer algorithms are available on commercial and research EMG machines intended to perform QEMG studies and we undertook a study to evaluate these algorithms' efficiency and accuracy. The algorithms are proprietary and specific to the EMG machine. Heretofore there has been no direct comparison to guide the selection of an EMG machine. Since QEMG provides statistical data it offers the possibility of more sensitive analysis and comparison of data from different clinics. This can only be realized if the performance of the data collection devices is comparable. In this study we evaluated three different algorithms, two commercial and one in

development (that was soon after commercialized) against simulated signals and biologically obtained EMG signals (40).

We tested the algorithms, one against another, using biological signals because this is the intended use. We brought all three EMG machines together and split the signal from the electrode three ways to allow each machine to capture the exact same data. We could not obtain input impedance values from the manufacturers of the various machines, but did determine that there was little or no decrement of the signal when multiple machines were connected. We collected data from normal (healthy) muscles, and muscles from a patient with amyotrophic lateral sclerosis (a neurogenic condition). We felt it important to include a range of MUAP morphologies to more fully test the algorithms.

Each of the machines was also fed simulated data (trains of simulated MUAPs) so that we could compare their performance against a set of known values. We sought to create as realistic a test as possible. First we created simulated MUAPs by recording from a variable power supply through an analog-to-digital converter. The waveforms were produced by manually adjusting the output of the power supply over time. The resultant waveforms were imported into MATLAB (MathWorks, Natick, Massachusetts) and adjusted to even more closely mimic biologic MUAPs. Twenty-eight different waveforms were selected that were similar to naturally occurring MUAPs, and each was analyzed to determine standard metrics. They were mixed together in various combinations.

Simulation of a normal interference pattern required that we mimic discharge frequencies of each individual motor unit independent one from another. From each

MUAP a train of discharges was created. The mean frequency of discharge is known to be 8-15 Hz for healthy muscle (41). There is a nearly normal distribution of actual frequency variation around these central frequencies. We chose a single central discharge frequency for each of the simulated MUAPs and used a normal random number generator in MATLAB to create variability of the interdischarge interval. Each of the resulting distributions of discharge intervals was then compared with biologic data. The distributions were statistically similar to biologic data. Each train, consisting of the firing of a single MUAP repeatedly over 30 seconds, was saved and combined to make interference patterns.

The creation of interference patterns, the signal resulting from several MUAPs discharging near the electrode, was accomplished by simply adding several of the previously created trains together. These voltages are known to add algebraically. This resulted in a realistic interference pattern where many discharges of each of the MUAPs had free baseline on either side and occasional overlapping of one or more MUAPs resulting in both constructive and destructive interference, creating a unique waveform that did not recur repeatedly in the interference pattern. The interference patterns were played back as if a routine clinical examination were performed and we determined that they were virtually indistinguishable from biologic data. Figure 2.1 shows a simplified illustration of the process used with the simulated data. The obvious advantage of the simulated interference patterns in the algorithm comparison is that the precise number of MUAPs and their metrics are known.

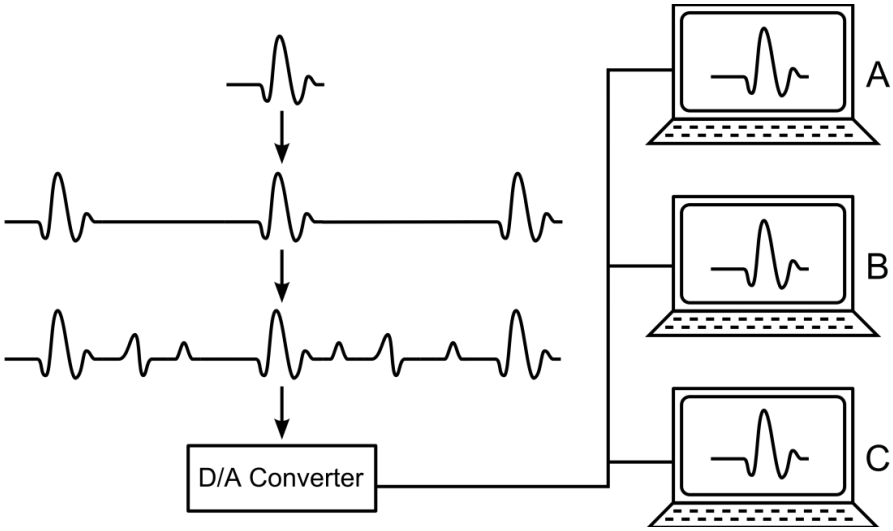

Figure 2.1: Illustration of how single MUAPs are incorporated into trains of single MUAPs then full interference patterns which are then presented to the different EMG systems.

Comparison of Three Algorithms for Multi-
Motor Unit Detection and Waveform Marking

Reprinted with permission from Muscle & Nerve 33: 538-545

ABSTRACT: Quantitative EMG (QEMG) techniques include automated motor unit action potential (MUAP) detection and marking of clinically useful waveform metrics. Different computer algorithms are available on modern EMG machines to perform these operations rapidly. However, the efficiency and accuracy of available algorithms are rarely directly compared. We have assessed three commercially available algorithms using both synthesized and biologic interference patterns and found differences among algorithms, some of which are clinically significant. Our results point out the importance of assessing for duplicate MUAPs (same waveform detected as two separate waveforms) and accuracy of markings used to determine MUAP metrics.

Muscle Nerve **33:** 538–545, 2006

COMPARISON OF THREE ALGORITHMS FOR MULTI-MOTOR UNIT DETECTION AND WAVEFORM MARKING

ALEXANDER A. BROWNELL, BS,[1] OLIVER NI, MD,[2] and MARK B. BROMBERG, MD, PhD[2]

[1] Department of Biomedical Engineering, University of Utah, Salt Lake City, Utah, USA
[2] Department of Neurology, University of Utah, 50 North Medical Drive, Salt Lake City, Utah 84132, USA

Accepted 27 October 2005

Quantitative EMG (QEMG) can be valuable in diagnosis and in tracking the progression of muscle and nerve disorders that may not be possible easily with routine qualitative EMG. The utility of QEMG lies in its objective and detailed data that can be compared to population values.[7] QEMG, defined herein as motor unit action potential (MUAP) isolation and quantitative assessment of waveform metrics (multi-MUAP analysis), relies on software that automatically performs three major functions: extraction of constituent MUAPs from an interference pattern (IP); averaging trains to obtain representative MUAP waveforms; and marking points on the waveform to determine and calculate various metrics of the extracted MUAPs. Algorithms differ among EMG machine manufacturers and are proprietary. The ability of these algorithms to accurately detect and mark MUAPs is assumed by the electromyographer, but issues of accuracy are infrequently discussed[5] and rarely directly tested.[2]

We have assessed and compared three sets of algorithms available on different EMG machines. Assessment of MUAP detection was made by two methods. We synthesized trains of MUAPs and combined them to simulate a number of IPs in order to assess the ability of the algorithms to identify known constituent MUAPs. We have also presented a variety of biologic IPs simultaneously to each EMG machine and compared how many MUAPs each algorithm could detect. Accuracy of MUAP marking algorithms for waveform metrics was assessed on both synthesized and biologic IPs.

Abbreviations: ALS, amyotrophic lateral sclerosis; CCC, concordance correlation coefficient; D/A, digital to analog; EMG, electromyography; IP, interference pattern; MUAP, motor unit action potential; MUAPT, motor unit action potential train; QEMG, quantitative electromyography

Key words: electromyography; EMG simulation; motor unit action potential; motor unit action potential waveform marking; quantitative electromyography

Correspondence to: M. Bromberg; e-mail: mbromberg@hsc.utah.edu

Published online 28 December 2005 in Wiley InterScience (www.interscience.wiley.com). DOI 10.1002/mus.20490

MATERIALS AND METHODS

We compared three commercially available EMG machines (labeled A, B, and C) with QEMG software packages that included algorithms to detect, isolate, average, and mark MUAPs. Default settings were used.

MUAP Modeling. The primary program for simulating IPs was MATLAB (MathWorks, Natick, Massachusetts). Individual MUAP waveforms were created

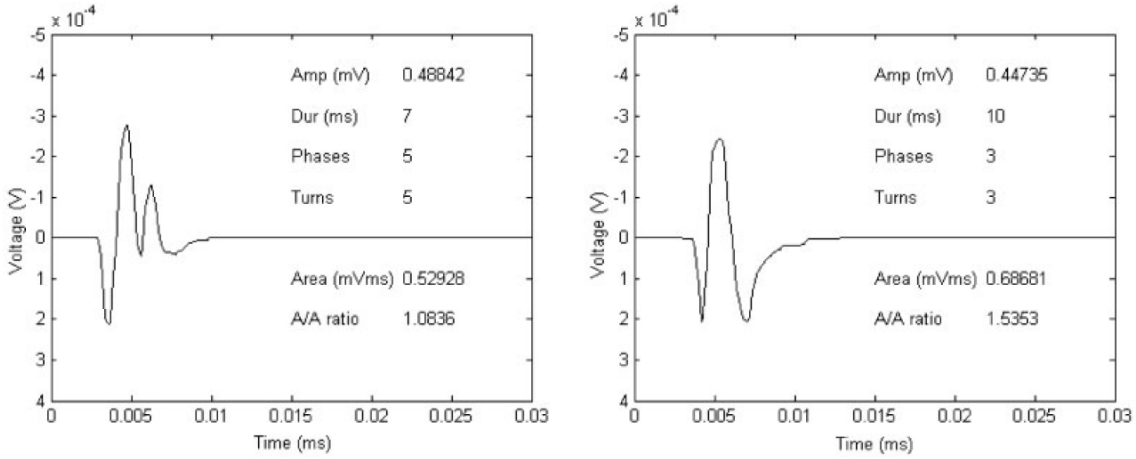

FIGURE 1. Two simulated MUAPs with metric values.

using a variable power supply with an output fed to an analog-to-digital (A/D) converter. By manually increasing and decreasing the output voltage, waveforms were generated that were similar in shape to biologic MUAPs. These waveforms were imported to MATLAB. Approximately 150 potential MUAPs were created, and 28 were selected for their similarities to biologic MUAPs (Fig. 1).

Calculation of Modeled MUAP Metrics. The following MUAP metrics were assessed: (1) peak-to-peak amplitude, as the difference between the maximum and minimum values of the MUAP; (2) duration, by markers which were set manually, based on accepted criteria[6]; (3) area, by calculations performed by numeric integration techniques; (4) area-to-amplitude ratio, determined by division of the appropriate values; (5) phases, counted as portions of the waveform that were either above or below the baseline, with an amplitude criterion of $\geq$25 μV so that noise about the baseline was not counted[6]; and (6) turns, counted as changes in slope direction that do not cross the baseline, with a voltage criterion of $\geq$25 μV so that noise was not counted.[6]

IP Simulation. During a weak contraction, a motor unit does not discharge at a constant frequency. Rather, there is a distribution of firing frequencies about a central firing frequency for any given level of muscle contraction, and this was integrated into the model. Central firing frequencies were used in a range from 8 to 15 Hz[1] to simulate real motor unit discharge frequencies during a weak contraction. Using the random number generator in MATLAB, a small value was either added to or subtracted from the interdischarge interval, with a coefficient of variation of 0.09 (standard deviation/mean), to give a normal distribution of frequencies on either side of the central frequency. An interdischarge interval corresponding to the central firing frequency desired was assigned to each motor unit. In order to randomly space motor unit discharges, an arbitrary start time was assigned to each motor unit. Within the first tenth of a second of the simulated IP, all motor units had fired their first MUAP and continued to do so around their central firing frequency throughout the entire run. Thus, a library of discharge patterns or motor unit action potential trains (MUAPT) was created for each of the 28 MUAPs.

Weak IPs were simulated by combining several MUAP discharge libraries. Because electrical potentials add algebraically, the IP is the sum of the various MUAPTs. Several different types of MUAP discharge libraries were selected to create a realistic IP. Within each IP, at least one MUAP was large with a short rise-time, indicating close proximity to the needle, whereas others were of lesser amplitude and longer rise-times to simulate more distant motor units. Simulated and biologic IPs are similar in appearance (Fig. 2).

Conversion of Digital Model to Analog Signals. A PCI-DAS6025 D/A converter card (Measurement Computing, Middleboro, Massachusetts) was used to create an analog signal from MATLAB digital signals. Because these cards are more accurate with larger voltages, the output values for the simulated IP were scaled so that the largest output of the IP did not

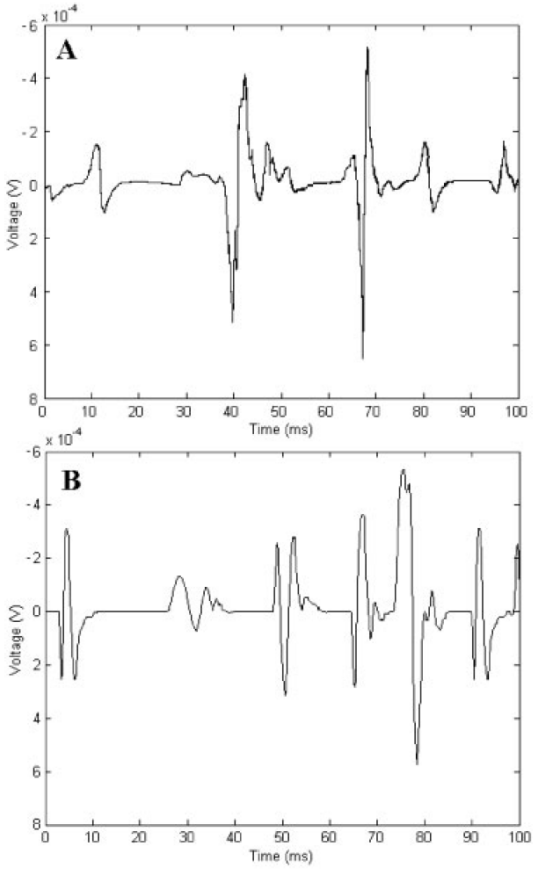

FIGURE 2. Interference patterns showing 100 ms of activity. **(A)** Activity from a normal subject. **(B)** Simulated activity from combining six synthesized MUAPTs.

exceed ±10 V. This voltage was then put through a voltage divider for appropriate scaling.

There was concern that, because the D/A card had a maximum sampling frequency of 10 kHz, the MUAP waveforms would appear stepped. This was not a problem because the EMG machines have a low-pass filter that sufficiently eliminates any of the stepped nature of the simulated waveforms. Default filter settings for each machine are: machine A, 10 Hz to 5 kHz; machine B, 10 Hz to 10 kHz; and machine C, 20 Hz to 10 kHz.

Simulated IP Testing. Five different simulated IPs with various combinations of MUAPs were administered to each machine. The maximum number of MUAPs that each algorithm could extract varied: four for machine C; six for machine A; and no programmed limit for machine B. Taking this into consideration, one simulated IP contained only four MUAPs, one had five, one had six, and two had seven MUAPs. Each simulated IP was administered to each machine separately. It was assumed that the D/A card was consistent throughout the testing process. The same computer was used to drive the card for all testing. The three EMG machines included algorithms to mark and determine MUAP metrics automatically, with the exception of machine C, which did not calculate area-to-amplitude ratios; this metric was therefore calculated manually.

Biologic IP Testing. This portion of the study was approved by our institutional review board, and informed consent was obtained from all subjects. Needle EMG records were obtained with a pediatric-sized concentric electrode (25-mm length, 0.3-mm diameter, 0.03-mm^2 recording area; Teca–Oxford Instruments, Hawthorne, New York). The EMG needle was connected to the three EMG machines simultaneously. The assumption was made that the amplifiers of the machines had nearly equal input impedance (values not available in operator manuals), which would allow all three to detect the same signal. Filter settings were left unchanged from default values. IPs were obtained from the anterior tibial muscle on two occasions in the same healthy subject, and from the first dorsal interosseous muscle in a subject with amyotrophic lateral sclerosis (ALS). Data were gathered during a weak IP from a muscle contraction, similar to that used for routine EMG studies. The needle was repositioned within the muscle to record a different IP. Muscle contractions were recorded until all three machines had at least 20 acceptable MUAPs. The prescribed data acquisition recording time for each algorithm varied: 30 s for machine B; 10 s for machine A; and no programmed limit for machine C (until four MUAPs were decomposed). Recording of the IP was started simultaneously for all three machines, and machines A and B were allowed to record for their respective default recording time, whereas machine C was stopped at 30 s (extended times well beyond 30 s did not routinely result in detection of more MUAPs if fewer than four were identified at 30 s).

After each IP, the detected MUAPs were examined to determine acceptability. MUAPs felt to be duplicates as determined by non-overlapping discharge patterns and by similar waveform "signature" characteristics—patterns of phases and turns and similar amplitudes—were rejected. Cannula potentials, defined as predominantly positive waveforms, were rejected.[6] For each IP, the waveforms were also compared to determine which ones were identical in

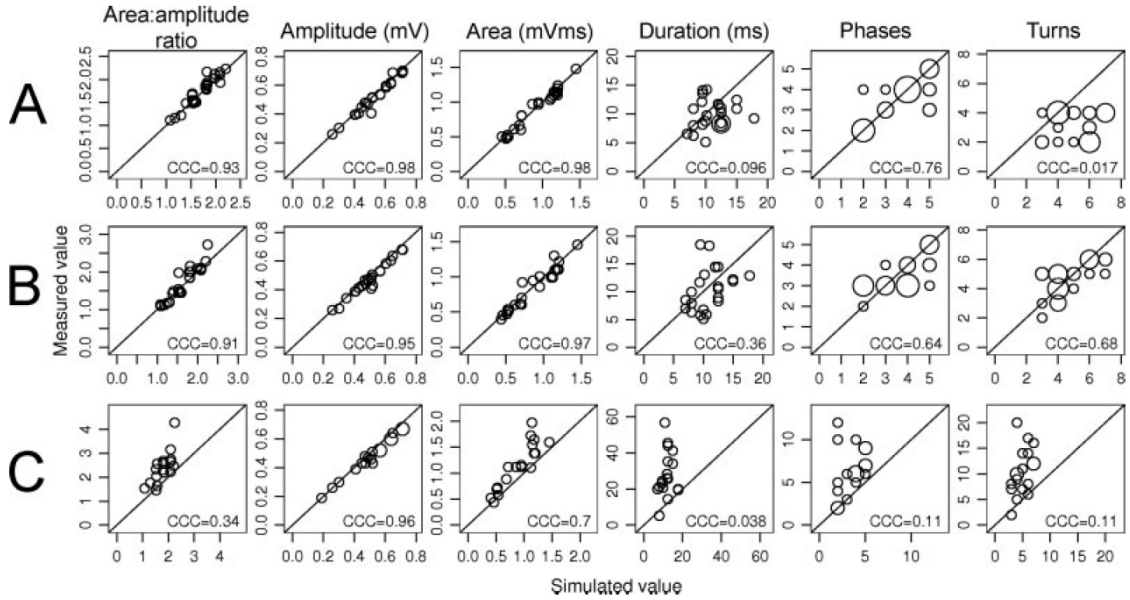

FIGURE 3. Scatterplots of motor unit action potential (MUAP) metric values from simulated interference patterns (IPs). Comparisons are between values assessed by three algorithms (**A, B, C**) against the values from the simulated MUAPs. Values are pooled from all seven IPs. The diagonal line visualizes the line where the two measurements are equal. The area of each circle is proportional to the number of points falling at its center. The CCC value is the concordance correlation coefficient (see Materials and Methods section).

all three machines. Identification was based on waveform signature characteristics, as noted earlier. The marking algorithms were allowed to identify the same metrics as determined for the simulated MUAPs, and no marks were manually changed.

Statistical Analysis. The software package R 2.0.1 was used for all statistical analyses.[4] Inspection of scatterplots for the same metric plotted against each EMG machine indicated that the measurement of errors were multiplicative, and it was believed that analysis of ratios as opposed to differences was more suitable. Technically, this was achieved by performing the analyses on log-transformed data. Pairwise comparison between the machines could be performed using three paired *t*-tests. Although the distribution of the differences of the log-readings (log-ratios) is clearly not normal for several of the measurements, the moderately large sample sizes justified the use of the test. Because three (dependent) tests are performed for each measurement, an adjustment for multiple testing was performed using the Bonferroni adjustment with 0.017 (0.05/3) as the cut-off for declaring significance. A more sophisticated analysis comparing all three machines simultaneously is possible, but proved to be unnecessary with these data.

Figure 3 shows algorithm-measured metrics plotted against simulated MUAP metrics. The concordance correlation coefficient (CCC) was used to measure agreement.[3] The CCC measures how well points line up on the diagonal of perfect agreement (in contrast to the Pearson correlation coefficient, which measures how well the points line up on any line) and ranges from -1 to 1, the extremes indicating perfect disagreement and perfect agreement, respectively. Values >0.8 are interpreted as excellent agreement.

RESULTS

Simulation Data. The extracted MUAP waveforms with their metrics from the five simulated IPs were compared to the modeled MUAPs to identify matching waveforms. The efficiency of each of the machines is shown in Table 1. The ability to detect known MUAPs in the simulated IPs varied among machines. Machine B detected the greatest number of MUAPs, and missed only three MUAPs among the five simulated IPs. Machine C missed at least one MUAP in every simulated IP, and machine A missed at least one MUAP in all but one IP. Machine A, and in one instance machine B, detected the same MUAP and presented it as two distinct MUAPs. Ma-

Table 1. Correspondence of detected to simulated motor unit action potentials (MUAPs).*

	IP Alpha								IP Beta								IP Gamma								IP Delta								IP Epsilon								
	a	b	c	d	e	f	g	No. detected (efficiency)	h	i	j	k	l	m	No. detected (efficiency)	n	o	p	q	r	No. detected (efficiency)	t	u	v	w	No. detected (efficiency)	x	y	z	aa	bb	cc	dd	No. detected (efficiency)	Overall
Machine A				1	2	2	1	4 (57%)	1		1	1	1	2	5 (83%)		2		1	1	3 (60%)	1	2	2	1	4 (100%)		1		1	1	2		4 (57%)	20 (69%)
Machine B	1	1	1	1	1	1	1	7 (100%)	1	2	1	1	1	1	6 (100%)		1		1	1	3 (60%)	1	1	1	1	4 (100%)	1	1	1	1	1	1		6 (86%)	26 (90%)
Machine C		1		1		1	1	4 (57%)	1		1		1	1	4 (67%)		1		1	1	3 (60%)		1	1	1	3 (75%)			1		1	1	1	4 (57%)	18 (62%)

*Machines are designated A, B, and C. Interference patterns (IP) are designated alpha, beta, gamma, delta, and epsilon. A value of 1 indicates that the MUAP was identified once, a value of 2 indicates the MUAP was identified twice as two separate MUAPs. Empty spaces indicate that the algorithm did not detect a particular MUAP. Efficiency of machine algorithms is shown by the number of MUAPs detected compared to the number of MUAPs in the simulated IP.

chine C detected its limit of four MUAPs for all but one trial—the trial that included only four MUAPs. Machine A, which has a limit of six MUAPs per IP, was able to detect in only one instance more than four MUAPs when five or more were available in the IP.

Figure 3 plots metric values determined from marking algorithms compared to those measured and manually assessed from simulated MUAPs. Differences are apparent for the metrics of duration, area, area–amplitude ratio, and number of phases and turns, most notably for machine C.

Biologic Data. Table 2 shows the efficiency of MUAP detection by each machine, as well as the numbers of matching MUAPs detected between machines. Machine B detected the greatest number of MUAPs, whereas machines A and B had the most matching MUAPs.

Table 3 shows the average values for each metric for matching MUAPs. Because the number of matching MUAPs is different for each pair of machines, the results are given separately for each pair. Table 4 shows pairwise ratios for matched MUAPs with their statistical analysis. Ratios of 1.0 would indicate a perfect match between the reported metric values. All metrics except MUAP amplitude are statistically significantly different between machines. However, there are fewer clinically significant differences in metrics between machines. Figure 4 provides a visual representation of correlation for all six metrics between each of the three combinations of machines plotted against one another. Metrics for matching MUAPs are most similar for machines A and B. The greatest differences are markedly long MUAP duration measurements by machine C. This, in turn, results in greater values for area, area–amplitude ratio, phases, and turns, all of which are likely clinically significant for machine C.

DISCUSSION

We have previously assessed algorithms for averaging and marking as applied to individual MUAPs isolated manually by a voltage trigger, and the current study represents an extension to automated detection algorithms.[2] As more EMG equipment manufacturers and electromyographers take advantage of sophisticated software packages, assurances that appropriate data are extracted are essential. Comparisons are complicated by different approaches taken by the algorithms, including different methods to extract constituent MUAPs (template matching, decomposition), different data acquisition times, limits

Table 2. Summary of MUAPs detected by each machine (A, B, C) from biologic interference patterns.

	A vs. B		A vs. C		B vs. C	
Number of common MUAPs	56		27		34	
Total number of MUAPs detected	62	94	62	66	94	66
Percent in common	90.3%	59.6%	43.5%	40.9%	36.2%	51.5%

on the number of extractable MUAPs, and which waveform metrics are determined.[8] Our approach has been to make comparisons with simulated IPs of known MUAP composition and with biologic data. Within the overall limitations, we have determined that there are clinically important differences between algorithms.

Comparisons with simulated IPs showed that no algorithm was absolutely accurate in extracting MUAPs. The detection programs are proprietary and two of the three tested were unavailable for review, but all likely differ in design. They clearly differ in how many MUAPs they can extract, and the five simulated IPs included at least four MUAPs, the upper limit for machine C. Machine A had the highest number of repeated MUAPs. Machine B missed only three MUAPs total and only repeated the same MUAP once. Repeat MUAPs are due presumably to enough baseline noise (superimposition of MUAPs) to render a train of MUAPs sufficiently different to be considered unique by the algorithm. The simulated IPs are somewhat simpler than biologic IPs due to less background noise from very distant MUAPs.

In IP Gamma, where all three machines missed two MUAPs, one of the missed MUAPs, it was found later, did not meet the detection threshold due to a low amplitude and insufficient initial slope. The other undetected MUAP had sufficient amplitude and slope for detection, but possibly was not easily isolated from other MUAP firings. The MUAP not meeting detection criteria is a simulation-model problem, and the other missed MUAP can be considered a deficiency in the algorithms.

When applied to biologic IPs, differences in the maximum number of MUAPs capable of being extracted affected the overall clinical efficiency of QEMG. Also affecting efficiency is how well the algorithms can extract their maximum numbers. Machine C had the least capacity, but also had difficulty in reaching that number in one trial. Machine B had the greatest efficiency of any of the machines, extracting more MUAPs from the IPs. Two algorithms counted the same MUAP as two different MUAPs at least once, and thus it is important to visually inspect extracted MUAPs for repeats.

More problematic was the marking algorithms. All three machines recorded the peak-to-peak voltage within microvolts of the model value. This is the most straightforward metric to identify. It also indicates that the amplifiers are essentially equal. Whereas there were statistical differences for the other metrics, only values for duration, and other values dependent upon it, are likely to be clinically significant. Waveform duration affects the metrics of area, area–amplitude ratio, phases, and turns. Designing algorithms that detect the onset and termination of MUAPs is challenging, and small differences in parameters can affect marker placement.[6] It will be difficult for any algorithm to improve upon those used in machines A and B, and this emphasizes the need to visually inspect extracted waveforms and reset markers as necessary.

Correlations were poor between the number of turns determined by the machines and those counted in the modeled data. Machine A reported numbers of turns well below the number of turns in

Table 3. Average metric values for matched motor unit action potentials (MUAPs) detected by each machine (A, B, C) from biologic interference patterns.

	A vs. B			A vs. C			B vs. C		
	No.	A	B	No.	A	C	No.	B	C
Amplitude (mV)	56	0.88	0.86	27	0.89	0.95	34	1.01	1.14
Area (mV/ms)	56	1.75	1.61	27	1.72	2.52	34	1.86	2.99
Area-to-amplitude ratio	55	2.24	1.98	26	2.1	3.19	33	1.96	3.33
Duration (ms)	56	16.02	13.67	27	14.9	37.65	34	14.86	42.68
Phases	56	3.75	3.11	27	3.74	6.59	34	3.26	7.76
Turns	56	3.14	3.66	27	3.33	14.04	34	3.88	17.12

Table 4. Pairwise ratios for matched motor unit action potentials (MUAPs).

	B/A				C/A				C/B			
Measure	Ratio			*P*-value	Ratio			*P*-value	Ratio			*P*-value
Amplitude (mV)	0.95	**0.98**	1.01	0.13	0.91	**1.03**	1.18	0.62	0.94	**1.05**	1.17	0.39
Area (mV.ms)	0.85	**0.91**	0.96	<0.001	1.22	**1.42**	1.65	<0.001	1.34	**1.54**	1.77	<0.001
Area-to-amplitude ratio	0.8	**0.88**	0.96	0.01	1.24	**1.4**	1.58	<0.001	1.34	**1.61**	1.92	<0.001
Duration (ms)	0.74	**0.83**	0.94	<0.001	2.01	**2.39**	2.85	<0.001	2.3	**2.78**	3.35	<0.001
Phases	0.79	**0.85**	0.93	<0.001	1.33	**1.66**	2.07	<0.001	1.67	**2.08**	2.58	<0.001
Turns	1.07	**1.16**	1.26	<0.001	3.05	**3.89**	4.95	<0.001	3.16	**3.97**	4.98	<0.001

P-values are for a two-sided t-test unadjusted for multiple testing. "Ratio" columns (a ***b*** *c) show the geometric mean* **b** *with its 95% confidence interval a–c.*

the modeled data. This suggests that the voltage criterion was >25 μV. Conversely, machine C reported numbers of turns far above the modeled data values. This was probably a result of extended durations determined for this machine and possibly a different voltage criterion. Ideally, a standard threshold value for this metric would have been used for the comparison, but this was not possible.

The results of this study indicate that there are differences among QEMG algorithms that detect and mark MUAPs in an IP. Although QEMG has clinical advantages over routine EMG, it requires continuous

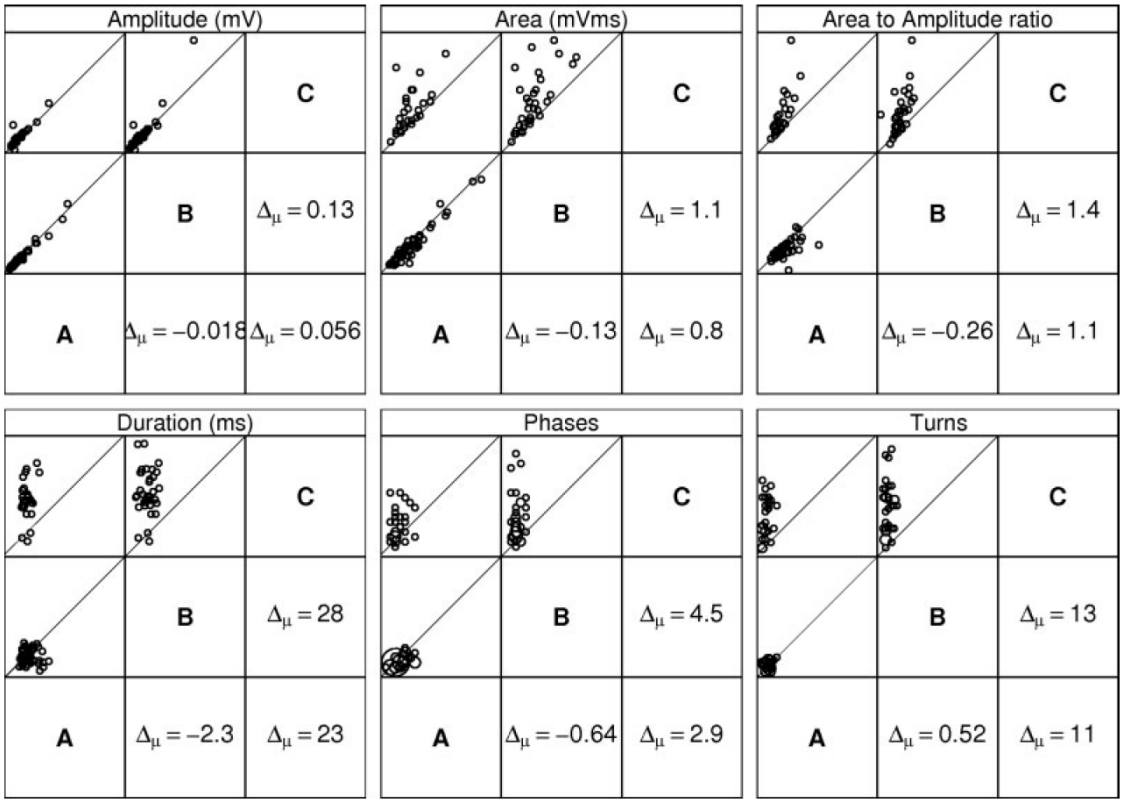

FIGURE 4. Scatterplots of motor unit action potential (MUAP) metric values from biologic interference patterns (IPs). Comparisons are between values assessed by three algorithms (A, B, C). Values are pooled from all trials. The diagonal line visualizes the line where the two measurements are equal. The area of each circle is proportional to the number of points falling at its center. Δ_μ is the mean difference between the measurement of the corresponding two machines (variable above − variable to the left).

oversight by the electromyographer. Further, it would be of interest to develop a variety of IP data libraries that could be used as test sources for algorithms.

Portions of this research were funded by the Richard K. and Shirley S. Hemingway Foundation. This work was undertaken in partial fulfillment of a master's degree (A.A.B.), Department of Biomedical Engineering. The authors thank Summer Davis, BA, for her assistance with data recording; Aniko Szabo, PhD, Biostatistics Shared Resource of the Huntsman Cancer Institute, for her statistical analysis; and Daniel Stashuk, PhD, for his comments concerning this work.

REFERENCES

1. Boe S, Stashuk D, Brown W, Doherty T. Decomposition-based quantitative electromyography: effect of force on motor unit potentials and motor unit number estimates. Muscle Nerve 2005;31:365–373.
2. Bromberg M, Smith A, Bauerle J. A comparison of two commercial quantitative electromyographic algorithms with manual analysis. Muscle Nerve 1999;22:1244–1248.
3. Lin L. A concordance correlation coefficient to evaluate reproducability. Biometrics 1989;45:255–268.
4. R Development Core Team. R: A language and environment for statistical computing. 2.0.1. Vienna; 2003.
5. Spitzer A. Multi-motor unit action potential analysis (MMA). Muscle Nerve 1997;20:250.
6. Stålberg E, Andreassen S, Falk B, Lang H, Rosenfalck A, Trojaborg W. Quantitative analysis of individual motor unit potentials: a proposition for standardized terminology and criteria for measurement. J Clin Neurophysiol 1986;3:313–348.
7. Stålberg E, Falck B, Sonoo M, Stålberg S, Astrom M. Multi-MUP EMG analysis-a two year experience in daily clinical work. Electroencephalogr Clin Neurophysiol 1995;97:145–154.
8. Stålberg E, Nandedkar S, Sanders D, Falck B. Quantitative motor unit potential analysis. J Clin Neurophysiol 1996;13:401–422.

High-pass Filtering

Electrical signals from muscle fiber action potentials are attenuated by the surrounding tissues. The rapid rise times of muscle fiber potentials close to the electrode can be brought out if low rise times from more distant potentials are filtered out. Previous studies have suggested that high-pass filtering at various cutoff frequencies (1,600-3,200 Hz) can reveal increased complexity within the MUAP that may be clinically relevant (42). Such signal filtering could be useful, as most EMG machines are already equipped with high-pass filters that can approach these numbers. If we could determine some utility of performing such filtering it could then be immediately implemented in the EMG laboratory. We undertook a study to determine if the MUAP metrics of filtered signals offered any insight into the physiology, anatomy, or pathology of the muscle (43).

MUAPs were recorded from healthy and diseased muscle initially with default filter settings (band-pass from 10-10,000 Hz). These were initially analyzed by the system algorithm (DQEMG), and metric marker adjustments were made manually as necessary. The signals were then exported to MATLAB to be filtered digitally. We initially filtered with a 1^{st} order digital Butterworth filter. We did this because it would be the simplest implementation, and all machines could match or exceed the performance of this filter design. Subsequently, we investigated the effects of filtering with more aggressive and sophisticated digital filters, but the results were not significantly changed. After filtering, the data were reintroduced to the DQEMG program. This was done two ways to determine which method was best. First, we introduced the data as if they had just been recorded. Second, we used the information determined from unfiltered data

about the firing times of MUAPs, so that the algorithm need not try to decompose the signal, just average the MUAPs. The two different methods yielded nearly identical results, and we introduced all the data presented as *de novo*.

In the initial version of this study we attempted to correlate high-pass filtered turn count with fiber density measurements. The hope was that we could use a conventional concentric needle electrode, which is much less expensive and is disposable, to glean a portion of the same information available with a single fiber needle determination of fiber density. We collected fiber densities for each of the muscles studied in the high-pass filter study. Our initial data looked extremely promising, but as we collected data from more muscles the correlation became very poor. Ultimately we concluded that this portion of the study was not feasible.

We measured the number of turns and phases using several different threshold values of the change in voltage direction: 50 μV which many laboratories use, the more sensitive 25 μV value that some laboratoies use, and all visible turns that we as experienced electromyographers felt were not noise (approx 2-6 μV depending on the noise in the signal). These different groups of data were evaluated against fiber density and it was determined that the best fit (signal to noise ratio) to the initial data was with the 25 μV threshold.

We also performed simulation studies to evaluate the effects of filtering. Two models were used (44-46). The Stålberg and Karlsson model is commercially available and the Hamiltron-Wright and Stashuk model is available from Stashuk (personal gift). Correlations between filtered turn and phase counts and fiber density were relatively good for the simulated data. The models allowed for simulations of the clinical single

fiber study. The Stålberg model allows direct visualization of the muscle fibers within the motor unit, so the results of the single fiber study were visually verified. We validated the results of the Hamilton-Wright model by extracting the muscle fiber placement information and modeling a single fiber study with MATLAB. Both models showed very good correlation between the actual fiber density and the simulated clinical study.

Effects of High-Pass Filtering on MUAP Metrics

Reprinted with permission from Muscle & Nerve 40:1008-1011

ABSTRACT: Previous observations suggest that elevated high-pass filter settings (1,600–3,200 Hz) can reveal greater motor unit action potential (MUAP) complexity (turns). We assessed the effect of high-pass filter settings (500, 1,000, 2,000 Hz) on MUAP metrics. MUAPs were recorded with a concentric needle and initially extracted by a decomposition software algorithm at 10 Hz–10 kHz and further filtered offline at 500, 1,000, and 2,000 Hz. When reanalyzed by the decomposition software there were marked reductions in peak–peak amplitude, area, area-to-amplitude ratio, and duration at the 500 Hz filter with lesser subsequent reductions at higher filter settings. In contrast, turn and phase counts did not change significantly. Individual MUAPs tracked across filter settings showed rare increases in turn count at the 500 Hz setting but a subsequent decrease in counts with higher filter settings. We conclude that the routine use of elevated high-pass filters, as in quantitative EMG analysis, does not enhance turn count.

Muscle Nerve **40:**1008–1011, 2009

EFFECTS OF HIGH-PASS FILTERING ON MUAP METRICS

ALEXANDER A. BROWNELL, MS and MARK B. BROMBERG, MD, PhD

Department of Neurology, Clinical Neurosciences Center, University of Utah, 175 North Medical Drive, Salt Lake City, Utah 84132, USA

Accepted 21 April 2009

Motor unit action potential (MUAP) waveform complexity can be expressed in part by the number of turns and phases. Identification of MUAPs with greater complexity is clinically important, because excessive numbers of turns and phases represent changes in motor unit architecture that reflect pathology. MUAP waveforms are altered by filtering the original biologic signal. Default high-pass (10–20 Hz) and low-pass (10,000–20,000 Hz) filter settings are a reasonable compromise for removing low-frequency mechanical-based noise and high-frequency electrical noise. However, raising the high-pass filter has been suggested to accentuate sharp (high frequency) waveform components, and a 500 Hz filter is used for single fiber EMG studies.[1] Very high high-pass filter settings (1,600–3,200 Hz) have been proposed to bring out turns in MUAP waveforms that may not be apparent with default filter settings.[2] While such filtering may accentuate sharp waveform features it also attenuates waveform amplitudes. We are not aware of a systematic assessment of the effects of increasing high-pass filtering on MUAP metrics and whether routine high-pass filtering could have a useful role as an adjunct to quantitative electromyography (QEMG) waveform analysis. We thus undertook such a study with a focus on turn count as a measure of MUAP complexity.

Abbreviations: ALS, amyotrophic lateral sclerosis; EMG, electromyography; MUAP, motor unit action potential; QEMG, quantitative EMG

Key words: needle electromyography; EMG; quantitative electromyography; QEMG; motor unit action potential; high-pass filtering

Correspondence to: M.B. Bromberg; e-mail: mbromberg@hsc.utah.edu

Published online 7 August 2009 in Wiley InterScience (www.interscience.wiley.com). DOI 10.1002/mus.21429

MATERIALS AND METHODS

MUAPs were recorded from biceps brachii and anterior tibialis muscles in seven subjects, three with normal neuromuscular function and four with amyotrophic lateral sclerosis (ALS), to represent a spectrum of waveform complexity. An interference pattern was generated that included 3-8 MUAPs with short rise time, as in routine QEMG studies. MUAPs were recorded with a concentric needle electrode and extracted from the interference pattern by a decomposition software program[3,4] running on a Compumedics EMG machine (El Paso, Texas). The initial MUAPs were recorded at default filter settings (10–10,000 Hz). MUAP metrics were set by algorithms in the DQEMG software and adjusted manually if necessary. The turn

Table 1. Mean, median, and range for motor unit action potential metrics at different high-pass filter settings in both normal muscles and those from patients with amyotrophic lateral sclerosis.

	Amplitude (μV)	Area (μVms)	Area amplitude ratio	Duration (ms)	Phases	Turns
Normal						
10 Hz	513;371 (174-3832)	832;611 (183-4955)	1.67;1.61 (0.74-3.26)	10.7;9.6 (4.1-24.4)	3.20;3 (1-6)	3.85;3 (2-8)
500 Hz	345;268 (78-2499)*	288;224 (36-2098)*	0.88;0.86 (0.30-1.65)*	6.1;5.7 (1.4-13.0)*	2.88;3 (1-6)*	3.58;3 (1-9)
1,000 Hz	294;212 (66-1984)*	172;139 (25-1231)*	0.64;0.62 (0.17-1.29)*	4.2;4.0 (0.7-10.8)*	2.53;2 (0-6)*	3.43;3 (1-9)
2,000 Hz	232;165 (72-1890)*	110;79 (16-617)*	0.54;0.50 (0.14-1.38)*	3.9;3.7 (0.5-8.6)*	2.05;2 (0-4)*	3.32;3 (1-9)
ALS						
10 Hz	695;596 (112-2563)	1635;1377 (116-6201)	2.34;2.23 (0.25-5.69)	14.8;15.0 (2.2-32.0)	3.04;3 (1-11)	4.26;3 (1-20)
500 Hz	387;297 (85-1837)*	403;333 (29-1444)*	1.05;1.02 (0.28-2.17)*	7.7;6.9 (1.2-19.2)*	2.80;3 (0-13)	4.19;3 (0-20)
1,000 Hz	300;249 (78-1267)*	232;199 (30-825)*	0.80;0.81 (0.22-1.78)*	6.3;6.0 (1.3-18.6)*	2.77;3 (0-11)	4.34;3 (1-16)
2,000 Hz	253;192 (64-993)*	138;110 (22-375)*	0.59;0.59 (0.18-1.28)*	4.6;4.4 (1.1-9.8)*	1.65;2 (0-3)*	3.53;3 (1-12)

Mean; median (range)
Asterisks represent a statistically significant difference from metrics ($P < 0.02$) measured with the 10-Hz high-pass filter.

amplitude criterion was 25 μV.[5] The MUAP data files from the DQEMG software were filtered off-line using MatLab (MathWorks, Natick, Massachusetts) at high-pass filter settings of 500, 1,000, and 2,000 Hz. Data files from the high-pass filtering were reanalyzed by the DQEMG software as a de novo interference pattern, and the metrics were set by the software and adjusted manually if necessary. These high-pass filter settings were chosen, because they represent a range that may be available on commercial EMG machines. The type and order of the filters used in commercial machines are not available in operator manuals, and thus we chose a first-order Butterworth filter. The study was approved by the Institutional Review Board and informed consent was obtained.

Statistically significant differences in MUAP metrics were identified by comparing values recorded at a high-pass filter setting of 10 Hz to values recorded at elevated high-pass filter settings using the Wilcoxon-Rank Sum test with $P < 0.02$ level to account for multiple comparisons.

RESULTS

Data were analyzed from two perspectives. When all MUAP data were analyzed the effect of raising the high-pass filter affected all metrics, but to varying degrees (Table 1). The effect on peak–peak amplitude, area, and area-to-amplitude ratio was greatest with 500 Hz filtering, where mean peak–peak amplitude fell by 33%, area by 65%, and area-to-amplitude ratio by 47%. Reducing the influence of low-frequency waveform components accounted for the marked reduction in duration values, with the greatest effect at 500 Hz filtering where mean duration was shortened by 43%. The attempt to sharpen and bring out high-frequency components by filtering and hence to show an increase in turn count was offset by the amplitude reduction, and the mean turn count dropped minimally with higher filter settings. The effects of filtering were statistically significant for most metrics at all elevated high-pass filter settings, with the most notable exception of turn and phase numbers (Table 1).

Because the variability in the combined data was large, turn counts for individual MUAPs from normal and ALS subjects were plotted to determine if high-pass filter settings increased turn counts in some MUAP waveforms. Figure 1 shows that an increase in turn counts occurred rarely, and most increases were observed at high-pass filter settings of 500 Hz. At higher filter settings all turns counts remained unchanged or fell. The effect of high-pass filtering on two individual MUAPs is illustrated in Figure 2, where no new phases or turns were evident at elevated high-pass filter settings.

DISCUSSION

Signal manipulation is a useful technique to extract specific data from MUAP waveforms, and one goal is to assess contributions from individual muscle fibers or groups of fibers. Changing filters is a readily available means to bring out potentially important features, and Payan[2] illustrated the utility of raising the high-pass filter for concentric needle electrode studies to bring out subtle features (turns) that might indicate pathology but were not visible with normal filter settings. Filter settings in that study were very high (1,600 and 3,200 Hz) and beyond those readily available on commercial EMG machines, and thus we sought to determine the effect of using readily available high-pass filters (500, 1,000, and 2,000 Hz) on MUAP metrics.

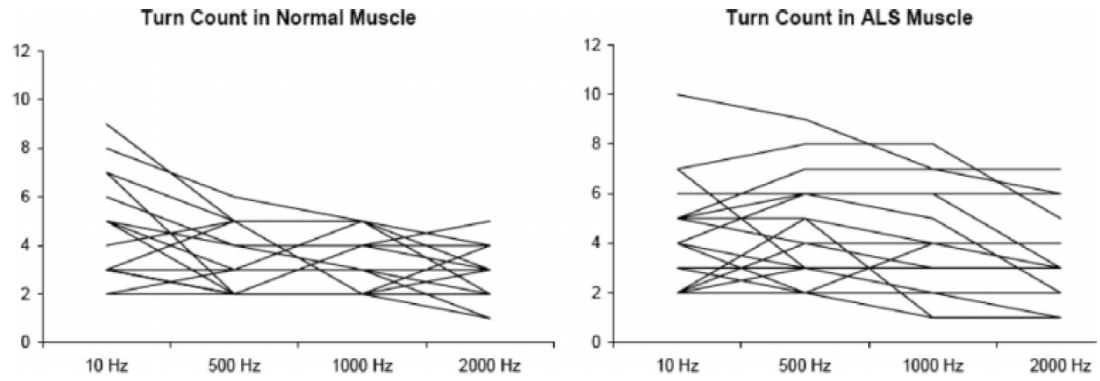

FIGURE 1. Plots of change in turn counts for the same motor unit action potentials tracked across different high-pass filter settings. $N = 20$ for both normal muscles and those from ALS patients.

We assessed the use of high-pass filtering on MUAP waveforms with two main questions: (1) Would routine filtering at raised high-pass filter settings be a useful manipulation for averaged MUAP data during QEMG studies; and (2) How often does filtering enhance individual MUAPs? In general, raising the high-pass filter affected MUAP amplitude and duration but had little effect on the number of turns despite using a low turn amplitude criterion of 25 μV.[5,6] We found the greatest change in metrics with 500 Hz filtering and did not find added benefit with 1,000 or 2,000 Hz filtering. An explanation as to why Payan[2] observed more turns with very high filter settings is likely his reliance on qualitative MUAP waveform inspection for any visible turns, and many of the turns brought out by such high value filtering were <5 μV in amplitude. Using such a low-amplitude turn criterion in a QEMG program would represent a challenge for the algorithm to distinguish a turn from noise. It can be argued that the averaging process in the DQEMG program may have eliminated very low amplitude turns. While this may be a factor, inspection of a large number of MUAP waveforms in raster format reveals little change in the number of turns with raised high-pass filter settings (Figs. 1, 2). It is possible that Payan's examples were from outlier MUAPs. In this regard, there is a spectrum of MUAP abnormalities in any disease process, and many MUAPs have metrics that fall within the normal range.[7,8] Many MUAPs from the subjects with ALS in this study were within the normal range (Table 1), and the diagnosis of ALS was based on outlying MUAPs in the muscle chosen for this study and in other muscles.

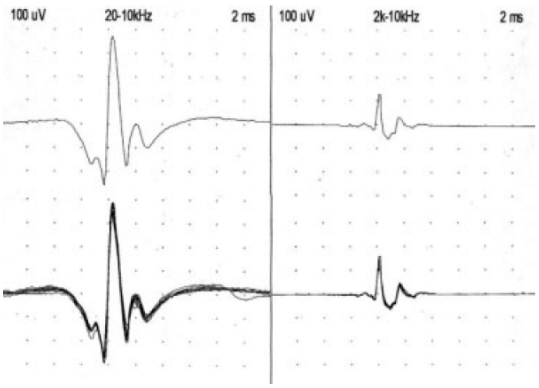

FIGURE 2. Two MUAP waveforms (upper and lower) recorded by conventional voltage trigger and delay line methods and displayed as single (upper) and in raster format (bottom). Left traces recorded with 20 Hz high-pass filter and right traces recorded with 2,000 Hz high-pass filter.

The effects of elevated high-pass filtering on MUAPs recorded with concentric needle electrodes have recently been discussed in terms of jitter measurements with these electrodes. Conclusions from these studies support our findings that there is a marked reduction in signal amplitude with high-pass filters greater than 1,000 Hz, including small components that represent phases and turns without making them more prominent.[9,10]

We find that routine use of elevated high-pass filtering is not effective in bringing out subtle or hidden MUAP complexity (turns) in the setting of QEMG analysis. Changing filter settings may serve to satisfy the electromyographer's curiosity about specific MUAPs (outlier MUAPs), but it is not promising as a routine technique to expose basic elements of the MUAP waveform.

Portions of this research were funded by the Richard K. and Shirley S. Hemingway Foundation.

REFERENCES

1. Stålberg E, Trontelj J. Single fiber electromyography. Studies in healthy and diseased muscle. New York: Raven Press; 1994.
2. Payan J. The blanket principle: a technical note. Muscle Nerve 1978;1:423–426.
3. Doherty T, Stashuk D. Decomposition-based quantitative electromyography: methods and initial normative data in five muscles. Muscle Nerve 2003;28:204–211.
4. Stashuk DW. Decomposition and quantitative analysis of clinical electromyographic signals. Med Eng Phys 1999;21: 389–404.
5. Pfeiffer G, Kunze K. Turn and phase counts of individual motor unit potentials: correlation and reliability. Electroencephalogr Clin Neurophysiol 1992;85:161–165.
6. Stålberg E, Andreassen S, Falk B, Lang H, Rosenfalck A, Trojaborg W. Quantitative analysis of individual motor unit potentials: a proposition for standardized terminology and criteria for measurement. J Clin Neurophysiol 1986;3: 313–348.
7. Stalberg E, Bischoff C, Falck B. Outliers, a way to detect abnormality in quantitative EMG. Muscle Nerve 1994;17: 392–399.
8. Stewart C, Nandedkar S, Massey J, Gilchrist J, Barkhaus P, Sanders D. Evaluation of an automatic method of measuring features of motor unit action potentials. Muscle Nerve 1989;12:141–148.
9. Kouyoumdjian JA, Stalberg EV. Reference jitter values for concentric needle electrodes in voluntarily activated extensor digitorum communis and orbicularis oculi muscles. Muscle Nerve 2008;37:694–699.
10. Kouyoumdjian JA, Stalberg EV. Concentric needle single fiber electromyography: comparative jitter on voluntary-activated and stimulated extensor digitorum communis. Clin Neurophysiol 2008;119:1614–1618.

Temporal Dispersion of the MUAP

When undertaking the work for the first study it was unclear what, if any, effect needle placement along the axial length of the muscle had on the MUAP waveform and metrics. Muscle fibers of the same motor unit do not share a uniform radial diameter; rather, there is some small distribution of diameters. Since signal propagation depends, in large part, on the diameter of the muscle fiber there would then be a similar distribution of action potential conduction velocities. In theory, and in computer simulations of muscle, this means that with the electrode nearer the motor end-plate zone (the area where the nerve innervates the individual muscle fibers of the motor unit—neuromuscular junctions) one could expect least temporal dispersion and greatest temporal overlap of individual muscle fiber action potentials making up the MUAP waveform. As the electrode is moved farther away from the motor end-plate zone one could then expect a greater degree of temporal dispersion in arrival of muscle fiber action potentials and change in MUAP waveform reflected in changes in metrics (increased number of turns and phases). Muscle fiber action potential conduction velocities in human skeletal muscle range from 1 m/s to 10 m/s with a mean velocity of approximately 4 m/s (47-50). Thus, at 4 m/s action potentials from two end-plate zones 50 mm apart results in a difference of 12.5 ms. This is certainly sufficient to distinguish two separate muscle fiber action potentials within the MUAP. Additional complexity comes from the concept that conduction velocities are variable along the length of the muscle fiber itself (51,52). For example, with large distances between the motor end-plate zone and the electrode separation of waveform components could reduce MUAP amplitude and increase the number of phases and turns. The hypothesis is that if there is a great degree

of variation in muscle fiber action potential propagation velocity a significant difference would exist in the same MUAP of the same motor unit if the recording electrode were placed near to or far from the motor end-plate zone.

We determined if large distances between the motor end-plate zone and electrode would be clinically significant, as it might be theoretically possible to induce false positives for neuropathic and myopathic diagnoses by placing the EMG electrode too far distant from the motor end-plate zone (53). Of note, the electromyographer does not know the distribution of end-plate zones and sites of needle electrode insertion are blind with respect to this variable.

The study was undertaken using the same two computer simulations as the filter study (Hamilton-Wright & Stashuk, 2005; Karlsson, Hammarberg, & Stålberg, 2003; Stålberg & Karlsson, 2001). The models allowed the creation of different numbers of muscle fiber action potentials, various distributions of muscle fiber diameters and resultant distributions of conduction velocities. Measurements of the resulting MUAPs were performed with the simulated electrode at various distances from a discrete motor end-plate zone.

Similar studies were performed in human subjects with both healthy and diseased muscle: diseased muscles from patients with amyotrophic lateral sclerosis was chosen because motor units will be in the process of denervation and reinnervation and a number of newly reinnervated muscle fibers will be atrophic, thus accentuating temporal dispersion. There is a distinction between the motor point, the site where the motor nerve enters the muscle, and the motor end-plate zone, the area where neuromuscular junctions are located. The motor point can be and was determined in the biceps brachii muscle.

The motor point can be identified electrophysiologically and the electrode positioned at varying distances away. The motor point is identified by stimulating with a small surface electrode over the belly of the muscle, using moderate current well below the maximal stimulation intensity, in various places until the greatest number of motor units are recruited for the given stimulus intensity (largest muscle twitch). This muscle was chosen because it is a relatively long muscle and anatomical studies indicate that the region in the muscle where motor end-plate zones are situated is relatively restricted.

It was found that while the predicted MUAP morphology and metric changes occurred in both the model and the human biceps, the changes rarely statistical significant in the human muscle and no changes would be considered to be clinically significant.

Effects of Intramuscular Needle Position on
Motor Unit Action Potential Metrics

Reprinted with permission from Muscle & Nerve 35: 465-470

ABSTRACT: It is unclear whether there are clinically significant differences in amplitude, duration, and numbers of turns and phases if an electromyographic (EMG) study is performed near to, or far from, the end-plate zone. The effects of temporal dispersion of arriving muscle-fiber action potentials on quantitative motor unit action potential (MUAP) metrics were assessed in simulated and biologic muscles. Two muscle simulation models were studied with electrode recording positions near the motor end-plate zone and 50–75 mm away. When the electrode was moved away from the end-plate zone, averages of 20 MUAPs significantly decreased in amplitude and area, and increased in numbers of turns and phases, but there was no significant change in duration. In biologic muscles (both normal and pathologic), similar changes in average metrics were observed, but to lesser degrees; few were statistically significant. Zones of innervation in biologic muscles are broadly distributed and, during routine electrode studies, distances between random electrode placements and end-plate zones are therefore relatively short, leading to clinically insignificant changes in quantitative MUAP metrics with distance from the end-plate zone. Thus, electrode position within a muscle is unlikely to affect clinical MUAP interpretation.

Muscle Nerve **35:** 465–470, 2007

EFFECTS OF INTRAMUSCULAR NEEDLE POSITION ON MOTOR UNIT ACTION POTENTIAL METRICS

ALEXANDER A. BROWNELL, MS,[1] and MARK B. BROMBERG, MD, PhD[2]

[1] Department of Biomedical Engineering, University of Utah, Salt Lake City, Utah, USA
[2] Department of Neurology, University of Utah, 50 North Medical Drive, Salt Lake City, Utah 84132, USA

Accepted 30 October 2006

A major component of electromyography (EMG) is assessment of motor unit action potential (MUAP) waveforms that can be described by metrics of amplitude, duration, turns, and phases. Modeling studies indicate that MUAP amplitude is influenced most by a few fibers within 0.5 mm of the electrode,[10] and can be optimized by adjusting the position of the electrode to achieve a rapid rise-time of the main spike component. MUAP duration is more complex and includes both clinically and physiologically defined components.[5] The number of turns and phases is largely influenced by temporal dispersion of arriving muscle-fiber action potentials.[10] Temporal dispersion is also influenced by the position of the electrode along the length of contributing muscle fibers. A question arises as to whether there are clinically significant differences in amplitude, duration, and numbers of turns and phases if an EMG study is performed near to, or far from, the end-plate zone. The effects of electrode position and the influence of muscle-fiber diameter and fiber density have been studied with respect to single MUAPs.[13] We examined the pragmatic implications, from the perspective of quantitative EMG, of the effects of these variables by two methods. First, two muscle simulation models were assessed to determine the effects of electrode position with respect to the end-plate zone on quantitative MUAP metrics. Second, the biologic counterpart was assessed in biceps brachii muscles in normal subjects and those with diseases affecting the motor unit by comparing quantitative MUAP metrics obtained with a decomposition algorithm for electrode positions near the physiologic end-plate zone and at a maximal longitudinal distance away.

Abbreviations: ALS, amyotrophic lateral sclerosis; DM, dermatomyositis; DQEMG, decomposition-based quantitative electromyography; EMG, electromyography; MUAP, motor unit action potential; MUAPT, motor unit action potential train

Key words: motor unit action potential; needle electromyography; QEMG; quantitative electromyography; simulation

Correspondence to: M. B. Bromberg; e-mail: mbromberg@hsc.utah.edu

Published online 12 January 2007 in Wiley InterScience (www.interscience.wiley.com). DOI 10.1002/mus.20718

MATERIALS AND METHODS

Simulated Data. Two muscle simulation models were studied. The Medtronic EMG Simulator version

3.5 (Karlsson and Stålberg, CD; Medtronic, Skovlunde, Denmark) developed by Karlsson and Ståberg[9] (thus designated the K/S model) was used with default settings for muscle-fiber properties: fiber diameter, 50 ± 5 μm; neuromuscular junction delay, 500 μs; jitter, 50 μs; muscle fibers per motor unit, 100; motor unit radius, 2,500 μm; firing frequencies, 5–30 Hz; frequency variability, ±2 Hz; and contraction force, 30%. An effort was made to distribute motor units randomly in the muscle by manually positioning the center of each unit so that a uniform density of muscle fibers was obtained. Each simulated muscle was restricted to a diameter of 2.5 cm.

Two concentric needle electrodes from the model were used in the simulation studies,[9] one with a large uptake area to simulate a standard-size concentric needle electrode, and one with a smaller uptake area to simulate a pediatric-size concentric needle. Recordings were made from different longitudinal positions along the muscle, resulting in several sets of MUAP data. In this muscle model, the "0" end-plate zone covers an area of ±2 mm, but because the "0" end-plate zone is artificially narrow, sets of 20 MUAPs were recorded starting nominally at +5 mm from the end-plate zone (±2 mm) and at a position 75 mm distant (maximum distance possible in the model). In the first set of recordings, the radial position of the electrode in the muscle (defined as the distance from the center of the muscle) was constant and the same MUAPs were recorded at both positions. In the second set, the electrode was placed at different radial positions and different MUAPs were recorded at both positions. Overall, 20 MUAPs were recorded at each of the sites. Duration markers were determined by the simulator software algorithm and could not be changed manually. Amplitude values were determined by the simulator software algorithm, but only MUAPs >200 μV were included because 200 μV is a reasonable visual limit during routine EMG studies. Numbers of turns and phases were counted manually using an amplitude criterion of >25 μV for both.

A second muscle simulation model (not commercially available; available from the author at stashuk@pami.uwaterloo.ca) was developed by Hamilton-Wright and Stashuk[8] (thus designated the H-W/S model) and creates whole muscles by taking the number of desired motor units and calculating the muscle diameter needed to contain that number of units. The center of the motor unit is placed within the muscle to simulate the even and random distribution of motor units. Muscle-fiber distribution within the motor unit is performed in a similar manner. Muscle-fiber diameters are selected from a Gaussian distribution specific to each motor unit so that the overall mean fiber diameter is 55 μm with a standard deviation of 9 μm.

A model of a standard concentric needle electrode was placed randomly within the radial plane of the muscle at the end-plate zone and a MUAP train (MUAPT) consisting of a number of motor units within the uptake area of the electrode was created. Similar placements of the electrode in the muscle were made in this model as in the first model to record sets of 20 MUAPTs at the end-plate zone (which represents a distribution ±5 mm from zero) and 50 mm away (maximal distance from the endpoint allowed by the software) and different MUAPTs at the end-plate zone and 50 mm away. Individual MUAPs were extracted from MUAPTs by software algorithms that detect the presence of each motor unit in the train. A total of 17 MUAPs were obtained at each site. Metrics of amplitude and duration of isolated MUAPs were initially determined by algorithms within the software. MUAPs with amplitudes >200 μV were included. Duration markers were occasionally changed. Numbers of turns and phases were manually counted using an amplitude criterion of >25 μV for both.

We also studied a model of a single-fiber electrode (available for the K/S model) to determine the effect of greater conduction distance on the separation of single muscle-fiber action potentials (based on default mean fiber diameter of 50 ± 5 μm). Detection of single-fiber action potentials was by established criteria.[12]

Biologic Data. This portion of the study was approved by our institutional review board, and informed consent was obtained. Studies were performed in the biceps brachii muscle: five muscles were from normal subjects, one was from a patient with dermatomyositis (DM), and five from patients with amyotrophic lateral sclerosis (ALS). A pediatric-size concentric needle electrode (25-mm long, 0.3-mm diameter, 0.03-mm^2 recording area; Teca-Oxford Instruments, Hawthorne, New York) was used for subject comfort. Data were acquired using decomposition-based quantitative electromyography (DQEMG) software[4] on a Compumedics Neuroscan EMG machine (El Paso, Texas). The physiologic end-plate zone was identified by moving a 10-mm disc cathode electrode (anode electrode placed proximally over the musculocutaneous nerve), using low-intensity shocks to locate the site of maximal muscle contraction. Twenty acceptable MUAPs were obtained with the electrode at the physiologic end-

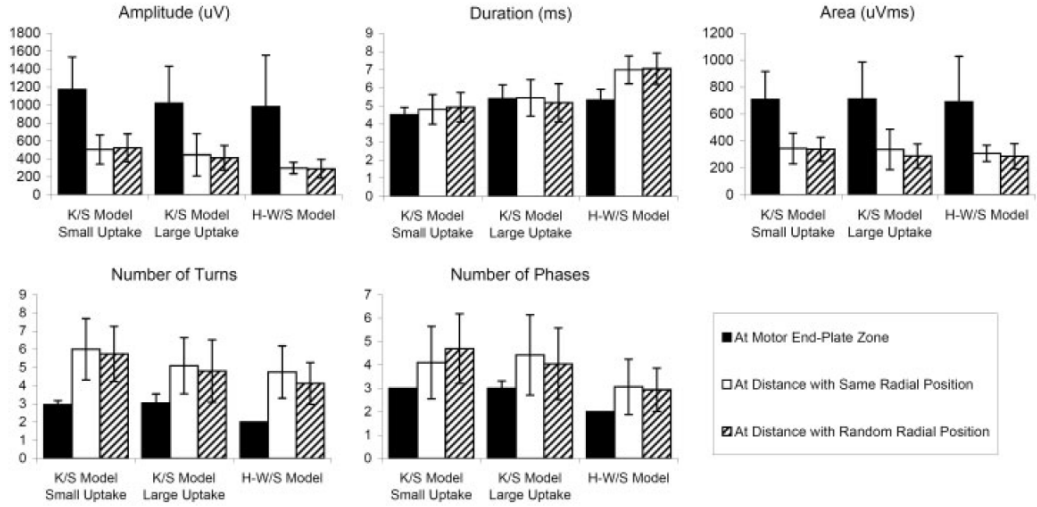

FIGURE 1. Average MUAP metric values for each of the modeled muscles (20 MUAPs for each K/S model and 17 MUAPs for H-W/S model) recorded at the end-plate zone (5 mm from "0") compared to the same (same radial position) or random (random radial position) MUAPs recorded at a distance from the end-plate zone (75 mm for each K/S model and 50 mm for H-W/S model). Error bars represent one standard deviation. There are statistically significant differences ($P < 0.05$) for measurements made at the end-plate zone compared to those made at both the same and different random radial positions for all metrics except duration.

plate zone and from a position 100 mm proximal to the end-plate zone. At the distal site, care was taken to avoid the tendon by assessing for insertional activity and voluntary motor units as indications of being in muscle. MUAP metrics were determined by the same algorithm used for the H-W/S model.

Statistical Analysis. Analysis was performed on averaged data from 20 MUAPs from each longitudinal site in modeled and biologic muscles. Statistically significant differences were determined by two-tailed *t*-tests. Significance was assumed at *P*-values <0.05 for single comparisons and <0.02 for multiple comparisons.

RESULTS

Simulated Data. Average MUAP metrics from modeled muscles (Fig. 1) show that all values change with greater distance from the end-plate zone (specifically, there are decreases in amplitude and area, and increases in duration and numbers of turns and phases). Among the metrics, amplitude values change the most with distance. The results are not different when the same MUAPs (identical radial position) are compared to different MUAPs (random radial position) for all metrics. The same results are found whether electrodes with large or small uptake areas are modeled (Table 1).

Within the model of a single-fiber electrode, there is an average increase in fiber density from 1.4 close to the end-plate zone to 2.4 when recorded 75 mm away.

Biologic Data. Average MUAP metrics from the biceps brachii muscle from normal subjects and those with DM and ALS are shown in Figure 2. With few exceptions among individual subjects, all metrics change in the expected directions with greater distance from the physiologically determined end-plate zone. Exceptions to the expected changes were not distributed in any consistent pattern among individual normal subjects and those with ALS. Few changes are statistically significant ($P < 0.02$ for multiple comparisons), and the magnitude of the changes is such that none are likely to be considered clinically significant. When the results from each muscle group type are combined, no significant differences are found in any metric. When the changes with longitudinal distance from simulated data are compared to biologic data, there are lesser effects of distance on the metrics of amplitude, area, and numbers of turns and phases in biologic data (Table 2).

DISCUSSION

We investigated the effects of longitudinal electrode position within muscle with respect to averaged quantitative MUAP metrics, as would be gathered with quantitative EMG techniques, to assess the clinical effects of temporal dispersion of arriving muscle-

Table 1. MUAP metrics comparing modeled concentric electrodes with large (standard size) and small (pediatric size) uptake areas.*

Site	Variable	Small uptake	Large uptake	Comparison (*P*-value)
5 mm	Amplitude (μV)	1,174 (360)	1,022 (411)	0.217
	Duration (ms)	4.52 (0.4)	5.40 (0.76)	<0.001
	Area (μVms)	709 (206)	712 (274)	0.971
	Turns	2.95 (0.22)	3.05 (0.5)	0.427
	Phases	3.00 (0.0)	3.00 (0.32)	1.000
80 mm	Amplitude (μV)	504 (162)	445 (235)	0.359
	Duration (ms)	4.81 (0.82)	5.44 (1.01)	0.033
	Area (μVms)	344 (114)	337 (150)	0.863
	Turns	6.00 (1.69)	5.10 (1.55)	0.081
	Phases	4.10 (1.55)	4.43 (1.72)	0.525

MUAP, motor unit action potential.
**MUAP metrics obtained at two longitudinal sites in the muscle (5 mm and 80 mm from the end-plate zone). Values represent averages with standard deviations in parentheses.*

fiber action potentials. Electrophysiologic modeling is useful to enhance understanding of the factors that influence MUAP waveform shape and metric values but it is important to test predictions in normal and diseased muscle to determine which aspects are numerically and clinically important. Two muscle simulation models were used that differ in the assembly of motor units within the muscle, but similar results were obtained with each model. There were no statistical differences whether the same or random MUAPs were compared at the two distances. Previous modeling studies assessed the effects of temporal dispersion on single[10,13] and multiple[11] MUAPs and found similar changes. Other studies have investigated gross needle position (at middle and distal sites) within biologic muscle.[7] We attempted to improve on these by locating the center of the end-plate zone and taking recordings at greater measured distances. By increasing the distances used in previous studies, we exaggerated the degree of dispersion and compared our simulated data to biologic data (in both normal and pathologic muscle).

In modeled muscles, we found a fall in MUAP amplitude distant from the end-plate zone that likely can be attributed to changes in the spatial relation of

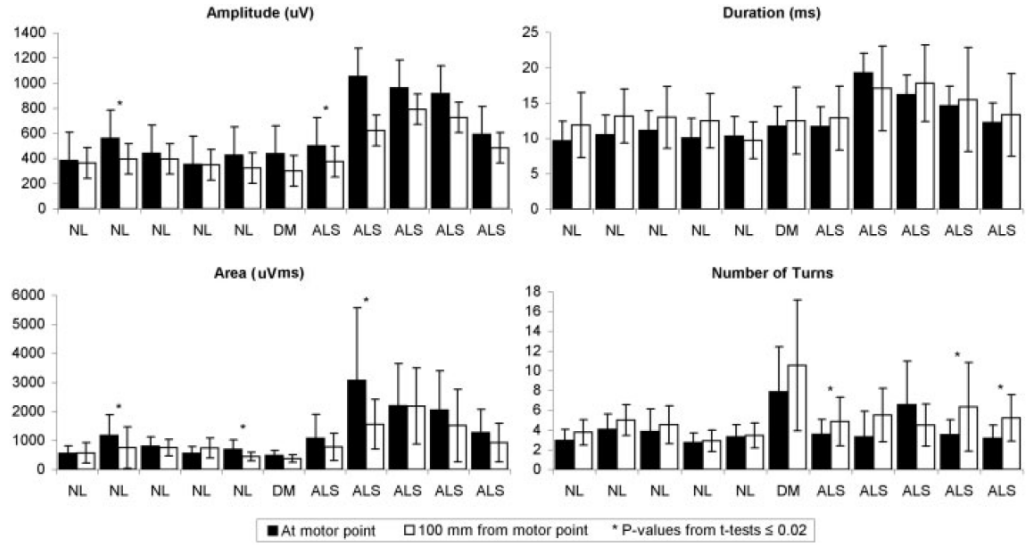

FIGURE 2. Average metric values of 20 MUAPs recorded in the biceps brachii muscle at the physiologically determined end-plate zone and 100 mm distant. NL represents normal subjects, DM subject with dermatomyositis, and ALS subjects with amyotrophic lateral sclerosis. Error bars represent one standard deviation. Bar graph of number of phases not shown, but trends are very similar to graph of number of turns. Only the last ALS patient had a statistical difference in number of phases.

Table 2. Percent change in MUAP metrics with greater conduction distance in modeled muscle (both models) compared to those from normal subjects and those with ALS.*

Muscle	Amplitude (μV)	Duration (ms)	Area (μVms)	Turns	Phases
Modeled	−53.6% (12.1)	31.6% (8.5)	−43.6% (11.7)	96.4% (55.4)	70.1% (51.6)
Normal	−13.8% (12.3)	16.8% (13.0)	−7.9% (29.2)	16.0% (9.8)	1.4% (6.4)
ALS	−24.4% (9.7)	4.8% (9.2)	−26.0% (17.4)	43.8% (45.0)	18.4% (25.5)

ALS, amyotrophic lateral sclerosis; MUAP, motor unit action potential.
**Percent values represent average metrics (and standard deviations) measured at the end-plate zone and at a distance (modeled muscles = 50 and 80 mm; biologic muscles = 100 mm).*

the contributing dipoles to the recording electrode and the effects of phase interaction.[10] The increase in the number of turns and phases can also be attributed to greater temporal separation of contributing muscle-fiber action potentials. MUAP duration is increased, but to a lesser degree than other metrics. A study using shorter interelectrode distances found no difference in average duration.[6] The effect of temporal dispersion on duration is emphasized by using greater interelectrode spacing. It has been noted that the greatest changes in metrics occur over the first 10 mm away from the end-plate zone,[11] but we assessed greater distances from the end-plate zone and found no differences in average metrics when different sizes of end-plate zones were studied.

There are a variety of electrodes to choose from with respect to configuration and size. We chose a pediatric-size concentric needle electrode for subject comfort. In a separate study (submitted for publication), we found no clinically significant difference in MUAP metrics recorded with standard- or pediatric-sized concentric electrodes in biologic muscles. We used models of concentric needle electrodes in the modeled muscle studies, including electrodes with large and small recording uptake radii, and found no significant differences (Table 1). Thus our results are applicable to any size of concentric (and likely monopolar) electrode.

When we studied a model of a single-fiber electrode to determine whether fiber pairs are merged into a single waveform when recorded close to the end-plate zone, we found an average increase in fiber density from 1.4 close to the end-plate zone to 2.4 when recorded 70–75 mm away. This shows the effects of temporal dispersion on the simplest motor unit.

For the study in biologic muscles we chose the biceps brachii because muscle fibers are long and parallel, matching more closely the modeled muscles and permitting comparisons of electrode recording distances up to 100 mm from the end-plate zone. We found similar changes in MUAP metrics recorded at greater distances from the endpoint zone. Duration values were larger, which contrasts with a study comparing both clinical and physiologic duration values from the same MUAP recorded at two sites 16–20 mm apart in the biceps brachii muscle in normal subjects where no differences are noted in either duration value.[6] However, another study based on multi-unit acquisition, and similar in design to our study, found increased duration between recording in the middle third and distal third of the biceps brachii muscle (interelectrode distances not given).[7] Thus, empiric evidence supports an increase in clinical MUAP duration with greater distance from the end-plate zone, but underlying factors remain unexplained.

Comparisons between modeled and biologic data from normal subjects obtained at the end-plate zone revealed higher average amplitude, shorter duration, but similar numbers of turns and phases in modeled muscles. MUAP amplitude in biologic recordings can be optimized by electrode adjustments, but we used multi-motor unit recording techniques that do not optimize amplitude.[2] Greater amplitude in modeled data likely also reflects simplifications in the model, including lack of background activity that could degrade amplitude. MUAP duration values vary among modeled muscles, but are always shorter than in biologic muscle by factors of 2 to 5 times. One factor in modeled MUAPs is the marking algorithm; some duration markers appeared short but could not be manually set and were placed in a consistent fashion. The longer duration values in biologic data reflect different marking algorithms and may also be due to the presence of more fibers in biologic than modeled MUAPs, since duration is proportional to the number of fibers in the electrode recording radius.[10] Other factors are the degree of background noise that is dependent upon the number of waveforms averaged to yield the measured MUAP waveform (52 waveforms are averaged in the decomposition algorithm), and the use of marking algorithms with manual resetting (visual assessment of duration was conservative, likely resulting in shorter rather than longer duration values).

Comparisons between biologic data in normal subjects and those with myopathic and neuropathic MUAPs reveals similar changes in all metrics with distance but greater variability among metrics within subjects, as is expected with a range of pathologic involvement. Degrees of change in pathologic MUAP metrics with distance are greater for amplitude and number of turns, and relatively less for duration and number phases (Table 2). Pathologic muscles were not modeled because MUAP changes at greater conduction distances are clearly evident in models of normal muscles. Similar discrepancies are noted between modeled and biologic data for numbers of phases, and have been attributed to assumptions about the relationship between muscle-fiber diameter and conduction velocity.[10]

A major difference in muscle architecture between simulated and biologic muscle is the precision of the size and position of the end-plate zone. In modeled muscles, it is over a zone of ±2 mm (K/S model) or of ±5 mm (H-W/S model). In biologic muscle, an end-plate zone was identified by physiologic methods, but its boundaries were not fully known. Histologic data on the distribution of neuromuscular junctions in the biceps brachii muscle indicate a primary clustering of end-plates in a longitudinally oriented "V" distribution that occupies at least the middle third of the muscle,[1] and in the tibialis anterior a diffuse distribution over the entire length.[1] Muscle fibers in complex muscles are relatively short, and the distance from the end-plate zone to the electrode will be much less than the 100-mm distances studied here. The zone of innervation for a single motor unit in human muscle is not known and likely spans 5–10 mm. Electrophysiologic data from surface multi-electrode recording techniques indicate that within a muscle the peak amplitudes of single MUAPs are distributed over a relatively broad area.[3] Further, clinical experience with recording end-plate activity suggests that the end-plate region may differ widely from person to person. We conclude that true distances for temporal dispersion are actually short in biologic muscle and this largely accounts for the minimal effect of electrode position within a muscle. Thus, electrode position within a muscle is unlikely to affect clinical MUAP interpretation.

Portions of this research were funded by the Richard K. and Shirley S. Hemingway Foundation. The authors thank Summer Davis, BA, for her assistance with data recording, as well as Erik Stålberg, MD, PhD, and Lars Karlsson, PhD, for their comments on the manuscript.

REFERENCES

1. Aquilonius S, Askmark H, Gilberg P, Nandedkar S, Olson Y, Stalberg E. Topographical localization of motor endplates in cryosections of whole human muscles. Muscle Nerve 1984;7: 287–293.
2. Bischoff C, Stålberg E, Falck B, Eeg-Olofsson K. Reference values of motor unit action potentials obtained with multi-MUAP analysis. Muscle Nerve 1994;17:842–851.
3. Blok JH, Van Dijk JP, Zwarts MJ, Stegeman DF. Motor unit action potential topography and its use in motor unit number estimation. Muscle Nerve 2005;32:280–291.
4. Doherty T, Stashuk D. Decomposition-based quantitative electromyography: methods and initial normative data in five muscles. Muscle Nerve 2003;28:204–211.
5. Dumitru D, King J. Motor unit action potential duration and muscle length. Muscle Nerve 1999;22:1188–1195.
6. Dumitru D, King J, Rogers W. Motor unit action potential components and physiologic duration. Muscle Nerve 1999;22: 733–741.
7. Falck B, Stalberg E, Bischoff C. Influence of recording site within the muscle on motor unit potentials. Muscle Nerve 1995;18:1385–1389.
8. Hamilton-Wright A, Stashuk D. Physiologically based simulation of clinical EMG signals. IEEE Trans Biomed Eng 2005; 52:171–183.
9. Karlsson L, Hammarberg B, Stalberg E. An application of a muscle model to study electromyographic signals. Comput Methods Programs Biomed 2003;71:225–233.
10. Nandedkar S, Sanders D, Stalberg E, Andreassen S. Simulation of concentric needle EMG motor unit action potentials. Muscle Nerve 1988;11:151–159.
11. Stalberg E, Karlsson L. Simulation of the normal concentric needle electomyogram by using a model. Clin Neurophysiol 2000;112:464–471.
12. Stålberg E, Thiele B. Motor unit fibre density in the extensor digitorum communis muscle. J Neurol Neurosurg Psychiatry 1975;38:874–880.
13. Zalewska E, Hausmanowa-Petrusewicz I, Stalberg E. Modeling studies on irregular motor unit potentials. Clin Neurophysiol 2004;115:543–556.

Needle Electrode Selection

A variety of needle electrodes are available for clinical use for an EMG study, and among the concentric needle design there are two sizes available; a standard size (described earlier) and a smaller pediatric sized needle. The difference in size of the needle is reflected in the uptake area of the active electrodes. The standard electrode has a recording surface of 0.07 mm^2 and the pediatric a surface of 0.03 mm^2. We sought to determine if there was a clinically significant difference in the MUAPs recorded from the two different sized electrodes (54).

Another reason for this study is that the smaller electrodes can be used in place of single fiber electrodes for measurement of neuromuscular jitter. Verifying the use of the smaller electrode for multi-MUAP analysis can expand the utility of a single electrode for complex cases. Further, the smaller electrode is more comfortable for the patient.

This question was first investigated using the Stålberg model and then in the biceps brachii, first dorsal interosseous, and anterior tibialis muscles of several volunteers, as these are commonly studied muscles in the clinical setting. To add robustness to the findings, subjects with both healthy and diseased muscle were studied. In this portion of the study in muscle, efforts were made to ensure that the same region of the muscle was studies with each needle in each subject. An attempt was made to insert both electrodes together to ensure recording from the same region of the muscle but this did not allow individual adjustment of the two electrodes to optimize recording features.

There were some issues using the model—which ultimately led to exclusion of this portion of the data from the published paper. The simulated electrodes were not created with the intention to precisely mimic the standard and pediatric sized needle

electrodes; rather, they were simply “large uptake” and “small uptake” area electrodes. We went forward and completed the simulated study with these different electrodes and found significant differences in duration and area, though amplitude, turns, and phases were statistically similar (Table 2.1).

Table 2.1: Results of needle size comparison using the Stålberg model. Results are similar for metrics of amplitude, turns and phases; while results for duration and area are markedly different. When differences were found in biologic muscle the differences did not match those found in the model.

Comparison of Simulated Needle Metrics

	Small Uptake Mean (SD)	Large Uptake Mean (SD)	P-value
Amplitude (μV)	407 (281)	433 (263)	0.505
Duration (ms)	4.51 (1.37)	5.90 (1.7)	< 0.001
Area (μVms)	294 (175)	403 (202)	< 0.001
Turns	4.75 (1.8)	4.71 (1.72)	0.873
Phases	3.94 (1.65)	3.67 (1.59)	0.244

Comparison of Standard and Pediatric Size
Concentric Needle EMG Electrodes

Reprinted with permission from Clinical Neurophysiology 118: 1162-1165

ELSEVIER

Clinical Neurophysiology 118 (2007) 1162–1165

www.elsevier.com/locate/clinph

Comparison of standard and pediatric size concentric needle EMG electrodes

Alexander A. Brownell, Mark B. Bromberg *

Department of Neurology, University of Utah, 50 North Medical Drive, Salt Lake City, UT 84132, USA

Accepted 20 January 2007

Abstract

Objective: To compare motor unit action potential (MUAP) metrics recorded by standard and pediatric size concentric EMG electrodes.
Methods: Commercial electrodes were used to record MUAPs from biceps brachii, first dorsal interosseous and tibialis anterior muscles in normal subjects and those with amyotrophic lateral sclerosis (ALS).
Results: In normal subjects, peak amplitude and area were significantly higher when recorded by the pediatric size electrode in tibialis anterior muscles and peak amplitude recorded in first dorsal interosseous muscles. In ALS subjects, peak amplitude was higher recorded by the pediatric size electrode in tibialis muscle but lower when recorded in first dorsal interosseous muscles.
Conclusions: Differences of MUAP metrics when recording with standard and pediatric size electrodes do not seem to have a clinical relevance.
Significance: Pediatric and standard concentric electrodes record similar MUAP metrics.

Keywords: EMG; Concentric electrodes; Motor unit action potential; MUAP; Electrode comparison

1. Introduction

There are two basic concentric needle EMG electrodes that differ in the diameter of the active electrode and thus exposed recording surface, the diameter of the reference (cannula), and total electrode length. We found no data comparing motor unit action potential (MUAP) metrics recorded by these two electrode configurations but our empiric observations are that MUAPs recorded by these electrodes are similar. Therefore, we undertook a formal comparison of a standard concentric electrode with a diameter of 0.45 mm to a pediatric size concentric electrode with a diameter of 0.30 mm assessing their respective MUAP metrics in biologic muscles.

2. Methods

This study was approved by the Institutional Review Board at the University of Utah and informed consent was obtained. Two disposable concentric needle electrodes were used: Teca standard (X553156) with 37 mm length, 0.45 mm diameter, and 0.07 mm^2 recording area; and Teca pediatric (X553153), with 25 mm length, 0.30 mm diameter, and 0.03 mm^2 recording area (Viasys Healthcare, Hawthorne, NY). MUAPs were recorded with both electrodes in the biceps brachii, the first dorsal interosseous of the hand, and tibialis anterior muscles. Each of these three muscles was studied in 5 normal subjects and 2 with probable or definite amyotrophic lateral sclerosis (ALS) and each muscle studied had Medical Research Counsel grade 4+ to 3+ strength.

Efforts were made to optimize the probability that the two electrodes recorded from similar regions of muscle and under similar contraction force. The electrodes were inserted perpendicular to the surface of the muscle and

Abbreviations: MUAP, motor unit action potential; ALS, amyotrophic lateral sclerosis.

* Corresponding author. Tel.: +1 801 585 5885; fax: +1 801 585 2054.
E-mail address: mbromberg@hsc.utah.edu (M.B. Bromberg).

1388-2457/$32.00
doi:10.1016/j.clinph.2007.01.016

within 3–4 mm of each other along the longitudinal axis of the muscles. The planes of the electrode bevels were kept as parallel as possible to each other. Adjustments of the electrode recording position were made to record crisp MUAP sounds. We initially tried to record from both electrodes simultaneously but it was difficult to ensure crisp sounds from each electrode and thus recordings were made consecutively at each depth. The level of muscle contraction was maintained as constant as possible with aural feedback from the EMG machine's speaker. Equipment to assess contraction force directly was not available for this study, but MUAP discharge rates were recorded as a measure of activation level. The electrodes are of different lengths, and the depth of the standard electrode was restricted to 25 mm.

MUAPs were extracted during a steady submaximal contraction by the Multi-MUP software program available on the Teca Synergy EMG machine (Viasys Healthcare, Hawthorne, NY). Ten-second epochs of a weak interference pattern were recorded from each electrode at similar depths in the muscles. Filters were set at 10–20,000 Hz. Two Synergy machines were used, one connected to each electrode. Extracted MUAPs and their discharge patterns were visually inspected and those accepted had at least 20 waveforms averaged and peak amplitude >50 μV. MUAPs were excluded if the main spike was exclusively positive (cannula potential) or markers were grossly aberrant. Recordings were made in each muscle until at least 20 MUAPs were obtained which met the stated criteria. MUAP marking algorithms from the Multi-MUP software were used and no marker adjustments were made allowing the marker algorithms to be applied consistently.

Statistical analysis for comparisons between standard and pediatric electrodes for both biologic and simulated muscles was made by two-sided *t*-tests. Because multiple comparisons are made, a Bonferroni adjustment was made (0.05/7 MUAP metrics) and *P* values <0.007 are considered significant.

3. Results

The average number of acceptable MUAPs per contraction is 3.01 for the standard needle and 3.09 for the pediatric needle ($P = 0.52$). When MUAPs from the three muscles are analyzed separately for normal subjects there are no significant differences between metrics for the biceps brachii muscle but there are for the first dorsal interosseous muscle for area and the tibialis anterior muscle for peak amplitude and area (Table 1). Similar analysis for the three muscles in ALS subjects indicates no significant differences in the biceps brachii muscle, but significant differences in the first dorsal interosseous muscle for peak amplitude, area and area:amplitude ratio, and in the tibialis anterior muscle for peak amplitude (Table 1). There are no significant differences in discharge rates recorded in the same muscle by the two electrodes in

Table 1
Motor unit action potential (MUAP) metric data from biceps brachii, first dorsal interosseous (FDIH), tibialis anterior muscles from normal subjects and those with amyotrophic lateral sclerosis (ALS)

	Biceps				FDIH				Tibialis anterior				
	Pediatric $N = 265$		Standard $N = 233$		*P*-value	Pediatric $N = 201$		Standard $N = 179$		*P*-value	Pediatric $N = 245$		Standard $N = 235$		*P*-value
Normal muscles															
Amplitude (μV)	395	(187)	376	(180)	0.270	850	(535)	749	(553)	0.070	853	(488)	610	(326)	<0.001
Duration (ms)	14.66	(3.83)	15.02	(3.53)	0.280	12.34	(3.77)	12.97	(3.91)	0.112	17.26	(3.82)	16.56	(3.53)	0.036
Phases	3.91	(1.27)	3.77	(1.21)	0.221	3.69	(1.54)	3.69	(1.29)	0.967	3.67	(1.11)	3.73	(1.23)	0.561
Turns	2.57	(.96)	2.46	(.81)	0.169	2.74	(.93)	2.81	(.97)	0.482	3.31	(1.07)	3.05	(1.08)	0.007
Area (μVms)	728	(379)	726	(375)	0.955	1220	(739)	1024	(596)	0.005	1829	(974)	1291	(689)	<0.001
Ratio	1.88	(.53)	1.97	(.53)	0.073	1.50	(.44)	1.46	(.48)	0.435	2.25	(.58)	2.20	(.63)	0.387
Rate (pps)	7.27	(2.4)	6.99	(2.53)	0.205	6.78	(2.27)	6.66	(2.51)	0.634	6.98	(1.89)	7.19	(2.12)	0.257
	$N = 79$		$N = 76$		*P*-value	$N = 77$		$N = 67$		*P*-value	$N = 59$		$N = 76$		*P*-value
ALS muscles															
Amplitude (μV)	1025	(631)	892	(543)	0.164	1570	(1124)	2368	(1317)	<0.001	1896	(1146)	1429	(745)	0.005
Duration (ms)	18.88	(4.84)	19.11	(4.26)	0.756	15.89	(5.36)	15.55	(4.11)	0.672	17.82	(3.81)	19.21	(5.13)	0.083
Phases	3.77	(1.25)	3.71	(1.24)	0.759	2.84	(.9)	3.25	(1.34)	0.031	3.32	(.86)	3.62	(1.15)	0.102
Turns	3.29	(1.04)	3.71	(1.29)	0.027	2.94	(1.08)	3.18	(1.03)	0.169	3.81	(1.25)	3.63	(1.18)	0.388
Area (μVms)	2374	(1384)	2344	(1658)	0.901	3111	(1779)	4297	(2313)	0.001	4486	(2974)	3687	(1938)	0.062
Ratio	2.39	(.64)	2.64	(.97)	0.057	2.13	(.56)	1.84	(.46)	0.001	2.41	(.56)	2.65	(.76)	0.042
Rate (pps)	9.11	(2.6)	9.09	(2.68)	0.959	8.70	(2.2)	9.33	(2.45)	0.108	8.69	(1.7)	8.74	(2.33)	0.908

Comparisons are between metrics recorded with pediatric and standard size concentric needle electrodes. Values are averages (standard deviations).

either normal or ALS muscles, but the discharge rate is higher in ALS subjects (Table 1).

4. Discussion

We compared two sizes of concentric electrodes, a larger standard electrode and a smaller electrode commonly used for pediatric age patients and for adult patients when comfort is an issue and only a few superficial muscles are to be studied. Three frequently studied muscles were chosen with different muscle fiber orientations to represent a suitable range of recording conditions. A Multi-MUP software program was used to extract a wide range of MUAPs that match the spectrum of MUAPs assessed qualitatively during routine EMG studies (Bischoff et al., 1994). No changes in the automated MUAP marker placements were made to ensure the application of uniform marking rules. The Multi-MUP software we used has been assessed in a comparison study and has been shown to be robust in terms of MUAP isolation and marking of metrics (Brownell et al., 2005).

MUAP metric values from normal muscle in our study are similar to those reported when consideration is given to differences in Multi-MUP software algorithms used (Howard et al., 1988; Bischoff et al., 1994). Our MUAP amplitude values are somewhat lower, most likely attributable to the low amplitude criterion (>50 μV) used as well as not using a rise-time criterion (not part of the Multi-MUP software) (Barkhaus and Nandedkar, 1996). Our MUAP duration values are longer because we did not change markers. Muscle contraction levels are consistent between electrode recordings within a muscle based on similar motor unit discharge rates.

We find few significant differences in MUAP metrics recorded with standard and pediatric size electrodes and note that the standard deviations are similar. Peak amplitude is significantly higher with the pediatric size electrode only for normal and ALS subjects from the tibialis anterior muscle. Conversely, MUAP amplitude is significantly lower for the pediatric size electrode in the first dorsal interosseous muscle in ALS subjects. MUAP area, not unexpectedly, is also occasionally observed to be significantly greater when amplitude is higher. The higher discharge rate in ALS subjects likely reflects the effects of reduced motor unit number and consequent compensatory increases in the rate component of recruitment. None of the scattered statistically significant differences between electrodes are likely to be of sufficient magnitude to be clinically significant from the perspective of quantitative EMG. Further, any quantitative MUAP differences are not likely to be detected from the perspective of routine qualitative EMG studies.

The lack of clinically significant and consistent differences in MUAP metrics from the pediatric size electrode with a recording area that is <50% of the area of the standard electrode (0.03 mm^2 vs. 0.07 mm^2) may be explained by simulation studies by Nandedkar and coworkers on the factors that influence MUAP metrics recorded by a standard concentric electrode (Nandedkar et al., 1988). In these studies, the amplitude of the main spike component is attributed to muscle fiber action potentials closest to the recording surface and both amplitude and area fall markedly and linearly with distances up to 1 mm from the electrode. The amplitude and area of a recorded MUAP depend both on the size of the recording surface (Ekstedt and Stålberg, 1973) and on the distribution of muscle fibers (Nandedkar et al., 1988). Even though the area of the standard and pediatric recording surfaces differs by a factor of two, the results of the present study show that this difference is not sufficient to cause a substantial difference in the size of the recorded MUAPs. The studies of Nandedkar and coworkers also show that the distance between the recording surface of the electrode and the nearest muscle fiber action potentials does not affect MUAP duration, and MUAP turn and phase number is dependent upon the temporal dispersion of arriving muscle fiber action potentials from the motor end-plate zone. These factors for duration and complexity should also apply for pediatric size electrodes.

We show that MUAPs recorded with the smaller pediatric size concentric electrode are similar to those recorded with the standard concentric electrode and differences in peak amplitude are not consistent between the two electrodes or across muscles and disease states and are not likely to be clinically significant. Further, any differences between concentric electrodes of different diameters are less than differences between monopolar and concentric electrodes (Howard et al., 1988; Pease and Bowyer, 1988; Chan and Hsu, 1991; Kohara et al., 1993; Trojaborg, 1998). Thus, MUAPs recorded with a pediatric size concentric electrode can be compared to data from a standard size concentric electrode.

Acknowledgements

Portions of this research were funded by the Richard K. and Shirley S. Hemingway Foundation. The authors thank Summer Davis and Luke Petersen for assistance with data recording.

References

Barkhaus PE, Nandedkar SD. On the selection of concentric needle electromyogram motor unit action potentials: is the rise time criterion too restrictive? Muscle Nerve 1996;19:1554–60.

Bischoff C, Stålberg E, Falck B, Eeg-Olofsson K. Reference values of motor unit action potentials obtained with multi-MUAP analysis. Muscle Nerve 1994;17:842–51.

Brownell AA, Ni O, Bromberg MB. Comparison of three algorithms for multi-motor unit detection and waveform marking. Muscle Nerve 2005;33:538–45.

Chan RC, Hsu TC. Quantitative comparison of motor unit potential parameters between monopolar and concentric needles. Muscle Nerve 1991;14:1028–32.

Ekstedt J, Stålberg E. How the size of the needle electrode leading-off surface influences the shape of the single muscle fibre action potential in electromyography. Comput Programs Biomed 1973;3:204–12.

Howard JE, McGill KC, Dorfman LJ. Properties of motor unit action potentials recorded with concentric and monopolar needle electrodes: ADEMG analysis. Muscle Nerve 1988;11:1051–5.

Kohara N, Kaji R, Kimura J. Comparison of recording characteristics of monopolar and concentric needle electrodes. Electroencephalogr Clin Neurophysiol 1993;89:242–6.

Nandedkar S, Sanders D, Stålberg E, Andreassen S. Simulation of concentric needle EMG motor unit action potentials. Muscle Nerve 1988;11:151–9.

Pease WS, Bowyer BL. Motor unit analysis. Comparison between concentric and monopolar electrodes. Am J Phys Med Rehabil 1988;67:2–6.

Trojaborg W. The concentric versus the monopolar needle electrode. The case for concentric needles. Muscle Nerve 1998;21:1806–8.

Optimizing Acquisition Time

The algorithms used to detect MUAPs in QEMG studies require that many discharges of the same MUAP be collected and averaged in order to ensure a fair representation of the isolated MUAP and distinguish it reliably from other MUAPs (40). As discussed earlier, the major contributions to the MUAP come from muscle fibers of the motor unit within 500 μm of the electrode. Thus, very small movements away from or toward the closest fibers may cause large changes in the MUAP morphology. Such movements come from respiratory and cardiac movements of both the patient and the operator, from physiologic tremor of the operator, and hysteresis of muscle tissue displaced by initial positioning of the electrode. Different QEMG algorithms collect data for varying amounts of time, 10-30 s. This study was undertaken to determine an optimal time for the collection of EMG data, balancing the need to collect sufficient MUAPs for a stable average with most noise removed and the likelihood of needle movement within the muscle that could change the MUAP morphology (55).

Thirty seconds of EMG data was collected in human volunteers using the DQEMG algorithm, commercially available (Neuroscan; Compumedics, Ltd., San Antonio, Texas) and the raw data were exported and analyzed in MATLAB (The MathWorks, Natick, Massachusetts). Two types of interference patterns were collected, simple with one MUAP and complex with two or more MUAPs.

For the simple interference patterns, data were exported for analysis with MATLAB. A custom waveform marking algorithm was created. It was determined at what time each MUAP fired and marked the metrics of each individual MUAP. Great care was taken during collection of these epochs of EMG data to reduce noise from any

source. This allowed for relatively good measurement on non-averaged MUAPs. Peak to peak amplitude was very straightforward to measure. Duration was the most difficult metric to determine. The difficulty arises due to the uncertainty of exactly when an excursion from baseline represents the beginning of an MUAP versus being part of the background noise, and when the waveform merges back to the baseline at the end of the MUAP (12). A threshold was set working forward through the signal using a moving average. When the threshold was met the algorithm would then work backward to determine the appropriate takeoff of the MUAP. A similar method was used to determine the termination of the MUAP. Once duration was determined the other metrics could be measured. Area was measured by a simple rectified numerical integration. Turns and phases were measured using a numerical derivative that provided sign changes. Once the sign of the slope changed, either from the beginning of the single MUAP or from the previous sign change, the algorithm examined the original waveform to determine if the appropriate turn or phase amplitude threshold was met. A threshold for numbers of turns and phases was set at a displacement of the signal of greater than or equal to 25 μV. If the turn or phase did not meet the amplitude criterion it was ignored and the algorithm continued to search from the last true turn or phase in order not to miss a legitimate turn or phase because of some small noise in the signal.

Metrics were measured for each firing of an MUAP (Figure 2.2) and for each contraction length (2, 5, 10, 15, and 30 s) it was determined what effect the changes in each metric over time would have on the averaged MUAP (Figure 2.3). Since not all algorithms choose the same MUAPs from the train for averaging the effect was measured in several different ways: using a running average, averaging all, and averaging randomly

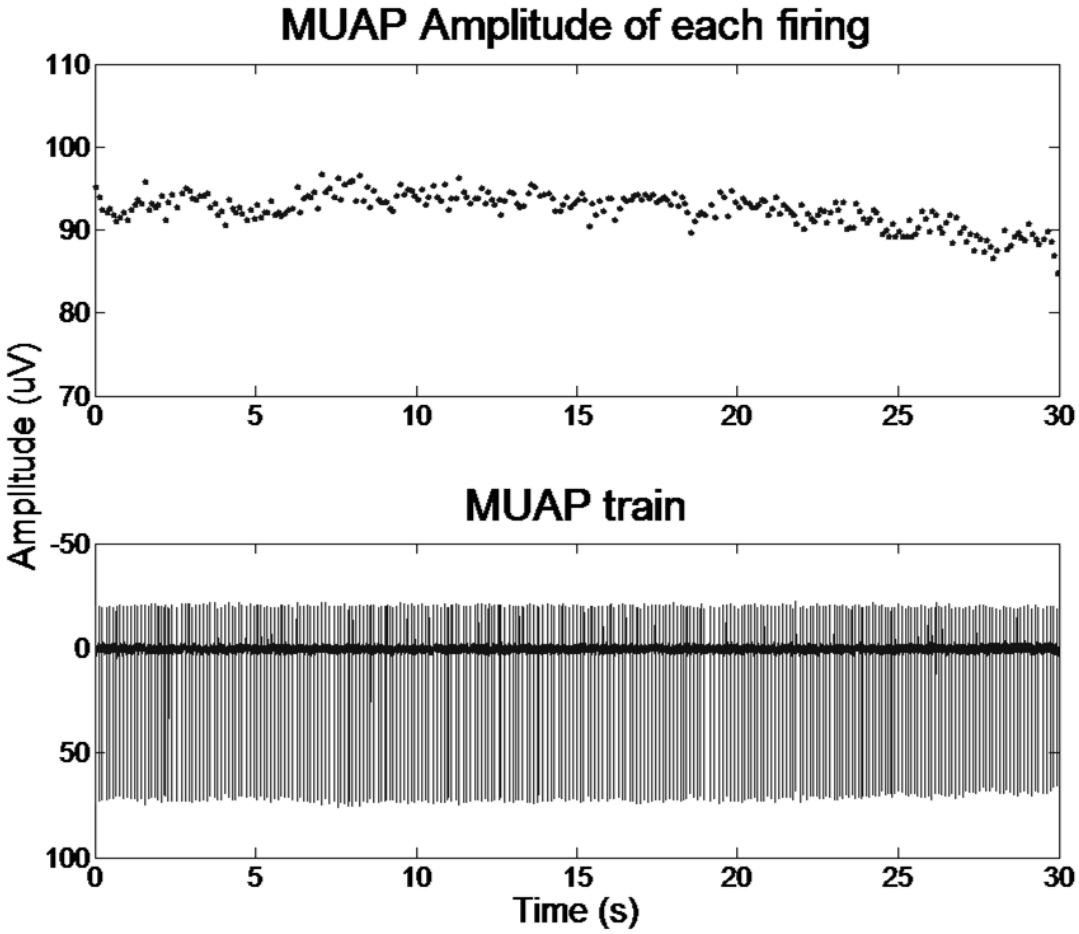

Figure 2.2: Example of measuring metrics of motor unit action potential trains—amplitude is shown here. Each MUAP is measured for all metrics. The amplitude of each MUAP, lower graph, is represented by a single point on the upper graph. Minor fluctuations in the amplitude can be seen throughout. Near the end of the 30 s epoch the amplitude begins to diminish visibly, indicating that the active surface of the electrode was moving away from the nearest fibers of the motor unit.

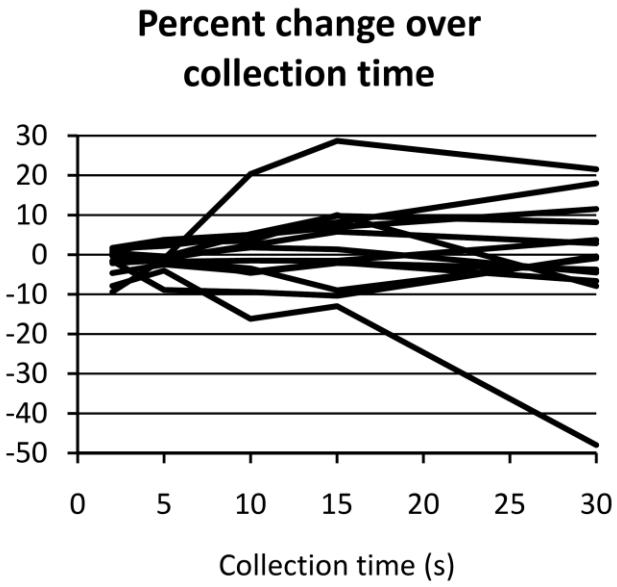

Figure 2.3: Representation of changes in MUAP amplitude, using a line fit of the data, of several MUAP trains at various collection times. At each time point after 5 s the range of percentage change spreads out. This figure includes only 12 MUAP trains for illustrative purposes.

selected MUAPs evenly spaced throughout the train. There were differences in the results of the various averaging methods for the longer collection epochs (15 and 30 s), but at 10 s or less all methods produced results which were roughly the same.

For complex interference patterns, those which contain two or more MUAP trains, these were cut at specific lengths (2, 5, 10, 15 and 30 s) to simulate having collected data for that specific amount of time. These were then reintroduced to the decomposition algorithm as if each were an independent study.

Optimizing Acquisition Time in Quantitative Electromyography

Reprinted with permission from Muscle & Nerve 40: 371-373

ABSTRACT: Quantitative electromyography (QEMG) relies on a number of discharges of the same motor unit action potential (MUAP) from a train to create an averaged MUAP considered to be representative of a true potential. The train of potentials may be affected by changes in position of the electrode relative to contributing muscle fibers of the motor unit due to operator or subject movement. The effect of changes in electrode position, along with consideration for patient comfort, prompted this study to determine the shortest duration of recording time necessary for sufficient data acquisition for QEMG studies. We determined that 10 seconds of moderate muscle activity is the most reasonable acquisition duration to isolate up to 6 MUAPs at a given electrode site and minimize the effects of movement artifact in the signal.

Muscle Nerve **40:** 371–373, 2009

OPTIMIZING ACQUISITION TIME IN QUANTITATIVE ELECTROMYOGRAPHY

ALEXANDER A. BROWNELL, MS, and MARK B. BROMBERG, MD, PhD

Department of Neurology, Clinical Neurosciences Center, University of Utah, 175 North Medical Drive, Salt Lake City, Utah 84132, USA

Accepted 3 February 2009

Factors that can affect the quality of quantitative electromyography (QEMG) analysis beyond those associated with hardware and software include movement of the electrode relative to muscle fibers of the motor unit in the uptake radius of the electrode. Electrode movement may occur from changes in posture of the patient due to factors such as fatigue, leading to activation of accessory muscles to maintain a suitable activation level, hand instability of the operator, and the heart beat of both the operator and patient. Electrode movement while collecting a motor unit action potential train (MUAPT) may ultimately result in changes in the motor unit action potential (MUAP) waveform over the acquisition time period. Acquisition time directly affects the number of MUAPs available for subsequent processing. There is a balance that allows for sufficient data to be obtained but minimizes artifactual changes during the MUAPT.

QEMG algorithms available on commercial EMG machines are proprietary and provide little information about their computational methods, but they generally follow a common analysis pattern. Waveforms from the interference pattern are first judged to represent individual MUAPs and are then grouped into one or more unique MUAPs. Further analysis based on discharge pattern and waveform similarities is carried out. For each unique MUAP signature, an average MUAP waveform thought to be representative of the actual MUAP is created and is used to determine metrics.[4] MUAPs within the interference pattern may be affected by electrode movement to a degree that does not cause the MUAP to be rejected but may change the average waveform and hence MUAP metrics. Automated QEMG algorithms use various lengths of data acquisition time for analysis, and thus data recording time is a factor in QEMG accuracy. Superimposed on the quantitative aspects of QEMG is consideration of patient comfort. These factors prompted this study to determine the shortest duration of recording time necessary for sufficient data acquisition in QEMG studies.

METHODS

Two different types of interference patterns were used in this study. The first are weak interference patterns, with only a single MUAP per MUAPT. The second were moderate interference patterns optimized to a couple of MUAPs. Interference patterns were obtained from biceps brachii and anterior tibialis muscles in three normal subjects and four moderately to markedly weak muscles (Medical Research

Abbreviations: ALS, amyotrophic lateral sclerosis; EMG, electromyography; MUAP, motor unit action potential; MUAPT, motor unit action potential train; QEMG, quantitative electromyography

Key words: data acquisition; electromyography; motor unit action potential; quantitative electromyography

Correspondence to: M. Bromberg; e-mail: mbromberg@hsc.utah.edu

Published online 17 July 2009 in Wiley InterScience (www.interscience.wiley.com). DOI 10.1002/mus.21339

Council grade 4) in subjects with amyotrophic lateral sclerosis (ALS; definite or probable ALS according to El Escorial criteria). Placement of the electrode with relation to the motor unit was determined by optimizing the amplitude and rise-time of the MUAP. Thirty seconds of EMG data were collected for each muscle. Raw data files were exported to MATLAB (The MathWorks, Natick, Massachusetts), where each raw data file was cut at specific lengths from the beginning of the file to produce recording epochs of 2, 5, 10, and 15 seconds. Each epoch of raw data was imported back into a decomposition QEMG software program (DQEMG) and analyzed just as it would have been had they been collected for the specific duration of time. The study was approved by the institutional review board. The EMG signals were collected using an EMG machine (Neuroscan; Compumedics, Ltd., San Antonio, Texas) with DQEMG software.[3]

To ensure consistency of metric measurement, MUAP metrics were determined by the internal algorithms of the DQEMG software, and there was no operator intervention. MUAPs that were not well defined were excluded from the study: for instance, if there were too few (<30) instances of MUAP or presence of dissimilar individual MUAP firings included in the averaged composite.

RESULTS

The number of individual MUAPs extracted from a moderate interference pattern increased linearly with longer acquisition epochs from both normal and ALS muscles. This resulted in larger numbers of average MUAPs detected with longer acquisition times, but the increase in number approached an asymptote with 5 or 6 MUAPs averaged at a 15-second acquisition epoch and no greater number with longer acquisition times (Fig. 1).

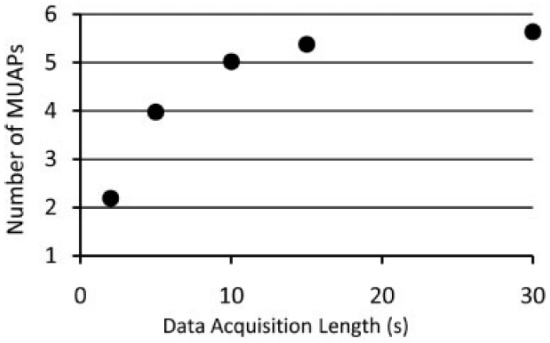

FIGURE 1. Average number of MUAPs detected based on length of acquisition epoch.

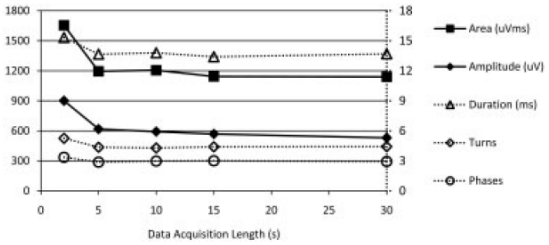

FIGURE 2. Change in average MUAP metrics based on length of acquisition epoch. Closed markers correspond to the left y-axis; open markers correspond to the right y-axis. Average metrics based on 1044 MUAPs.

MUAP metrics assessed by the algorithm included amplitude, duration, area, area-to-amplitude ratio, and number of turns and phases. The average values of all metrics decreased as acquisition time increased, and they reached stable values at and beyond 5 seconds (Fig. 2). MUAP amplitude and area decreased the most. Figure 3 shows examples of the variability in amplitude over 30-second epochs for individual MUAPs.

DISCUSSION

Automated QEMG algorithms rely on the ability to identify similar MUAPs in a discharge train to create a composite MUAP from which noise is essentially removed and which allows for more accurate marking of metrics. Data acquisition time is an important variable in order to collect a sufficient number of different MUAPs and to average them.[2] Commer-

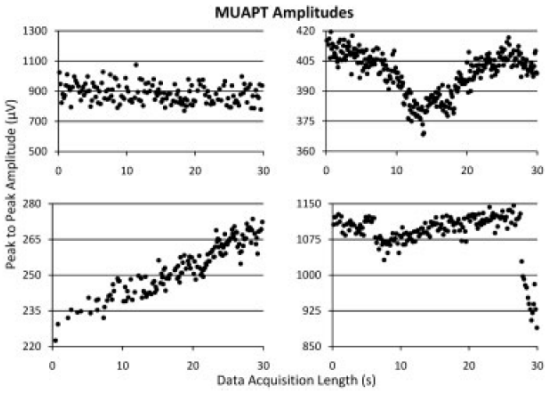

FIGURE 3. Examples of MUAP trains showing variations in amplitude. The amplitude of each MUAP is plotted over the 30-second acquisition time. Examples include a stable amplitude, increase, increase–decrease, and decrease over time attributed to changes in the position of the electrode in relation to individual muscle fibers of the motor unit.

cially available QEMG algorithms have differing requirements for the number of similar MUAPs needed to compile the composite MUAP used for averaging. If a single MUAP is recorded, the acquisition time would be a simple calculation based on the mean firing frequency (9–13 Hz) and the number used in the average. As contractions become more vigorous, and additional MUAPs are included, many instances of single MUAPs are obscured by the incidental simultaneous firing of two or more MUAPs. Although probability statistics might be used to approximate a reasonable acquisition time, most commercial algorithms rely on a set acquisition time. Another factor is the actual number of similar MUAPs that are averaged. With the software used in this study, a maximum of 51 similar MUAPs are averaged regardless of the number collected.

Our findings demonstrate the following: (1) There was a realistic maximum of 5 or 6 MUAPs that can be extracted from a moderate interference pattern regardless of the data acquisition time (Fig. 1). This and a previous study[2] have shown that an average of 6 distinct MUAPs per contraction is a practical upper limit; this number of MUAPs can typically be achieved with acquisition times of 10 seconds. Shorter data acquisition epochs may lead to inadequate numbers of individual MUAP firings due to the occasional superimposition of different MUAPs. Longer data acquisition epochs may lead to a reduction in the metric values of amplitude and area-to-amplitude ratio, most likely due to enhanced probability of electrode movement. These findings are supported empirically by studies using several different commercially available QEMG algorithms.[1–3] (2) There were changes in the averaged MUAP waveform when a larger number of MUAPs were averaged due to changes in needle position relative to the motor unit muscle fibers—and these changes affected the placement of markers and metric values (Fig. 3). In the algorithms used in this study, the maximum number averaged (51 MUAPs) was reached at 5 seconds of recording time (Fig. 1), and the averaged MUAP waveforms stabilized after 5 seconds of data acquisition. (3) The degree of change in individual MUAPs in the discharge train, as measured by amplitude, varied among trains from very stable to gradual or abrupt changes, and most changes appeared to occur later in the recording epoch (Fig. 3). The increases and decreases in amplitude were likely due to small movements of the electrode toward and away from one or more muscle fibers of the motor unit close to the active electrode surface. Because MUAP area is directly related to amplitude, changes in area were likely also caused by changes in electrode position.[5] (4) The findings were similar for normal and denervated muscle.

This and a previous study[2] have shown that an average of 6 distinct MUAPs per contraction represents a practical upper limit; this number of MUAPs can typically be achieved with an acquisition time of 10 seconds. Shorter data acquisition epochs may lead to inadequate numbers of individual MUAP firings due to the occasional superimposition of different MUAPs. Longer data acquisition epochs may lead to a reduction in the metric values of amplitude and area-to-amplitude ratio, most likely due to enhanced probability of electrode movement. QEMG is more widely available on commercial EMG machines and is being used more in both research and clinical settings. It is reasonable, in the interest of the patient, to attempt to minimize the time necessary for data acquisition in QEMG studies, because patients can exhibit fatigability and may change their posture in order to sustain the requisite contraction. This study reassures the researcher and clinician that adequate data for an accurate QEMG study can be obtained relatively quickly.

The authors are grateful for the grant support for this study (Short-Term Training: Students in Health Professional Schools).

REFERENCES

1. Boe S, Stashuk D, Brown W, Doherty T. Decomposition-based quantitative electromyography: effect of force on motor unit potentials and motor unit number estimates. Muscle Nerve 2005;31:365–373.
2. Brownell AA, Ni O, Bromberg MB. Comparison of three algorithms for multi-motor unit detection and waveform marking. Muscle Nerve 2005;33:538–545.
3. Doherty T, Stashuk D. Decomposition-based quantitative electromyography: methods and initial normative data in five muscles. Muscle Nerve 2003;28:204–211.
4. McGill KC, Lateva ZC, Marateb HR. EMGLAB: an interactive EMG decomposition program. J Neurosci Methods 2005;149: 121–133.
5. Nandedkar S, Sanders D, Stalberg E, Andreassen S. Simulation of concentric needle EMG motor unit action potentials. Muscle Nerve 1988;11:151–159.

3 CONCLUSIONS AND DISCUSSION

Overall, the contributions made by this series of studies aid in refining QEMG techniques in the clinical setting. We have followed a theme in evaluating a number of issues related to the accuracy and practical use of QEMG. We have validated many tools used for QEMG, and assured that comparable results are to be had regardless of needle selection or recording site. We have also sought to make the QEMG examination as efficient as possible so that the technique may be more readily used by the clinician who is always pressured for time.

Algorithm comparison

This study was undertaken to determine if the various QEMG algorithms available to clinicians were sufficiently similar in performance to allow the comparison of data between clinics and laboratories. We found that: 1) there were significant differences between the algorithms. We determined that one of the algorithms was able to distinguish fewer MUAPs and also marked their metrics with less accuracy. 2) None of the algorithms was perfectly efficient in extracting MUAPs out of the interference patterns when tested with simulated data. 3) Marking algorithms are difficult to design and none agreed perfectly with our measurements of known (simulated) data, but two of the algorithms performed well.

Simulated EMG data were used for this study to give us full control of the system, with knowledge of every component of the signal, including the basic noise. The fact that we created our signal means that it is likely less complex than a biologic signal in that we did not include as many motor units. We created a fully complex interference pattern in the sense that it contained a full complement of large MUAPs. However, we did not include tiny MUAPs from distant units. These are clinically insignificant, and their main effect on the signal would have been a simple shift in the background noise. The addition of such distant units would almost certainly not change the results of this study, as they would not be detected according to the criteria for detection set forth in the algorithms and would be averaged out in creating the composite MUAPs. We did create a distribution of inter-discharge intervals to vary the firing times of individual MUAPs throughout the interference pattern, but did this via a mathematical normal distribution function rather than create a velocity recovery function as described by Stålberg (56). However, the resulting distribution of interdischarge intervals should be sufficiently similar to the biologic reality. Some of the subtle complexities of a biologic system were not included such as low frequency deviations from baseline due to respiratory artifact, miniscule EKG components of the signal, and physiologic tremor both of the patient and electromyographer, but this refinement would add little and would be difficult to include in a meaningful way.

The expectations for MUAP extraction have not been specified or discussed in the literature. We included MUAPs of reasonable amplitude. Extracting all MUAP signals is not necessary for clinical utility and could be counterproductive. There is a greater spectrum of MUAPs identified by the multi-MUAP technique than by isolation of single

MUAPs and thus there is greater overlap of MUAPs from neuropathic and myopathic muscles with normal muscles (see Figure 1.17). Since the completion of this study a software program has been created which can extract all but the minutest noise in a biologic signal, and we discuss this further in the Future Work section.

Overall, this study showed that two of the algorithms are very useful tools in the clinical and research settings. However, they cannot currently be used without sophisticated oversight. The state of the art requires that a trained clinician review the results to discard duplicate MUAPs (MUAPs identified as unique but represent the same motor unit with slight changes in waveform morphology) and occasionally change duration markers. These algorithms do allow for efficient gathering and analysis of QEMG data which is useful in the clinical setting.

High-pass filtering

Modeling results suggested that there would be utility in further filtering the data—indeed it was suggested that with such filtering there would be a very high correlation between filtered turn count and fiber density as measured with a single fiber electrode. The fact that this was not verified in biologic muscle suggests that there are deficiencies within the models. These models are sophisticated, but even so have many assumptions and simplifications compared to biologic muscle. We believe that the line source representation of muscle fibers does not realistically allow for physiologic attenuation of the signal and does not recreate the anisotropy found in biologic muscle.

Additionally, it could be that the arrangement of muscle fibers does not accurately represent that found in biologic muscle.

We determined with this study that there was minimal utility in high-pass filtering EMG data in routine QEMG studies to extract increased complexity. This increased complexity, while real, did not correlate with any clinically useful information about the motor unit. We investigated this against fiber density measured using single fiber EMG techniques and looked at it in healthy and neuropathically diseased muscle. In neither case did high-pass filtering reveal pathology in greater degree than did EMG data obtained at conventional filter settings.

We did not extensively study the effects of filtering EMG signals obtained from myopathies. However, from the findings in normal and neuropathic muscles, in addition to the unique characteristics of myopathic MUAPs, there is likely to be no additionally useful clinical data from filtering myopathic EMG data.

Temporal dispersion of the MUAP

From the study on needle position and its effect on MUAPs, it was determined that any increase in the degree of temporal dispersion in arrival times of muscle fiber action potentials generated from more distant neuromuscular junctions does not clinically affect the MUAP to a significant degree. The modeling study suggested a greater change in the measurements than was found in muscle. This means that the effects of the distributions of muscle fiber propagation velocities are exaggerated in the models. Most likely, the distribution of muscle fiber diameters used in the models exceeded the actual

physiologic distribution in the biceps muscle. This was confirmed by a later study using a different electrodiagnostic technique (57). However, each of these models base their default values on physiologic studies (58,2,59). We could not, from this study, determine whether the equations relating fiber diameter to muscle fiber action potential velocity are accurate or exaggerated. These models are excellent teaching tools, and as such it is beneficial for the learner to observe exaggerated changes in MUAP morphology. Many experiments have found that models appropriately demonstrate physical phenomena, but do not necessarily exactly mirror physiology (60,29,34,61).

There is still much debate about the size and distribution of motor points (57,62-65). Knowing the location of the motor point is clinically useful from the perspective of treatment of spastic disorders with destructive lesions. However, determining that axial position of the electrode within the muscle in relation to the motor point does not create a clinically significant difference in EMG studies is an important finding. This speeds the electrodiagnostic testing by obviating the need to locate the motor point.

Needle electrode selection

Among the two electrode sizes tested there was no clinical significance in MUAP waveform metrics. Though significant differences between the two types of needles exist in certain metrics of certain muscles, these differences are not of sufficient magnitude to cause a problem with clinical studies. This issue is further ameliorated by consistent study practices such as collecting a laboratory normal database, and using the same needle for similar studies.

These findings were significant because they allow comparisons to be made across the reports in the literature. Many studies use either the standard or pediatric sized electrodes exclusively. Previously, these studies could not have legitimately been directly compared directly. Similar type studies had been performed in the past to examine the difference between the concentric and monopolar style electrodes (66,67). Together, these studies allow for most EMG data to be compared to that reported in the literature.

The model used for this study insufficiently represented the reality of the electrodes to include its results in the article. While excellent at mimicking the important principles in EMG studies, there are simplifications and assumptions that render the model deficient for full scientific studies.

Optimizing acquisition time

In the study that investigated the optimum collection time it was found that 10 seconds of moderate muscle activity was the most reasonable duration of acquisition. Less time would most likely be inadequate to generate sufficient numbers of MUAPs to reduce noise and create a reliable and accurate average. Longer acquisition times could more likely result in movement of the electrode and lead to a change in the MUAP morphology over time. This would distort the resulting averaged MUAP. It is likely that if there were even moderate movement the resulting MUAP could change enough that it would be recognized by the algorithm as two distinct MUAPs—as if one motor unit were

dropping out and another coming in. These observations are supported empirically by other studies (41,68).

Thought was given to the idea of a device to support the needle electrode, rather than having the clinician simply attempt to keep it steady. A number of different devices were drawn up, but none were deemed appropriate for many reasons. These included the inability of the clinician to easily adjust the needle position the many times required throughout the study, the concern for infection control (using the same device with many patients), obscuration of direct visualization of the insertion site, and added time and expensive not justifiable by the benefit.

Part of the problem with such devices is the radial expansion of muscle as it contracts. This means that all points of reference external to the muscle are going to be inadequate if muscle contraction either increases or decreases. It was decided that minimizing the time required to hold the electrode in place, during a steady contraction, was sufficient for most studies. This is because of both the limited time for drift, but also because the clinician can make small adjustments to recover if drift is noted. Additionally, if there is noticeable change in the MUAP morphology, the clinician can throw away a contraction completely. This is much easier to do if the individual contraction times are shorter.

It is also common practice to tape the electrode leads to the skin not far from the needle, which may be more steady than the clinician holding the electrode if a patient is uncooperative or there is other reason to keep the needle in one position for an extended time. We looked at this practice using the same techniques employed in this study and

found that there was significant drift in the MUAP morphology if the patient moves much, and minor drift otherwise. This was determined to be inadequate steadying.

Another significant consideration is patient comfort during an EMG study. Many patients experience discomfort, both physical and emotional, from the experience of having needles in their muscles. In fact, there is a defined medical condition called needle phobia (69), which makes these studies difficult, and reducing the amount of time the needle must be within the muscle to obtain adequate data would therefore reduce discomfort and anxiety.

Future Work

Library of known data

The algorithm comparison study used a known data source against which we compared the performance of the various systems. We could create an even more sophisticated known data set from biologic data. Kevin McGill and his colleagues have been working on the problem of superimposition of MUAPs which occurs during natural contractions (70-72). He has a technique where he can manually extract every MUAP from an interference pattern. This technique still requires a great deal expert manipulation, but it does make it possible to have a biologically derived signal where all variables are eventually known. It could be of great use to have a library of such known interference patterns which could be distributed to clinics and laboratories against which they could test their systems and algorithms. We would want to collect data from a variety of different conditions—normal muscle, myopathic, neuropathic, traumatic injury.

These could then be used to validate the system and allow for greater assurance that comparison of data from laboratory to laboratory was appropriate and accurate.

Finite element model of muscle fiber membrane

Most of the work in modeled EMG data is created using a line source model (Figure 3.1) (73,74,44,45,75,10,76,77,46). This assumes that the contributions from the muscle fiber action potential act as if from a line which is centered within the muscle fiber. As the current in muscle is generated across the fiber membrane, there is no point

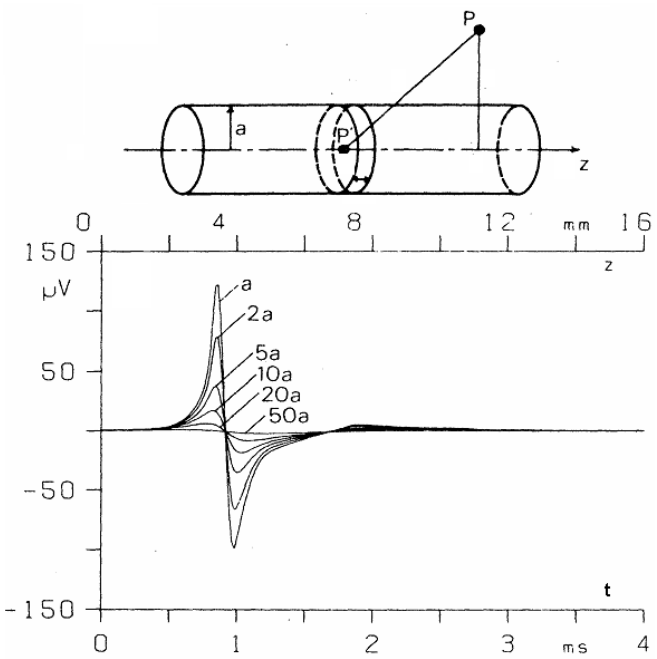

Figure 3.1: Basics of line source model. Model assumes a characteristic muscle fiber action potential (MFAP) based on the radius (a) of the muscle fiber. Electrode placement (P) dictates the recorded MFAP, the more distant the electrode placement the smaller the MFAP. The lower graph shows MFAPs recorded at increasing electrode distances from the muscle fiber.

source; rather, there is a roughly cylindrical surface source. As the needle is very close to the muscle fiber the muscle fiber action potential may contribute differently to the MUAP due to differences in near field effect versus the far field contribution from other muscle fibers. Additionally, there may be changes in the muscle fiber action potential from different morphologies of the muscle fiber membrane. One modeling study used a 3D muscle fiber as the source (78); however, muscle fibers are rarely perfectly cylindrical. They may have concavities and sharp corners where they border other muscle fibers as seen in histologic sections (Figure 3.2).

While we (43) and others (79,80) have investigated filtering as a method to pick out the contribution of single muscle fiber action potentials to MUAPs, it has not been investigated whether these morphological changes would significantly change the resulting muscle fiber action potential, or the MUAP. It is reasonable that a finite

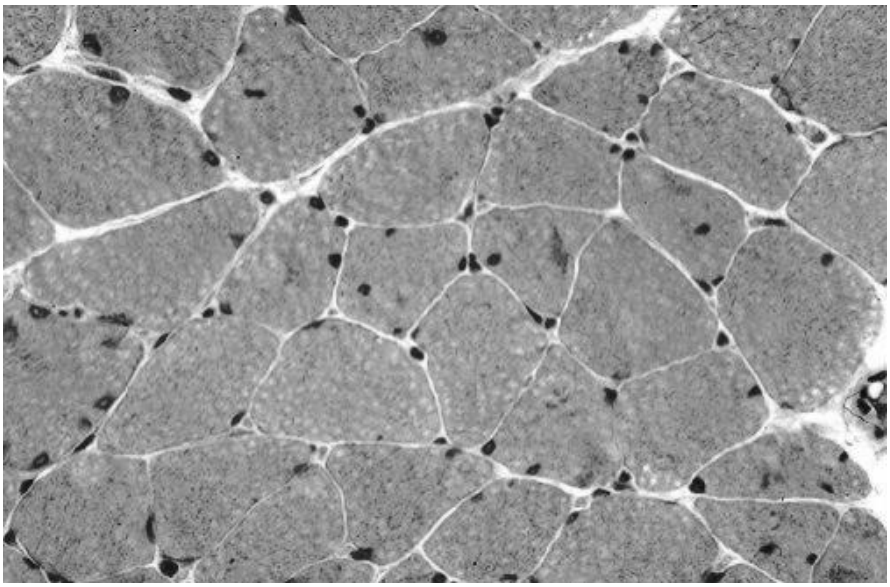

Figure 3.2: Cross section of deltoid muscle biopsy showing irregularity of muscle fibers. Though most are basically cylindrical, there are many flat sections, sharp edges, and concavities.

element model could be created which would allow a more accurate representation of the shape of a muscle fiber membrane to be studied. Many different muscle fiber morphologies could be investigated for action potential differences at both near field and far field distances. The simulated electrode should also be positioned at different positions relative to the various morphologic features. This could possibly show that a sharp corner or concavity of membrane affects the resulting action potential. If so, it is important that models be made more sophisticated to incorporate this information. If there is no significant difference in the potentials then we can continue to rely on the simpler models and look for other areas of inaccuracy to explain the deficiencies in the models. Also, this could lead to an increased understanding of the anisotropy of volume conduction in muscle tissue (81,26).

Distribution of conduction velocity based on muscle fiber diameters appears, from the results of our studies, to be an area of disagreement between the models and biology. A finite element model would allow for calculation of the muscle fiber conduction velocity based on membrane characteristics as well as diameter. This may resolve some of the disagreement.

One difficulty in creating such a model is that it is not know whether muscle fibers retain the same basic shape over their entire length or if there are many changes throughout based on the forces exerted by neighboring fibers. To create the finite element model we would first have to perform a study in which serial histological sections all along the length of many muscles mapped out the outline of muscle fiber membranes. The results of this study could serve as the basic framework for the finite element mesh model.

Motor unit number estimation

Additionally, there are other electrodiagnostic techniques that utilize EMG and nerve conduction study data to estimate the number of motor units in a muscle, called motor unit number estimation (MUNE). MUNE is particularly useful in assessing the progression of motor neuron disease. The basic idea is to stimulate the entire nerve which innervates a muscle and obtain a maximal summed compound muscle action potential (CMAP). Then, individual MUAPs are obtained. It is important to note that a surface electrode is used to record activity of all muscle fibers in the muscle (CMAP) and of motor units (surface motor unit potential—SMUP). Since motor units vary in amplitude, a representative sample is obtained to calculate an average SMUP. Once these two values have been determined, the MUNE is calculated as the CMAP divided by the average SMUP. The difficulty lies in obtaining a truly representative average SMUP. We have investigated and reviewed many different techniques employed to obtain these estimates (82). Unfortunately, these techniques have poor correlation one to another in the results, and only moderate test-retest reliability. We are continuing to evaluate new MUNE techniques and hope to find greater consistency in the results.

REFERENCES

1. Lidell EGT, Sherrington CS. Recruitment and some other factors of reflex inhibition. Proceedings of the Royal Society of London. Series B, Containing Papers of a Biological Character. 1925 Apr;97(686):488-518.

2. Edström L, Kugelberg E. Histochemical composition, distribution of fibres and fatiguability of single motor units. Anterior tibial muscle of the rat. J. Neurol. Neurosurg. Psychiatr. 1968 Oct;31(5):424-433.

3. Burke RE, Tsairis P. Anatomy and innervation ratios in motor units of cat gastrocnemius. J. Physiol. (Lond.). 1973 Nov;234(3):749-765.

4. Burke RE. Motor unit properties and selective involvement in movement. Exerc Sport Sci Rev. 1975;3:31-81.

5. Buchthal F, Guld C, Rosenfalck F. Multielectrode study of the territory of a motor unit. Acta Physiol. Scand. 1957 Apr 10;39(1):83-104.

6. Stålberg E, Antoni L. Electrophysiological cross section of the motor unit. J. Neurol. Neurosurg. Psychiatr. 1980 Jun;43(6):469-474.

7. Bischoff C, Stålberg E, Falck B, Eeg-Olofsson KE. Reference values of motor unit action potentials obtained with multi-MUAP analysis. Muscle Nerve. 1994 Aug;17(8):842-851.

8. Bromberg MB. EMG assessment of denervation. Critical Reviews in Physical and Rehabilitation Medicine. 1993;5:83-127.

9. Nandedkar SD, Sanders DB, Stålberg EV. Selectivity of electromyographic recording techniques: a simulation study. Med Biol Eng Comput. 1985 Nov;23(6):536-540.

10. Nandedkar SD, Sanders DB, Stålberg EV, Andreassen S. Simulation of concentric needle EMG motor unit action potentials. Muscle Nerve. 1988 Feb;11(2):151-159.

11. Gath I, Stålberg E. The calculated radial decline of the extracellular action potential compared with in situ measurements in the human brachial biceps. Electroencephalogr Clin Neurophysiol. 1978 May;44(5):547-552.

12. Stålberg E, Andreassen S, Falck B, Lang H, Rosenfalck A, Trojaborg W. Quantitative analysis of individual motor unit potentials: a proposition for standardized terminology and criteria for measurement. J Clin Neurophysiol. 1986 Oct;3(4):313-348.

13. Stålberg E, Nandedkar SD, Sanders DB, Falck B. Quantitative motor unit potential analysis. J Clin Neurophysiol. 1996 Sep;13(5):401-422.

14. Exner S. Notiz zu der Frage von der Faservertheilung mehrerer Nerven in einem Muskel. Pflüger, Arch. 1885 12;36(1):572-576.

15. Edds MV. Collateral nerve regeneration. Q Rev Biol. 1953 Sep;28(3):260-276.

16. Kugelberg E, Edström L, Abbruzzese M. Mapping of motor units in experimentally reinnervated rat muscle. Interpretation of histochemical and atrophic fibre patterns in neurogenic lesions. J. Neurol. Neurosurg. Psychiatr. 1970 Jun;33(3):319-329.

17. Stålberg E. Electrophysiological studies of reinnervation in ALS. Adv Neurol. 1982;36:47-59.

18. Wohlfart G. Collateral regeneration in partially denervated muscles. Neurology. 1958 Mar;8(3):175-180.

19. Mihelin M, Trontelj JV, Stålberg E. Muscle fiber recovery functions studied with double pulse stimulation. Muscle Nerve. 1991 Aug;14(8):739-747.

20. Stålberg E, Ekstedt J, Broman A. The electromyographic jitter in normal human muscles. Electroencephalogr Clin Neurophysiol. 1971 Nov;31(5):429-438.

21. Stålberg EV, Sonoo M. Assessment of variability in the shape of the motor unit action potential, the "jiggle," at consecutive discharges. Muscle Nerve. 1994 Oct;17(10):1135-1144.

22. Kingston WJ, Moxley RT. Inflammatory myopathies. Neurol Clin. 1988 Aug;6(3):545-561.

23. Nandedkar SD, Sanders DB. Simulation of myopathic motor unit action potentials. Muscle Nerve. 1989 Mar;12(3):197-202.

24. Stålberg E. Single fibre electromyography. Old Woking Eng.: Mirvalle ; Pleasantville N. Y. distributed in the U. S. by Teca Corp.; 1979.

25. Epstein BR, Foster KR. Anisotropy in the dielectric properties of skeletal muscle. Med Biol Eng Comput. 1983 Jan;21(1):51-55.

26. Gath I, Stålberg E. On the volume conduction in human skeletal muscle: in situ measurements. Electroencephalogr Clin Neurophysiol. 1977 Jul;43(1):106-110.

27. Gath I, Stålberg E. Frequency and time domain characteristics of single muscle fibre action potentials. Electroencephalogr Clin Neurophysiol. 1975 Oct;39(4):371-376.

28. Pattichis CS, Elia AG. Autoregressive and cepstral analyses of motor unit action potentials. Med Eng Phys. 1999 Sep;21(6-7):405-419.

29. Duchêne J, Hogrel JY. A model of EMG generation. IEEE Trans Biomed Eng. 2000 Feb;47(2):192-201.

30. Falck B, Stålberg E, Stålberg S, Aström M. Multi-MUP EMG analysis in clinical routine. Neurol. Neurochir. Pol. 1996;30 Suppl 3:55-70.

31. Mambrito B, De Luca CJ. A technique for the detection, decomposition and analysis of the EMG signal. Electroencephalogr Clin Neurophysiol. 1984 Aug;58(2):175-188.

32. Stålberg E, Falck B, Sonoo M, Stålberg S, Aström M. Multi-MUP EMG analysis--a two year experience in daily clinical work. Electroencephalogr Clin Neurophysiol. 1995 Jun;97(3):145-154.

33. Stashuk DW, Naphan RK. Probabilistic inference-based classification applied to myoelectric signal decomposition. IEEE Trans Biomed Eng. 1992 Apr;39(4):346-355.

34. Zhou P, Rymer WZ. MUAP number estimates in surface EMG: template-matching methods and their performance boundaries. Ann Biomed Eng. 2004 Jul;32(7):1007-1015.

35. Freund HJ, Büdingen HJ, Dietz V. Activity of single motor units from human forearm muscles during voluntary isometric contractions. J. Neurophysiol. 1975 Jul;38(4):933-946.

36. Milner-Brown HS, Stein RB, Yemm R. Changes in firing rate of human motor units during linearly changing voluntary contractions. J. Physiol. (Lond.). 1973 Apr;230(2):371-390.

37. Norris FH, Gasteiger EL. Action potentials of single motor units in normal muscle. Electroencephalogr Clin Neurophysiol. 1955 Feb;7(1):115-125.

38. Olney RK, Aminoff MJ, Gelb DJ, Lowenstein DH. Neuromuscular effects distant from the site of botulinum neurotoxin injection. Neurology. 1988 Nov;38(11):1780-1783.

39. Stewart CR, Nandedkar SD, Massey JM, Gilchrist JM, Barkhaus PE, Sanders DB. Evaluation of an automatic method of measuring features of motor unit action potentials. Muscle Nerve. 1989 Feb;12(2):141-148.

40. Brownell AA, Ni O, Bromberg MB. Comparison of three algorithms for multi-motor unit detection and waveform marking. Muscle Nerve. 2006 Apr;33(4):538-545.

41. Boe SG, Stashuk DW, Brown WF, Doherty TJ. Decomposition-based quantitative electromyography: effect of force on motor unit potentials and motor unit number estimates. Muscle Nerve. 2005 Mar;31(3):365-373.

42. Payan J. The blanket principle: a technical note. Muscle Nerve. 1978 Oct;1(5):423-426.

43. Brownell AA, Bromberg MB. Effects of high-pass filtering on MUAP metrics. Muscle Nerve. 2009 Dec;40(6):1008-1011.

44. Hamilton-Wright A, Stashuk DW. Physiologically based simulation of clinical EMG signals. IEEE Trans Biomed Eng. 2005 Feb;52(2):171-183.

45. Karlsson L, Hammarberg B, Stålberg E. An application of a muscle model to study electromyographic signals. Comput Methods Programs Biomed. 2003 Jul;71(3):225-233.

46. Stålberg E, Karlsson L. Simulation of EMG in pathological situations. Clin Neurophysiol. 2001 May;112(5):869-878.

47. Hopf HC. Anticonvulsant drugs and spike propagation of motor nerves and skeletal muscle. J. Neurol. Neurosurg. Psychiatr. 1973 Aug;36(4):574-580.

48. Nishihara K, Futami T, Hosoda K, Gomi T. Validation of estimated muscle fiber conduction velocity with the normalized peak-averaging technique. J Electromyogr Kinesiol. 2005 Feb;15(1):93-101.

49. Okajima Y, Tsubahara A, Kondo K, Chino N, Noda Y, Tomita Y. A new method of estimating the distribution of muscle fiber conduction velocities. Electroencephalogr Clin Neurophysiol. 1995 Dec;97(6):310-317.

50. Yaar I, Shapiro MB, Mitz AR, Pottala EW. A new technique for measuring muscle fiber conduction velocities in full interference patterns. Electroencephalogr Clin Neurophysiol. 1984 May;57(5):427-434.

51. Li W, Sakamoto K. Distribution of muscle fiber conduction velocity of M. biceps brachii during voluntary isometric contraction with use of surface array electrodes. Appl Human Sci. 1996 Jan;15(1):41-53.

52. Mito K, Kaneko K, Makabe H, Takanokura M, Sakamoto K. Comparison of experimental and numerical muscle fiber conduction velocity (MFCV) distribution around the end-plate zone and fiber endings. Med. Sci. Monit. 2006 Apr;12(4):BR115-123.

53. Brownell AA, Bromberg MB. Effects of intramuscular needle position on motor unit action potential metrics. Muscle Nerve. 2007 Apr;35(4):465-470.

54. Brownell AA, Bromberg MB. Comparison of standard and pediatric size concentric needle EMG electrodes. Clin Neurophysiol. 2007 May;118(5):1162-1165.

55. Brownell AA, Bromberg MB. Optimizing acquisition time in quantitative electromyography. Muscle Nerve. 2009 Sep;40(3):371-373.

56. Stalberg E. Propagation velocity in human muscle fibers in situ. Acta Physiol Scand Suppl. 1966;287:1-112.

57. Navallas J, Stålberg E. Studying motor end-plate topography by means of scanning-electromyography. Clin Neurophysiol. 2009 Jul;120(7):1335-1341.

58. Brooke MH, Engel WK. The histographic analysis of human muscle biopsies with regard to fiber types. 1. Adult male and female. Neurology. 1969 Mar;19(3):221-233.

59. Stålberg E, Dioszeghy P. Scanning EMG in normal muscle and in neuromuscular disorders. Electroencephalogr Clin Neurophysiol. 1991 Dec;81(6):403-416.

60. van Veen BK, Wolters H, Wallinga W, Rutten WL, Boom HB. The bioelectrical source in computing single muscle fiber action potentials. Biophys. J. 1993 May;64(5):1492-1498.

61. van Veen BK, Mast E, Busschers R, Verloop AJ, Wallinga W, Rutten WL, et al. Single fibre action potentials in skeletal muscle related to recording distances. J Electromyogr Kinesiol. 1994;4(1):37-46.

62. Lee NG, You JH, Park HD, Myoung HS, Lee SE, Hwang JH, et al. The validity and reliability of the motor point detection system: a preliminary investigation of motor points of the triceps surae muscles. Arch Phys Med Rehabil. 2009 Feb;90(2):348-353.

63. Amirali A, Mu L, Gracies J, Simpson DM. Anatomical localization of motor endplate bands in the human biceps brachii. J Clin Neuromuscul Dis. 2007 Dec;9(2):306-312.

64. Harrison TP, Sadnicka A, Eastwood DM. Motor points for the neuromuscular blockade of the subscapularis muscle. Arch Phys Med Rehabil. 2007 Mar;88(3):295-297.

65. Harris AJ, Duxson MJ, Butler JE, Hodges PW, Taylor JL, Gandevia SC. Muscle fiber and motor unit behavior in the longest human skeletal muscle. J. Neurosci. 2005 Sep 14;25(37):8528-8533.

66. Howard JE, McGill KC, Dorfman LJ. Properties of motor unit action potentials recorded with concentric and monopolar needle electrodes: ADEMG analysis. Muscle Nerve. 1988 Oct;11(10):1051-1055.

67. Pease WS, Bowyer BL. Motor unit analysis. Comparison between concentric and monopolar electrodes. Am J Phys Med Rehabil. 1988 Feb;67(1):2-6.

68. Doherty TJ, Stashuk DW. Decomposition-based quantitative electromyography: methods and initial normative data in five muscles. Muscle Nerve. 2003 Aug;28(2):204-211.

69. Hamilton JG. Needle phobia: a neglected diagnosis. J Fam Pract. 1995 Aug;41(2):169-175.

70. Koch VM, McGill KC, Loeliger H. Resolution of superpositions in EMG signals using belief propagation: results for the known constituent problem. Conf Proc IEEE Eng Med Biol Soc. 2006;1:1260-1263.

71. Marateb HR, McGill KC. Resolving superimposed MUAPs using particle swarm optimization. IEEE Trans Biomed Eng. 2009 Mar;56(3):916-919.

72. McGill KC. Optimal resolution of superimposed action potentials. IEEE Trans Biomed Eng. 2002 Jul;49(7):640-650.

73. Cohen MH, Lester JM, Bradley WG, Brenner JF, Hirsch RP, Silber DI, et al. A computer model of denervation-reinnervation in skeletal muscle. Muscle Nerve. 1987 Dec;10(9):826-836.

74. Dumitru D, King JC, Nandedkar SD. Concentric/monopolar needle electrode modeling: spatial recording territory and physiologic implications. Electroencephalogr Clin Neurophysiol. 1997 Oct;105(5):370-378.

75. Nandedkar SD, Sanders DB, Stålberg EV. EMG of reinnervated motor units: a simulation study. Electroencephalogr Clin Neurophysiol. 1988 Aug;70(2):177-184.

76. Nandedkar SD, Stålberg E. Simulation of single muscle fibre action potentials. Med Biol Eng Comput. 1983 Mar;21(2):158-165.

77. Rattay F. Current distance relations for fiber stimulation with pointsources. IEEE Trans Biomed Eng. 2008 Mar;55(3):1122-1127.

78. Stickler Y, Martinek J, Rattay F. Modeling needle stimulation of denervated muscle fibers: voltage-distance relations and fiber polarization effects. IEEE Trans Biomed Eng. 2009 Oct;56(10):2396-2403.

79. Lateva ZC, McGill KC. Estimating motor-unit architectural properties by analyzing motor-unit action potential morphology. Clin Neurophysiol. 2001 Jan;112(1):127-135.

80. Stashuk DW. Detecting single fiber contributions to motor unit action potentials. Muscle Nerve. 1999 Feb;22(2):218-229.

81. De Lisa JA, Brozovich FV. Volume conduction in electromyography: experimental and theoretical review. Electromyogr Clin Neurophysiol. 1983 Dec;23(7):651-673.

82. Bromberg MB, Brownell AA. Motor unit number estimation in the assessment of performance and function in motor neuron disease. Phys Med Rehabil Clin N Am. 2008 Aug;19(3):509-532, ix.